



Faculty of Nursing, Pharmacy and Health Professions

Master Program in Industrial Pharmaceutical Technology

**Master Thesis**

**Formulation of Topical Mebendazole and Studying its  
Permeation Behavior.**

تحضير علاج موضعي من ميبندزول و دراسة خصائص نفاذته

This thesis was submitted in partial fulfillment of the requirements for the Master's Degree in Industrial Pharmaceutical Technology from the Faculty of Graduate Studies at Birzeit University, Palestine

**By**

**Huda Awadallah Obaid**

**Supervisor: Dr. Moammal Qurt**

**Co. Supervisor Dr. Numan Malkieh**

**5<sup>th</sup> June 2021**

**Formulation of Topical Mebendazole and Studying its  
Permeation Behavior.**

توضير علاج موضعي من ميبنذول و دراسة خصائص نفاذته

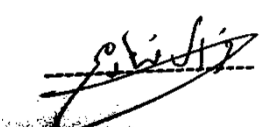
**By**

**Huda Awadallah Obaid**

**ID: 1165106**

*This thesis was defended successfully on* 5/6/2021

**Examination Committee members:**

<i>Name</i>	<i>Signature</i>	<i>Date</i>
<b>Dr. Moammal Qurt</b> <i>Head of committee</i>		<u>28/6/2021</u>
<b>Dr. Numan Malkieh</b> <i>Head of committee</i>		<u>28/6/2021</u>
<b>Dr. Hani Shtaya</b> <i>Internal Examiner</i>		<u>28/6/2021</u>
<b>Dr. Feras Qanaze</b> <i>Internal Examiner</i>		<u>28/6/2021</u>

## **Dedication**

*To my great Mom and Dad  
Who have never left my side;  
and who always picked me up on time  
and encouraged me to go on every challenge  
especially this one...*

## **Acknowledgements**

I would like to express my deepest gratitude and appreciation to my advisors, Dr. Moammal Qurt and Dr. Numan Malkieh for their guidance and encouragement throughout my master thesis.

My sincere gratitude also goes to my committee members for their advices and for providing critical comments that improve the content of this thesis.

I would like to gratefully and sincerely thank Eng. Ramzi Muqedi and Dr. Amin Thawabteh at Samih Darwazeh institution for providing the working space and for their research assistance.

My family is the long-term source of energy for my life. I wish to express my deepest gratitude to my father, Awadallah Obaid, my mother, Ahlam Shoman, my sisters, Noor, Fatima and Shatha, my brothers, Ibraheem and Ismaeel, and my dear friend Mariana for their unconditional love and for giving me the strength to take up this work and complete it to the best of my ability.

Finally, I would like to thank all my friends, work colleagues in Qimam Academy, and study colleagues for their faith, encouragement, and pushing me for tenacity.

## Table of Contents

Dedication.....	II
Acknowledgements .....	III
List of Tables.....	VIII
List of Figures.....	XIII
List of abbreviations and symbols.....	XVI
List of Appendices .....	XIX
Abstract .....	XX
المخلص.....	XXIII
Chapter 1.....	1
Introduction .....	1
1.1. Transdermal drug delivery system (TDDS).....	1
1.1.1. Structure of the human skin.....	2
1.1.2 Dermal and transdermal permeation pathway .....	3
1.1.3 Properties that influence transdermal drug delivery .....	5
1.1.4 Ideal physicochemical properties for transdermal drug delivery .....	7
1.1.5 Transdermal permeation enhancement techniques .....	7
1.1.6 Techniques and methods for modeling permeation / penetration through human skin .....	9
1.2. Microemulsion .....	19
1.2.1 Advantages of microemulsion.....	19
1.2.2 Disadvantages of microemulsion.....	20
1.2.3 Composition of microemulsion .....	20
1.2.4 Types of microemulsion .....	23
1.2.5 Phase diagram study.....	24
1.2.6 Preparation of microemulsion.....	25
1.2.7 Factors affecting microemulsion.....	26
1.2.8 Characterization of microemulsion .....	28
1.2.9 Accelerated stability studies for microemulsion.....	30

1.2.10	Long term stability studies for microemulsion.....	30
1.2.11	In vitro skin permeation studies.....	32
1.3	Mebendazole.....	32
1.3.1	Description.....	32
1.3.1.1	Solubility.....	32
1.3.1.2	Polymorphs.....	33
1.3.1.3	Octanol/ water partition coefficient and dissociation constant.....	33
1.3.1.4	Melting point.....	33
1.3.1.5	Biopharmaceutical Classification System (BCS).....	33
1.3.1.6	Method of manufacturing.....	33
1.3.1.7	Mode of action.....	33
1.3.2	Mebendazole as anti-cancer.....	34
1.3.2.1	Treating melanoma with mebendazole.....	34
Chapter 2	.....	35
Problem, Objectives and work plan	.....	35
2.1	Problem.....	35
2.2	Objectives.....	36
2.3	Work plan.....	37
Chapter 3	.....	38
Methodology	.....	38
3.1	Materials.....	38
3.1.1	Materials for formulation.....	38
3.1.2	Materials for analysis.....	39
3.1.3	Membranes.....	39
3.2	Equipment and tools.....	40
3.3	Methods.....	41
3.3.1	High performance liquid chromatography (HPLC) analysis.....	41
3.3.2	Preparation method for linearity, LOD, and LOQ.....	41
3.3.3	Preparation method for solubility tests.....	42
3.3.3.1	The Saturation solubility of MBZ in oils.....	42

3.3.3.2	The Saturation solubility of MBZ in surfactants and co-surfactant.....	42
3.3.4	Analysis method for solubility tests .....	42
3.3.5	Preparation method for microemulsion.....	43
3.3.6	Characterization and stability of microemulsion formulation trials .....	44
3.3.6.1	Type of microemulsion .....	44
3.3.6.2	Viscosity measurement.....	44
3.3.6.3	Refractive index measurement.....	45
3.3.6.4	Droplet size and size distribution.....	46
3.3.6.5	Centrifugation stress test.....	46
3.3.6.6	Freeze thaw cycle .....	46
3.3.7	Permeation study of various microemulsion formulations of mebendazole using Franz diffusion cells.....	47
3.3.7.1	Description of Franz diffusion cell apparatus.....	47
3.3.7.2	Preparation of receptor medium .....	48
3.3.7.3	Preparation of membrane.....	49
3.3.7.4	In vitro skin permeation studies procedures.....	49
3.3.7.5	Calculation of permeation membrane parameters .....	51
3.3.8	Mebendazole solubility in receptor medium.....	53
3.3.9	Statistical analysis.....	53
Chapter 4	.....	54
Results and discussion	.....	54
4.1	Linearity, LOD, and LOQ for HPLC method .....	54
4.2	Solubility studies of mebendazole in various oils .....	56
4.3	Solubility studies of mebendazole in various surfactants and co-surfactants .....	58
4.4	Microemulsion formulations trials.....	60
4.4.1	Stage1: By Experimental Trials .....	60
4.4.2	Stage 2: Using ternary diagram tables.....	62
4.5	Solubility studies of mebendazole in various formulations of microemulsion.....	70
4.6	Type and composition of the selected microemulsion formulations trials .....	71
4.7	Viscosity of selected formulations of microemulsion.....	73

4.8	Refractive index of the selected microemulsion formulation trials.....	74
4.9	Droplet size of the selected microemulsion formulation trials .....	75
4.10	Stability studies for formulations of microemulsion without mebendazole .....	78
4.11	Stability studies of the selected formulations of microemulsion with MBZ .....	79
4.11.1	Stability study of the selected microemulsion formulations with MBZ at room temperature .....	79
4.11.2	Accelerated Stability study for selected formulations of microemulsion with MBZ at room temperature .....	82
4.12	Permeation study using Franz diffusion cells .....	83
4.12.1	Permeation study using nylon (polyamide)0.45 $\mu\text{m}$ membrane.....	84
4.12.2	Permeation study using Start-M membrane 300 $\mu\text{m}$ .....	98
Chapter 5	.....	113
Conclusion	.....	113
Future work	.....	115
References	.....	116
Appendices	.....	132



## List of Tables

<b>Table 1:</b> Materials for formulation and its function-----	<b>38</b>
<b>Table 2:</b> Materials for analysis-----	<b>39</b>
<b>Table 3:</b> Description of synthetic membranes-----	<b>39</b>
<b>Table 4:</b> Equipment and Tools-----	<b>40</b>
<b>Table 5:</b> Chemicals used for phosphate buffer preparation-----	<b>48</b>
<b>Table 6:</b> Summary of diffusion parameters and their method of calculation met----- -----	<b>55</b>
<b>Table 7:</b> Statistical analysis of the HPLC method validation-----	<b>55</b>
<b>Table 8:</b> Saturation solubility of MBZ in various oils-----	<b>57</b>
<b>Table 9:</b> Saturation solubility of MBZ in various surfactants and co-surfactants--- -----	<b>58</b>
<b>Table 10:</b> Microemulsion formulations by experimental trials-----	<b>60</b>
<b>Table 11:</b> Microemulsion formulation ratios using titration method and pseudo- ternary diagram tables.-----	<b>63</b>
<b>Table 12:</b> Microemulsion formulations properties for IPP: Tween 80/DEGME---- -----	<b>64</b>
<b>Table 13:</b> Microemulsion formulations properties for Oleic acid: Tween80/ benzyl alcohol-----	<b>65</b>

<b>Table 14:</b> Microemulsion formulations properties for Oleic acid: Tween 80/N-methyl pyrrolidone-----	<b>66</b>
<b>Table 15:</b> Microemulsion formulations properties for Oleic acid: RH 40/ N-methyl pyrrolidone-----	<b>67</b>
<b>Table 16:</b> Saturation solubility of MBZ in various microemulsion formulation trials-----	<b>70</b>
<b>Table 17:</b> Selected formulation trials of microemulsion with (v/v%) using ternary diagram tables-----	<b>70</b>
<b>Table 18:</b> Viscosity of the selected microemulsion formulation trials-----	<b>73</b>
<b>Table 19:</b> Refractive index of the selected microemulsion formulation trials----	<b>74</b>
<b>Table 20:</b> Droplet size of the selected microemulsion formulation trials-----	<b>75</b>
<b>Table 21:</b> Summary of physical properties for the selected microemulsion formulation trials-----	<b>77</b>
<b>Table 22:</b> Stability studies for formulations of microemulsion without mebendazole-----	<b>78</b>
<b>Table 23:</b> Assay % and droplet size of the selected formulations of microemulsion with MBZ at time zero-----	<b>80</b>
<b>Table 24:</b> Assay % and droplet size of the selected formulations of microemulsion with MBZ after one week at room temperature-----	<b>80</b>
<b>Table 25:</b> Assay % and droplet size of the selected formulations of microemulsion with MBZ after 2 weeks at room temperature-----	<b>81</b>

<b>Table 26:</b> The assay % and visual appearance of the selected microemulsion formulations after freeze-thaw cycle-----	<b>82</b>
<b>Table 27:</b> The visual appearance of the selected microemulsion formulations after centrifugation stress test-----	<b>83</b>
<b>Table 28:</b> Data obtained from Franz diffusion cells for formulation ME#4 (Oleic acid: T80/Pyrrrol) using polyamide membrane-----	<b>84</b>
<b>Table 29:</b> Data obtained from Franz diffusion cells for formulation ME#4 (Oleic acid: T80/Pyrrrol) using polyamide membrane-----	<b>85</b>
<b>Table 30:</b> Diffusion parameters for formulation ME#4-----	<b>86</b>
<b>Table 31:</b> Data obtained from Franz diffusion cells for formulation ME#6 (IPP:T80/DEGME) using polyamide membrane-----	<b>83</b>
<b>Table 32:</b> Data obtained from Franz diffusion cells for formulation ME#6 (IPP:T80/DEGME) using polyamide membrane-----	<b>88</b>
<b>Table 33:</b> Diffusion parameters for formulation ME#6-----	<b>89</b>
<b>Table 34:</b> Data obtained from Franz diffusion cells for formulation ME#7 (Oleic:RH40/Pyrrrol) using polyamide membrane-----	<b>90</b>
<b>Table 35:</b> Data obtained from Franz diffusion cells for formulation ME#7 (Oleic:RH40/Pyrrrol) using polyamide membrane-----	<b>91</b>
<b>Table 36:</b> Diffusion parameters for formulation ME#7-----	<b>92</b>
<b>Table 37:</b> Data obtained from Franz diffusion cells for formulation ME#8 (Oleic: RH40/Pyrrrol) using polyamide membrane-----	<b>93</b>

<b>Table 38:</b> Data obtained from Franz diffusion cells for formulation ME#8 (Oleic:RH40/Pyrrrol) using polyamide membrane-----	<b>94</b>
<b>Table 39:</b> Diffusion parameters for formulation ME#8-----	<b>95</b>
<b>Table 40:</b> Steady state flux for microemulsion formulations (with polyamide membrane)-----	<b>96</b>
<b>Table 41:</b> Data obtained from Franz diffusion cells for formulations trial ME#4 (Oleic acid: T80/Pyrrrol) using Start-M membrane-----	<b>98</b>
<b>Table 42:</b> Data obtained from Franz diffusion cells for formulation ME#4 (Oleic acid: T80/Pyrrrol) using Start-M membrane-----	<b>99</b>
<b>Table 43:</b> Diffusion parameters for formulation ME#4-----	<b>100</b>
<b>Table 44:</b> Data obtained from Franz diffusion cells for formulation ME#6 (IPP:T80/DEGME) using Start-M membrane-----	<b>101</b>
<b>Table 45:</b> Data obtained from Franz diffusion cells for formulation ME#6 (IPP:T80/DEGME) using Start-M membrane-----	<b>102</b>
<b>Table 46:</b> Diffusion parameters for formulation ME#6-----	<b>103</b>
<b>Table 47:</b> Data obtained from Franz diffusion cells for formulation ME#7 (Oleic acid: RH 40/Pyrrrol) using Start-M membrane-----	<b>104</b>
<b>Table 48:</b> Data obtained from Franz diffusion cells for formulation ME#7 (Oleic acid: RH 40/Pyrrrol) using Start-M membrane-----	<b>105</b>
<b>Table 49:</b> Diffusion parameters for formulation ME#7-----	<b>103</b>
<b>Table 50:</b> Data obtained from Franz diffusion cells for formulation ME#8 (Oleic acid: RH40/Pyrrrol) using Start-M membrane-----	<b>107</b>

**Table 51:**Data obtained from Franz diffusion cells for formulation ME#8 (Oleic acid: RH 40/Pyrrrol) using Start-M membrane-----**108**

**Table 52:** Diffusion parameters for formulation ME#8-----**109**

**Table 53:** Steady state flux for microemulsion formulations (with Start-M membrane)-----**110**

**Table 54:** Permeation parameters for microemulsion formulations using polyamide and Start-M membrane-----**112**

## List of Figures

<b>Figure 1:</b> Cross section of skin-----	<b>3</b>
<b>Figure 2:</b> Schematic of dermal and transdermal permeation pathway-----	<b>5</b>
<b>Figure 3:</b> Drug transport processes across the skin-----	<b>6</b>
<b>Figure 4:</b> Vertical Franz Diffusion cell-----	<b>11</b>
<b>Figure 5:</b> A match in Morphology between Start- M membrane and human skin-- -----	<b>13</b>
<b>Figure 6:</b> Determination of steady state flux and lag-time -----	<b>18</b>
<b>Figure 7:</b> Aqueous Phase Titration Method-----	<b>25</b>
<b>Figure 8:</b> Chemical structure of mebendazole-----	<b>32</b>
<b>Figure 9:</b> Thesis work plan-----	<b>32</b>
<b>Figure 10:</b> Vertical Franz diffusion cell apparatus (ORCHD science)-----	<b>47</b>
<b>Figure 11:</b> Standard calibration curve of mebendazole-----	<b>55</b>
<b>Figure 12:</b> Standard calibration curve of mebendazole for LOD and LOQ-----	<b>55</b>
<b>Figure 13:</b> Standard calibration curve of mebendazole for solubility of MBZ in oils-----	<b>56</b>
<b>Figure 14:</b> Saturation solubility of mebendazole in oils-----	<b>57</b>
<b>Figure 15:</b> Relation btwn Standards Conc. ( $\mu\text{g}/\text{ml}$ ) Vs Area / for solubility of MBZ in surfactant and co-surf-----	<b>58</b>

<b>Figure 16:</b> Saturation solubility of mebendazole in surfactants and co-surfactants-----	<b>59</b>
<b>Figure 17:</b> Formulations by experimental trials after a period of time. ME#1 and ME#5 were separated while other formulations were clear and monophasic---	<b>61</b>
<b>Figure 18:</b> Some formulations after prepared. ME#1 and ME#5 were turbid while ME#4 and ME#6 were clear-----	<b>61</b>
<b>Figure 19:</b> Ternary phase diagram for Oleic acid/T80: BL-----	<b>68</b>
<b>Figure 20:</b> Ternary phase diagram for Oleic acid/T80: N-methyl pyrrolidone---	<b>68</b>
<b>Figure 21:</b> Ternary phase diagram for Oleic acid/RH40: N-methyl pyrrolidone-----	<b>69</b>
<b>Figure 22:</b> Ternary phase diagram for IPP/T80: DEGME-----	<b>69</b>
<b>Figure 23:</b> Saturation solubility of mebendazole in various microemulsion formulation trials-----	<b>70</b>
<b>Figure 24:</b> Assay % of the selected formulations of microemulsion with MBZ at room temperature-----	<b>81</b>
<b>Figure 25:</b> In vitro cumulative permeation profile of formulation ME#4 obtained from studies in Franz Diffusion Cells using polyamide membrane-----	<b>86</b>
<b>Figure 26:</b> In vitro cumulative permeation profile of formulation ME#6 obtained from studies in Franz Diffusion Cells using polyamide membrane-----	<b>89</b>
<b>Figure 27:</b> In vitro cumulative permeation profile of formulation ME#7 obtained from studies in Franz Diffusion Cells using polyamide membranes-----	<b>92</b>

<b>Figure 28:</b> In vitro cumulative permeation profile of formulation ME#8 obtained from studies in Franz Diffusion Cells using polyamide membranes-----	<b>95</b>
<b>Figure 29:</b> In vitro cumulative permeation profile of formulations ME#4, ME#6, ME#7 and ME#8 obtained from studies in Franz Diffusion Cells using polyamide membrane-----	<b>96</b>
<b>Figure 30:</b> In vitro cumulative permeation profile of formulation ME#4 obtained from studies in Franz Cell using Start-M membranes-----	<b>100</b>
<b>Figure 31:</b> In vitro cumulative permeation profile of formulation ME#6 obtained from studies in Franz Cell using Start-M membranes-----	<b>103</b>
<b>Figure 32:</b> In vitro cumulative permeation profile of formulation ME#7 obtained from studies in Franz Cell using Start-M membranes-----	<b>106</b>
<b>Figure 33:</b> In vitro cumulative permeation profile of formulation ME#8 obtained from studies in Franz Cell using Start-M membranes-----	<b>109</b>
<b>Figure 34:</b> In vitro cumulative permeation profile of formulations ME#4, ME#6, ME#7 and ME#8 obtained from studies in Franz Diffusion Cells using Start-M membrane-----	<b>110</b>



### List of abbreviations and symbols

<b>Abbreviation</b>	<b>Description</b>
<b>BCS</b>	Biopharmaceutical Classification System
<b>BL</b>	Benzyl alcohol
<b>C<sub>d</sub></b>	Concentration of drug in the donor compartment
<b>Conc.</b>	Concentration
<b>Co-surf.</b>	Co-surfactant
<b>D</b>	Diffusion coefficient
<b>d</b>	Density
<b>DEGME</b>	Diethyleneglycol -mono ethylether
<b>DLS</b>	Dynamic light scattering
<b>EM</b>	Electron microscope
<b>FDC</b>	Franz diffusion cell
<b>FTC</b>	Freeze thaw cycle
<b>GI</b>	Gastrointestinal
<b>h</b>	Membrane thickness
<b>HLB</b>	Hydrophilic – lipophilic balance
<b>HPLC</b>	High performance liquid chromatography
<b>ICH</b>	International Council for Harmonisation of Technical Requirements for Pharmaceuticals for Human Use
<b>IPA</b>	Isopropyl alcohol

<b>IPP</b>	Isopropyl palmitate
<b>J<sub>ss</sub></b>	Steady state flux
<b>K</b>	Partition coefficient
<b>LOD</b>	Limit of detection
<b>LOQ</b>	Limit of quantitation
<b>Max.</b>	Maximum
<b>MBZ</b>	Mebendazole
<b>M.C.T</b>	Medium chain triglycerides
<b>ME</b>	Microemulsion
<b>Na<sub>2</sub>HPO<sub>4</sub></b>	Disodium phosphate
<b>O/W</b>	Oil in water
<b>P</b>	Permeability coefficient
<b>PAMPA</b>	Parallel Artificial Membrane Permeability Assay
<b>PEG</b>	Poly ethylene glycol
<b>Pyrrrol</b>	N-methyl pyrrolidone
<b>RH40</b>	Kolliphor® RH 40 (Polyoxyl 40 hydrogenated castor oil)
<b>RI</b>	Refractive index
<b>RPM</b>	Revolution per minute
<b>RT</b>	Room temperature
<b>SC</b>	Stratum corneum

<b>SD</b>	Standard deviation
<b>SEM</b>	Scanning electron microscope
<b>SLN</b>	Solid lipid nanoparticles
<b>SLS</b>	Sodium lauryl sulfate
<b>STDEV</b>	Standard Deviation
<b>t</b>	Flow time
<b>T80</b>	POE-20-sorbitan monooleate (Tween 80)
<b>TDDS</b>	Transdermal drug delivery system
<b>TEM</b>	Transmission electron microscopy
<b>T<sub>L</sub></b>	Lag time
<b>USA</b>	United States of America
<b>USP</b>	United States Pharmacopeia
<b>UV</b>	Ultra violet
<b>W/O</b>	Water in oil
<b>WHO</b>	World Health Organization

## List of Appendices

<b>Appendix 1:</b> Pseudo- ternary diagrams for some microemulsion formulations---	
-----	132
<b>Appendix 2:</b> Chromatograph of mebendazole using HPLC-----	134
<b>Appendix 3:</b> DLS report foe ME#8 using DLS Brookhaven Instruments-----	135
<b>Appendix 4:</b> Photos from work-----	136

## **Abstract**

Mebendazole is an essential drug against worms, roundworms, and hookworms. In recent years, anticancer activities of mebendazole have been reported, and that promoted us to develop a new dosage form for it.

However, the low water solubility of mebendazole makes it difficult to develop an oral dosage form an oral dosage form due to its very low bioavailability that may fail to achieve the required therapeutical effects. So, we were investigated delivering mebendazole topically as microemulsion because it is significantly enhanced the solubility of poorly water-soluble drugs by reducing the particle sizes of drug particles and then increasing the total surface area of particles.

In addition, microemulsion formulations of mebendazole can improve drug solubility by incorporating oil and surfactants in the formulations, and it would be beneficial as a topical anticancer drug for many types of cancer, especially Melanoma.

In this study, mebendazole were formulated as topical microemulsion and its permeation behavior was studied.

Mebendazole-loaded microemulsions for topical delivery were developed using oleic acid or isopropyl palmitate as the oil phase, Tween 80 or Kolliphor® RH40 as the surfactants, and N-methyl pyrrolidone, Diethylenglycol-mono- ethylether, isopropyl alcohol, benzyl alcohol, ethanol, and PEG 400 as the co-surfactants. The

pseudo-ternary phase diagrams were constructed to determine the composition of microemulsion formulations. In this study, pharmaceutical development, physical and chemical characterization, stability and in vitro permeation studies using synthetic membranes and Franz diffusion cells were performed. In terms of droplet size, visual appearance, and assay, the microemulsion formulations were stable over the period of study.

The mebendazole permeation flux of microemulsion formulations ME#4 (Oleic acid: T80/ Pyrrol 3:7), ME#6 (IPP: T80/DEGME 3:7), ME#7 (Oleic acid: RH 40/ Pyrrol 1:9), and ME#8 (Oleic acid: RH 40 / Pyrrol 3:7) through polyamide membrane was comparatively greater than mebendazole permeation flux of microemulsion formulations through Start-M membrane using Franz diffusion cells and phosphate buffer pH 7.4 +20% v/v PEG 400 as receptor medium for 5 hours.

In the permeation experiments using Start-M<sup>®</sup> membrane, ME#4 which has the highest ratio of oleic acid as oily phase showed the highest permeation flux of mebendazole (0.0042 mg/cm<sup>2</sup>/h) at 5 hours, followed by ME#6 which has a high ratio of isopropyl palmitate as oily phase , then ME#8 which contains less ratio of oleic acid than ME#4 , and ME#7 which has the lowest ratio of oleic acid.

Since formulation ME#4 (Oleic acid: T80/ Pyrrol 3:7) containing the highest oleic acid revealed a good in vitro release and permeation of mebendazole, ME#4 was

known to be the best-suited formulation amongst all for delivery of mebendazole across the skin safely and thus can be possibly used as an alternative delivery route for administration of mebendazole.

These preliminary results indicate the promise of microemulsion formulations for topical delivery of mebendazole.

## المخلص

يعتبر الميبندازول من أهم الأدوية المستخدمة لمعالجة الديدان، كالدودة الشريطية والخطافية. بالإضافة إلى فعاليته ضد السرطان و التي تم اثباتها في الدراسات خلال السنوات الأخيرة. و لذلك فإن سميته المنخفضة وتأثيره الفعال ضد السرطان قادنا لتطوير تركيبات جديدة له لاستخدامه لعلاج السرطان، و لكن ذائبته القليلة بالماء تشكل عقبة أمام تطوير مستحضرات فموية له؛ إذ أنها تؤدي إلى توافر حيوي ضعيف يقود لعدم تحقيق المطلوب وفشل العلاج. لذلك بحثنا عن توصيل الميبندازول عن طريق الجلد بتركيبة نانوية. حيث أنها تعمل على زيادة الذائبية بشكل ملحوظ للمواد قليلة الذوبان بالماء من خلال تقليل حجم الجزيئات وزيادة مساحة سطحها. و قد تم تحضير مستحضرات مايكروية موضعية؛ إذ أنها تحسن ذائبية الدواء من خلال مزج الزيت والمواد الخافضة للتوتر السطحي في هذه التركيبات. وهذا سيكون مفيداً كدواء موضعي مضاد لأنواع مختلفة من السرطان.

و قد تم تطوير تركيبات الميبندازول المايكروية الموضعية باستخدام حمض الزيت (الأوليك) أو إيزوبروبيل بالميتات للطور الزيتي وعديد السوربات (توين 80) والـ "كاليفور 40 RH" كمواد خافضة للتوتر السطحي بالإضافة إلى ميثيل بيروليدون و ثنائي ايثيلي غلايكول احادي ايتل ايثر والأيزوبروبانول والكحول البنزلي والإيثانول والبولي ايثيلين جلايكول 400 كمواد فاعلة للسطح (co-surfactant). وتم إنشاء مخطط pseudo-ternary phase diagrams لتحديد نسب تركيبات المستحلب المايكروي.

في هذا البحث، تم إجراء تطوير صيدلاني لدواء الميبندازول، و دراسة الخصائص الكيميائية والفيزيائية والثباتية الدوائية له بالإضافة إلى دراسة نفاذيته باستخدام أغشية اصطناعية و جهاز فرانز. وقد تبين ثبات الدواء خلال فترة الدراسة من حيث حجم القطرات، والمظهر البصري، وفحص الفرز للمادة الفعالة.



و تم اختيار 4 تركيبات مختلفة للمستحلب المايكروي لدراسة نفاذية الميبيندازول فيها باستخدام جهاز فرانز و أغشية اصطناعية . و هي ME#4 (Oleic acid: T80/ Pyrrol 3:7) و ME#6 (IPP: T80/DEGME 3:7) و ME#7 (Oleic acid: RH 40/ Pyrrol 1:9) و ME#8 (Oleic acid: RH 40 / Pyrrol 3:7). حيث كان التدفق من خلال غشان البولي أميد لجميع التركيبات أعلى من التدفق من خلال غشاء Start-M® خلال دراسة نفاذية الميبيندازول في محلول الفوسفات pH 7.4 + 20% PEG 400 v/v لمدة 5 ساعات .

وقد وجد أن أعلى تدفق من خلال غشاء Start-M® كان لتركيبة المستحلب المايكروي (ME#4) و التي تحتوي على أعلى نسبة لحمض الزيت (الأوليك) مقارنة بباقي التركيبات المختارة حيث يساوي (0.0042 ملغم/سم<sup>2</sup>/ساعة) بعد 5 ساعات من دراسة النفاذية. يتبعه التدفق لتركيبة المستحلب المايكروي (ME#6) و التي تحتوي على نسبة عالية من الأيزوبروبيل بالمينات كطور زيتي ، ثم التركيبة (ME#8). و أقل تدفق كان للتركيبة (ME#7) و التي كانت تحتوي على أقل نسبة من حمض الزيت (الأوليك).

و بالإعتماد على النتائج السابقة، فإن تركيبة المستحلب المايكروي (ME#4) و التي تحتوي على أعلى نسبة من حمض الزيت (الأوليك) أظهرت افضل النتائج لتدفق الميبيندازول من خلال غشاء Start-M® و بالتالي تعتبر التركيبة (ME#4) أفضل تركيبة من بين جميع تركيبات المستحلب المايكروي التي تم فحصها لتوصيل الميبيندازول عبر الجلد بأمان ، وبالتالي يمكن استخدامه على أنه طريق توصيل بديل لإعطاء الميبيندازول.

و تشير هذه النتائج الأولية إلى نجاح تركيبات الميبيندازول المستحلبة المايكروية موضعياً، وتعطي وعداً لبحوث أخرى.

# Chapter 1

## Introduction

### 1.1. Transdermal drug delivery system (TDDS)

Transdermal drug delivery system (TDDS) is one of the controlled drug delivery systems that can deliver predetermined amount of a drug in a controlled aspect through the skin. There are three main routes of drug penetration including the appendageal, intercellular and transcellular routes. Some factors such as skin age, environmental and physicochemical factors must be considered while delivering drug through these routes. Transdermal drug delivery system (TDDS) has various advantages, like reduced side-effects, prolonged therapeutic effect, improved bioavailability, easy termination of drug therapy and better patient compliance .

*(Porwal 2012)*

One of the main objectives of transdermal drug delivery system (TDDS) is to achieve systemic medication through topical application on intact skin, so it is important to review the biochemical features and structure of the human skin.

### **1.1.1. Structure of the human skin**

The skin is the outer tissue that considered as one of the most extensive organs of our body. It covers an area of about 2 m<sup>2</sup> in an average human adult . *(Porwal 2012)*

It is a barrier between the human body and the external environment, and being the first line of defense against pathogenic microorganisms. Skin performs many vital functions including prevention of excess water loss from the body, protection of the body against exogenous physical and chemical factors. *(Boer et al. 2016)*

The skin can be divided into three layers: epidermis, dermis, and subcutaneous fat tissues. The epidermis is the outer layer of the skin that acts as a barrier against pathogenic microorganisms and protects the internal organs from external injuries. Its thickness approximately 150 µm and contains no blood vessels. It can be divided into four layers: stratum corneum, granular cell layer, prickle cell layer, and basal cell layer .*(Yagi and Yonei 2018)*

The dermis or the corium provides strength and elasticity to the skin, and contains tough connective tissue, hair follicles, and sweat glands with a thickness of 2000 - 3000 µm. It can be divided into three layers: the papillary layer, sub-papillary layer, and the reticular layer. *(Yagi and Yonei 2018)*

Subcutaneous tissues are a fatty layer that plays the role of energy storage and protect the body from the hotness or the coldness of the external environment, with a thickness of several mm depending on which part of the body it is located.

*(Yagi and Yonei 2018)*

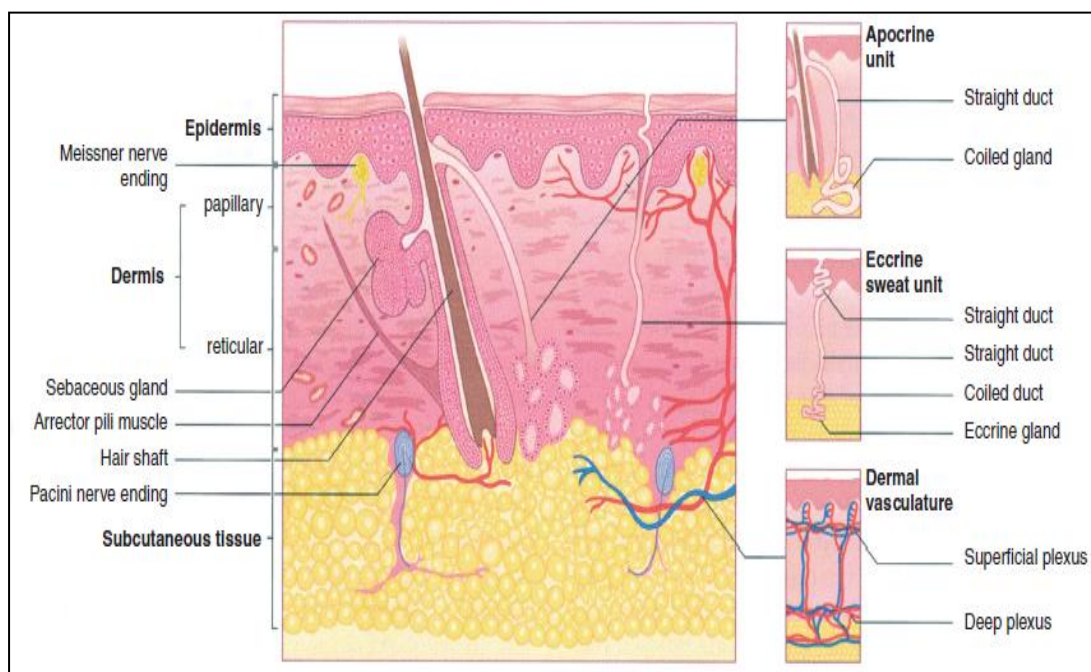


**Figure 1: Cross section of skin.** *(Yagi and Yonei 2018)*

### 1.1.2 Dermal and transdermal permeation pathway

Drug molecules penetrate through skin surface using two diffusional routes; the appendageal route ( through the hair follicles , the sweat ducts, and sebaceous glands) or the epidermal route directly across the stratum corneum.*(Rahman et al. 2011)*

### **1.1.2.1 Appendageal route:**

In the appendageal route, the transport of the molecules occurs via hair follicles, sweat glands, and sebaceous glands. The penetration carries out into approximately 0.1 % of the total skin area through the stratum corneum, so it is considered a minor route because of its relatively small area. *(Luís et al. 2016)*

### **1.1.2.2 Epidermal route:**

This route for drugs, which mainly cross-intact the stratum corneum by two potential micro routes, the paracellular and transcellular pathways. *(Sharma et al. 2011)*

#### **1.1.2.2.1 Transcellular:**

In the transcellular pathway, the transport of molecules occurs across the epithelial cellular membrane. These include active transport of polar and ionic compounds, passive transport of small molecules, transcytosis and endocytosis of macromolecules. *(Sharma et al. 2011)*

#### **1.1.2.2.2 Paracellular:**

In the paracellular pathway, the transport of molecules occurs around or between the cells. Lipophilic drugs traverse the stratum corneum via the intercellular route, whereas, Hydrophilic drugs traverse the stratum corneum via the intracellular domains. However, most drugs permeate the stratum corneum by both routes. *(Sharma et al. 2011)*

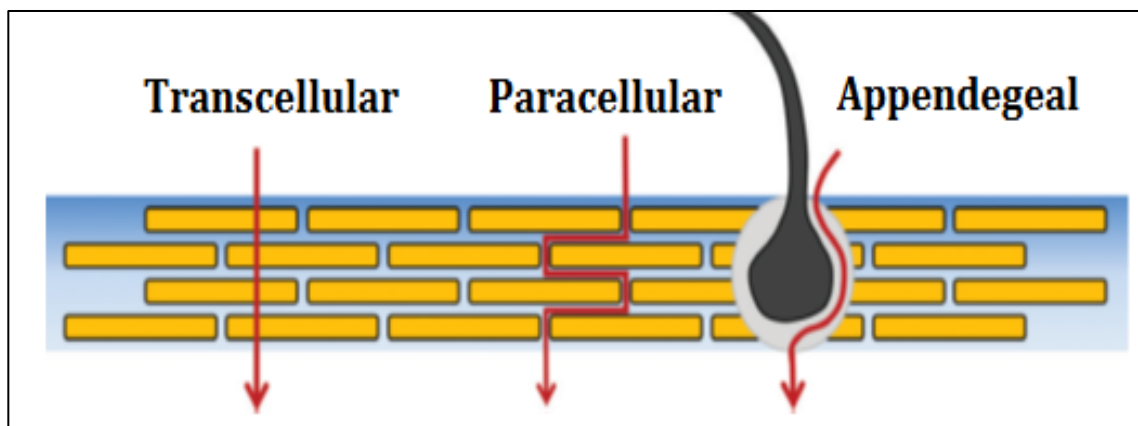
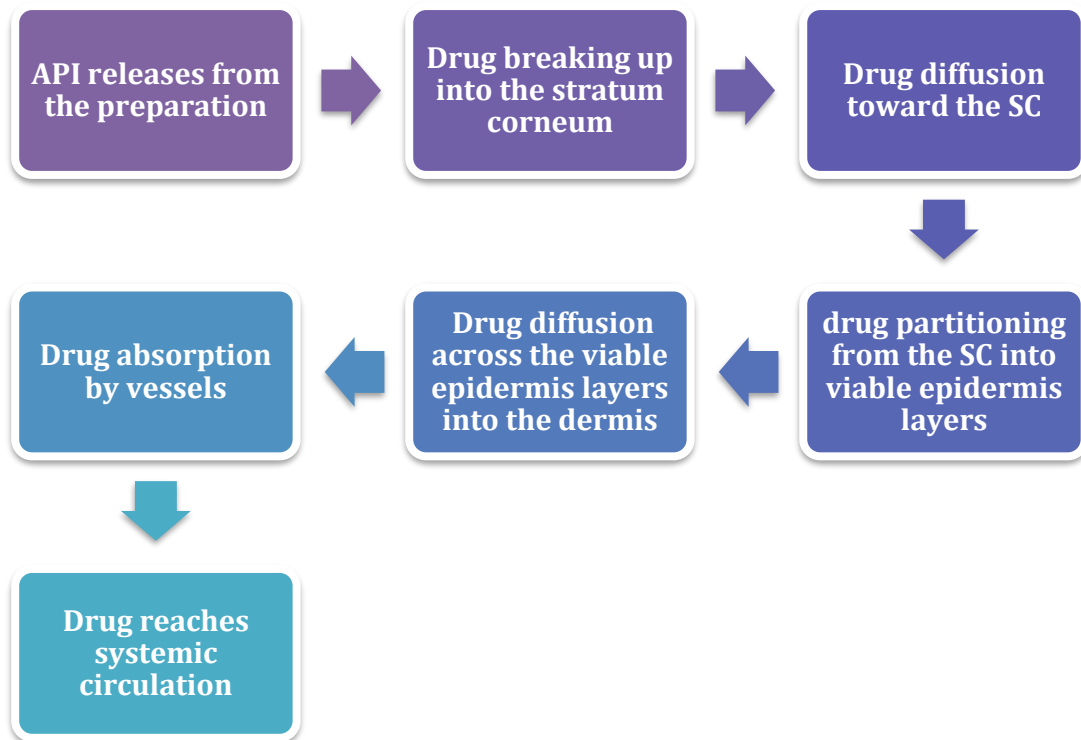


Figure 2: Schematic of dermal and transdermal permeation pathway. (Sharma *et al.* 2011)

### 1.1.3 Properties that influence transdermal drug delivery

The penetration of a drug through the SC and the drug release determined by the interactions between the skin, drug, and vehicle. However, the liberation of an API from a topical formulation and its transport to the systemic circulation is a complex process that includes the steps shown in Figure (3). (Zsikó *et al.* 2019)



**Figure 3 : Drug transport processes across the skin.**

The factors that affect the transdermal drug delivery can be divided into biological factors and physicochemical factors.

### ***1.1.3.1 Biological factors***

Biological factors have an impact on the penetration of a drug through the skin, these factors are: skin hydration level, skin condition, skin age, blood supply, skin metabolism, and regional skin site. *(Marwah et al. 2016)*

As the skin hydration level increases, the permeability of the skin may be improved. Skin age also affects the permeability, where damaged skin and baby skin have higher permeability. *(Zsikó et al. 2019)*

### **1.1.3.2 Physicochemical factors**

There are many physicochemical factors that can affect the penetration of drug through the skin such as : skin hydration , diffusion coefficient , drug concentration , molecular size , molecular shape, temperature, and pH. *(Marwah et al. 2016)*

### **1.1.4 Ideal physicochemical properties for transdermal drug delivery**

We can conclude some physicochemical properties for drug molecules to be an ideal molecule and has the highest penetration. The properties are:

- An adequate solubility in water and lipid (1mg/ml).
- The molecular weight of a drug should be less than 1000 Daltons.
- The saturated solution should have pH between 5 to 9.
- The melting point of the drug should be less than 200°C.
- The drug should be non-irritating, potent, and having short half-life.

*(Rahman et al. 2011)*

### **1.1.5 Transdermal permeation enhancement techniques**

Using the penetration enhancers is altering the barrier property of the stratum corneum and facilitates the absorption of drugs. *(Rizwan et al. 2009)*



Penetration enhancers are classified into:

**1.1.5.1 *Physical enhancers:***

- Iontophoresis
- Microneedle-based devices
- Needleless Injection
- Ultrasound

**1.1.5.2 *Chemical enhancers:***

- Urea
- Azone
- Fatty acids
- Surfactants
- Essential oil, terpenes and terpenoids
- Cyclodextrins

**1.1.5.3 *Carriers and Vehicles:***

- Micro or nanocapsules
- Microemulsions
- Nanoemulsions
- Multiple emulsions
- Solid lipid nanoparticles (SLN)
- Liposome

### **1.1.6 Techniques and methods for modeling permeation / penetration through human skin**

Recently, more and more regulations and researches are available for dermal and transdermal absorption studies from the United States and Europe. These documents present rules on, descriptions of how to conduct dermal/ transdermal studies and how to perform dermal/transdermal absorption assays. *(Zsikó et al. 2019)*

The researchers suggested different techniques for modeling permeation and penetration through human skin, these techniques divided into two main types. The first type is quantitative techniques that include diffusion cells, tape stripping methods, and the Parallel Artificial Membrane Permeability Assay (skin-PAMPA). While the other type is qualitative techniques that include different spectroscopic and microscopic methods. *(Zsikó et al. 2019)*

#### **1.1.6.1 Diffusion cells**

In 1970, Dr. Thomas J. Franz developed the Franz diffusion cell model for pharmaceutical formulations and determined the relationships between API, formulations, and skin. *(Zsikó et al. 2019)* This model consists of three components; the donor, a membrane, and the receptor chamber. *(Gaddam et al. 2009)*

### **1.1.6.2 Franz diffusion cells (FDC)**

The evaluation of the permeation of formulations that are released through the skin as topical formulations is very critical; to establish bioavailability for the drug, and to achieve the highest possible permeability of the active ingredient. *(Salamanca et al. 2018)*

Different types of in vitro skin permeation apparatus can be used to measure the permeation rate of the drug released through the skin. One of these types is Franz diffusion cells, which have many advantages, such as (a) Possibility to use synthetic membrane or animal skin as membrane barrier (b) few handling of membranes (c) require a small amount of drug for analysis, and (d) inexpensive to use. *(Salamanca et al. 2018)*

The test that done by Franz diffusion cells determines the amount of API that has permeate the membrane at each time point.

#### **1.1.6.2.1 Components of Franz diffusion cell**

Franz diffusion cell composed of two main parts: donor chamber and receptor chamber separated by a membrane, as shown in Figure 4. *(Gaddam et al. 2009)*

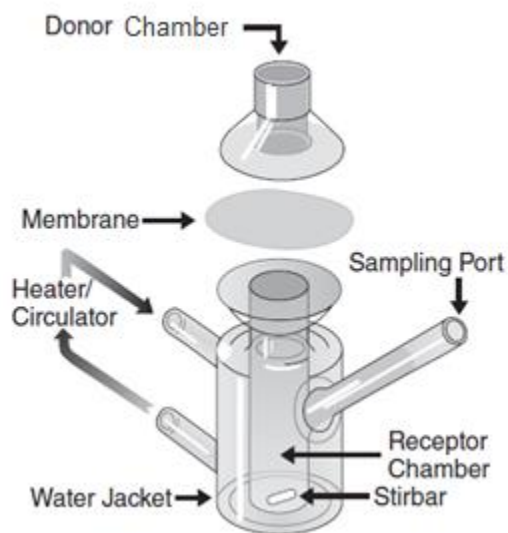


**Figure 4: Vertical Franz Diffusion cell.** (*Harunrasheed et al. 2011*)

The test of a topical formulation is applied to the membrane via the donor chamber, whereas the receptor chamber contains a homogeneous fluid from which samples are taken to analysis at predefined time intervals. (*Harunrasheed et al. 2011*)

#### **1.1.6.2.1.1 Donor chamber**

The donor chamber is the top component of the Franz diffusion cell. This chamber containing the active agent of the topical formulation. (*Fern et al. 2010*)

#### **1.1.6.2.1.2 Receptor chamber**

The receptor chamber of the Franz diffusion cell is the bottom component, and it is placed in circulation water in a water bath.

To mimic a real-life skin condition as much as possible, the temperature of the water bath should be 37°C to keep the temperature at the skin surface at 32°C. *(Harunrasheed et al. 2011)*

#### **1.1.6.2.1.3 Receptor fluid**

The fluid in the receptor chamber is called receptor fluid and it is manually sampled at specific time intervals, as well as, the concentration and temperature of this fluid kept homogenous by a magnetic stirring bar. *(Harunrasheed et al. 2011)*

#### **1.1.6.2.1.4 Membrane**

The membranes in Franz diffusion cell drug studies have two main functions: simulation of the human skin and quality control for the drug. *(Fern et al. 2010)*

The membrane can be either animal/human skin (biological membrane) or synthetic membrane. Hairless pig, rabbit, and mouse skin are examples of biological membranes, while cellulose, nylon, and polymethylsiloxane are examples of synthetic membranes. *(Zsikó et al. 2019)*

The advantages of synthetic membranes are low cost, easier setup than biological membrane, reproducibility, and absence of biological variability. *(Naik et al. 2016)* However, synthetic membranes for quality control should only act as a support to separate the topical formulation from the receptor fluid and should have minimum diffusion resistance to drugs. *(Fern et al. 2010)*

The membrane can be either full-thickness or split-thickness; moreover, the thickness of the skin affects the experimental results for drug permeation.

*(Harunrasheed et al. 2011)*

One of the synthetic membranes is Strat-M® membrane that engineered with the intent to mimic the structural and chemical characteristics found in the human skin. *(Uchida et al. 2015)*

Strat-M® membrane is composed of multilayers that create morphology of this membrane similar to that of human skin as shown in Figure 5. The top layer resembling the lipid chemistry of the human stratum corneum (SC) and supported by two layers of porous polyether sulfone (PES) on top of one single layer of polyolefin non-woven fabric support. *(Neupane et al.2020)*

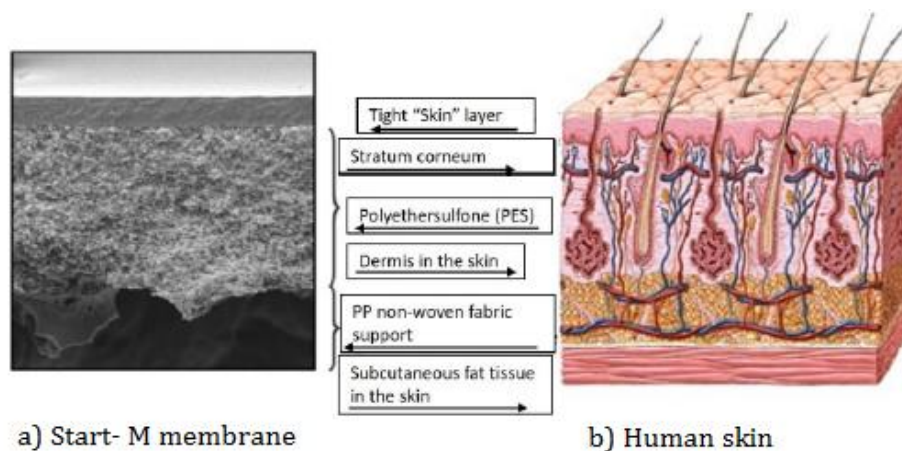


**Figure 5: A match in Morphology between Start- M membrane and human skin. *(Neupane et al.2020)***

To mimic different layers of human skin such as epidermis, dermis, and subcutaneous tissue, Strat-M® membrane layers are increasingly more porous and also increasingly larger in thickness. Besides, this synthetic membrane contains different lipids such as cholesterol, ceramides, free fatty acids, and other components in a specific ratio similar to what is found in the human stratum corneum. *(Haq et al. 2018)*

Recent studies showed that Strat-M® membrane has better correlations compared with other biological membranes such as rat and other animal skins. Moreover, it has equivalency to human skin for the skin permeation of many complex topical formulations such as cosmetics. *(Arce et al. 2020)*

The thickness of each Strat-M® membrane is approximately 300 µm, and its various advantages as its simplicity of handling, and low variability of lot -to-lot quality compared to biological membranes. *(Arce et al. 2020)*

#### **1.1.6.2.2 Parameters that affect drug release rate in FDC**

To obtain reliable permeation rate data, several parameters have to be considered for the design of the Franz diffusion cell test system, which is influenced by the drug release rate. These parameters are temperature, sink condition, speed of stirring, the volume of chambers, pH, the composition of receptor fluid, the solubility of drug, and the amount of API. *(Naik et al. 2016)*

### 1.1.6.2.3 Principle of diffusion through membrane using FDC

Mathematically, in Franz diffusion cells, skin absorption can be described by Fick's laws of diffusion. (*Bartosova and Bajgar 2012*)

Fick's first law of diffusion is specific to an infinite dose condition:

$$J = -D \frac{dC}{dx} \text{----- (1)}$$

where:

**J**: is the rate of transfer per unit area (flux) (g.cm<sup>2</sup>/h)

**D**: is the diffusion coefficient (cm<sup>2</sup>/h)

**C**: is the concentration gradient (g/cm<sup>3</sup>)

**x**: is the linear distance travelled (cm)

The negative sign means that the transfer of molecules is in the opposite direction to the concentration gradient. (*Bartosova and Bajgar 2012*), (*Ng et al. 2010*)

In diffusion process, steady state is an important condition, equation (1) of Fick's first law gives the flux/ area in steady state conditions of the flow, while the second law explains the change in concentration of diffusion with time at any distance (x) as shown in equation (2).

$$\frac{\partial C}{\partial t} = D \frac{\partial^2 C}{\partial x^2} \text{----- (2)}$$



From Fick's first law and Fick's second law of diffusion, we can derive the following equations:

$$J_{ss} = P \cdot C_d \text{----- (3)}$$

Where;

$J_{ss}$ : is the steady state flux per unit area.

$P$ : is the permeability coefficient for a given solute in a given vehicle.

$C_d$ : is the concentration of the solute in the donor compartment.

The permeability coefficient can only be used to predict the penetration rate of a drug at a given concentration from the same vehicle. In addition, it is independent of concentration and time, and it is chemical specific, species dependent, and site specific.

The permeability coefficient is kinetically first order rate constant that is related to the diffusion coefficient (D) by the equation:

$$D = \frac{h^2}{6 T_l} \text{----- (4)}$$

Where;

$D$ : is the diffusion coefficient.

$T_l$ : is the lag time.

**h:** is the thickness of the membrane.

The partition coefficient is a measure of how well penetrant can diffuse from a vehicle into the biological or synthetic membrane. Partition coefficient is:

$$K = \frac{P \cdot h}{D} \text{----- (5)}$$

Where;

**K:** is the membrane partition coefficient.

**P:** is the permeability coefficient for a given solute in a given vehicle.

**h:** is the thickness of the membrane.

**D:** is the diffusion coefficient.

We measure the cumulative amount of diffusant, *m*, that passes per unit area through the membrane as a function of time and we obtain the plot shown in Figure 6.

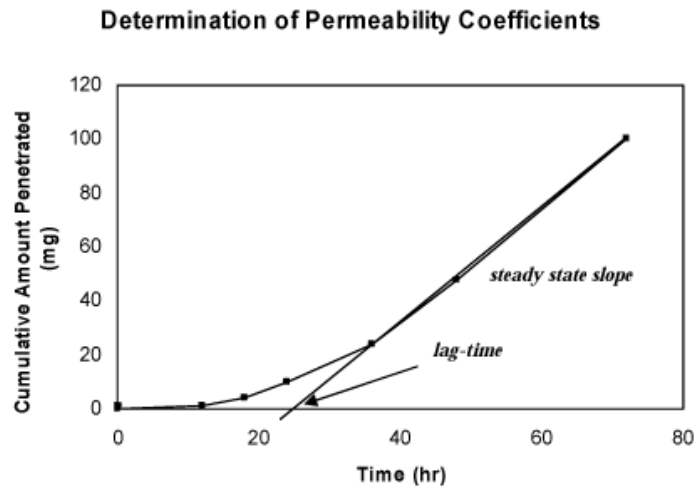


**Figure 6: Determination of steady state flux and lag-time.**

After prolonged times the plot has a straight line and a steady state flow is obtained. Intercept with x axis gives the lag time,  $T_L$  which can be expressed by the following equation:

$$T_L = h^2/6D \text{ ----- (6)}$$

The time it takes to permeate through the membrane and diffuse into the receptor fluid and then finally reach a steady state of diffusion is referred to as the lag time that can be calculated as the intercept with x-axes for the curve in (Figure 6).

## **1.2. Microemulsion**

Microemulsion is transparent and thermodynamically stable drug delivery system. It consists of an isotropic liquid mixture of oil, water, surfactant, and co-surfactant. Microemulsion can be used for hydrophilic drugs by solubilizing in the aqueous phase and can be used for lipophilic drugs by solubilized it in oil or oil-surfactant mixtures. It has several interesting characteristics such as; good thermodynamic stability, small droplet size, low viscosity, enhanced drug solubilization, ease of preparation, high diffusion and absorption rates through skin and high drug-loading capacity. These properties make microemulsion a powerful alternative carrier system for drug delivery. *(Iqbal and Hamdard 2018)*

Microemulsion has very low water/oil interfacial tension and very small droplets size (10 nm-200 nm). Besides, microemulsion is transparent as a result of the size of droplets that are less than 25% of the wavelength of visible light. *(Mishra, Panola, and Rana 2014)*

### **1.2.1 Advantages of microemulsion**

Microemulsions have many advantages such as:

- Improves the bioavailability of drug.
- Converts fat soluble molecules to stable water dispersions.
- Long shelf life.
- The drug-loading capacity is high.

- Increase the rate of absorption.
- Taste masking.
- Improve solubility of lipophilic drugs.
- Stable from pH 2-8 and at temperatures up to 110° C.
- Excellent thermodynamic stability.
- Ease of preparation.
- It acts as a super solvent.
- Suited for most routes of administration.

### **1.2.2 Disadvantages of microemulsion**

Although microemulsion has many advantages, it has some disadvantages such as:

- Using large amount of surfactants and co-surfactants.
- Limited solubilizing capacity for high melting substances.
- The stability of microemulsion is influenced by various environmental parameters such as pH and temperature.

### **1.2.3 Composition of microemulsion**

Microemulsion consists of transparent isotropic liquid mixture of oil, water, surfactant, and co-surfactant. (*Bhattacharya, and Mukhopadhyay 2016*)

### **1.2.3.1 Oil component**

The most vital component in the microemulsion is the oil because of its ability to solubilize the desired quantity of the lipophilic drugs. The oil component has an ability to penetrate, thus it influences curvature and swells the tail group region of the surfactant monolayer. *(Bhattacharya, and Mukhopadhyay 2016)*

The short chain oils permeate the tail group region to a greater extent compared with the long chain oils, which decrease effective HLB and causes the increase in the negative curvature. *(Bhattacharya, and Mukhopadhyay 2016)*

Oil component has many types; unsaturated fatty acids as oleic acid and linoleic acid, saturated fatty acids as lauric, myristic and capric acid, and fatty acid esters such as methyl esters, ethyl esters of lauric, and oleic acid. *(Kale and Deore 2017)*

### **1.2.3.2 Aqueous phase**

Water is the most commonly aqueous phase used in the microemulsion; it can have the hydrophilic active ingredients and the preservatives. In some researches, a buffer solution is used as the aqueous phase. *(Kumar et al. 2011)*

The pH of the aqueous phase is very important and affects the phase behavior of microemulsions so it should be adjusted.

### **1.2.3.3 Surfactant**

Surfactants provide a flexible film that can readily form around the small droplets and reduce the surface tension to a very small value to aid in dispersion.

Surfactants should have appropriate curvature to form a correct curvature on the interfacial region.

The types of surfactants are ionic, non-ionic or amphoteric. The most type of surfactant that can be used in microemulsion is non-ionic because it has good cutaneous tolerance. *(Kumar et al. 2011)*

- **Hydrophilic – lipophilic balance (HLB)**

The Hydrophilic-Lipophilic balance of a surfactant expresses the balance between the hydrophilic and the lipophilic parts of an amphiphilic molecule. In addition, the HLB system was defined over 60 years ago first by Griffin and was later expanded by Davies. *(Muzaffar, Singh, and Chauhan 2013)*

Every surfactant has an HLB value of between 0 and 20, (0 being the oil soluble / very water insoluble) and (20 being the oil insoluble / completely water soluble). Surfactants have variable properties and applications from wetting to solubilizers depending on their HLB value.

#### ***1.2.3.4 Co-surfactants***

Generally, single-chain surfactants are unable to reduce the oil in water (o/w) interfacial tension sufficiently, thus co-surfactants such as propylene glycol, PEG, N-methyl pyrrolidone and benzyl alcohol must be used to allow the interfacial film sufficient flexibility and help to take up different curvatures required to form microemulsion. *(Kale and Deore 2017)*

### **1.2.4 Types of microemulsion**

Microemulsions have three types: oil in water microemulsion (O/W), water in oil microemulsion (W/O) and bi-continuous microemulsion. In these types, the interface is stabilized by an adequate combination of surfactants and co-surfactants. *(Muzaffar, Singh, and Chauhan 2013)*

#### ***1.2.4.1 Oil in water microemulsion (O/W)***

In this type droplets are dispersed in the continuous aqueous phase as water, increases temperature stability, and can be used as carriers for many organic compounds.

#### ***1.2.4.2 Water in oil microemulsion (W/O)***

In this type water droplets are dispersed in the continuous oil phase.

#### ***1.2.4.3 Bi-continuous microemulsion***

In this type micro domains of oil droplets and water droplets are inter dispersed in the system. So, water and oil both are continuous phases. It is like sponge and may exist as hexagonal liquid crystal structure.



## 1.2.5 Phase diagram study

### 1.2.5.1 Pseudo-ternary phase diagram

Pseudo ternary phase diagrams of the mixtures of water, oil, and surfactant/co-surfactants are constructed at fixed surfactant/co-surfactant weight ratios. Besides, ternary phase diagrams are obtained by mixing of all components, which shall be weighed, then titrated with water and stirred well at room temperature.

*(Mishra, Panola, and Rana 2014)*

The formation of a monophasic microemulsion system or biphasic system is determined by visual inspection. If the mixture is turbid then followed by phase separation, the mixture considered as biphasic system. However, the sample considered as monophasic if its transparent mixture and clear after stirring. Moreover, the area covered by the samples points in the phase diagram is considered as the microemulsion region as shown in Figure 7. *(Mishra, Panola, and Rana 2014)*

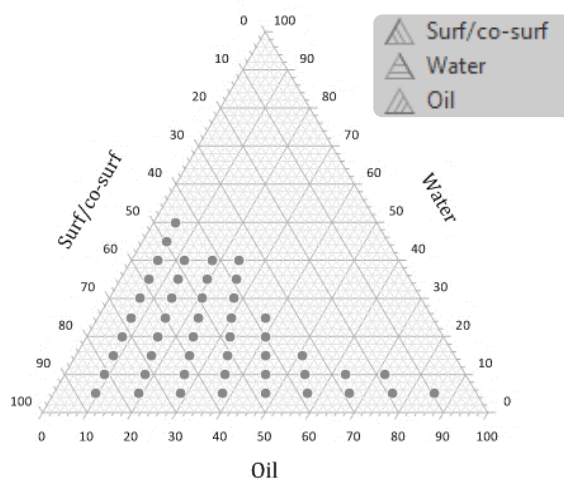


**Figure 7: Pseudo-ternary phase diagram for microemulsion.**

## 1.2.6 Preparation of microemulsion

### 1.2.6.1 Phase titration method

Spontaneous emulsification method depicted with the help of phase diagrams. By mixing of all components at once and dilution of an oil-surfactant mixture with water to make water in oil microemulsion or dilution of a water surfactant mixture with oil to make oil in water microemulsion. (*Bhattacharya, and Mukhopadhyay 2016*)

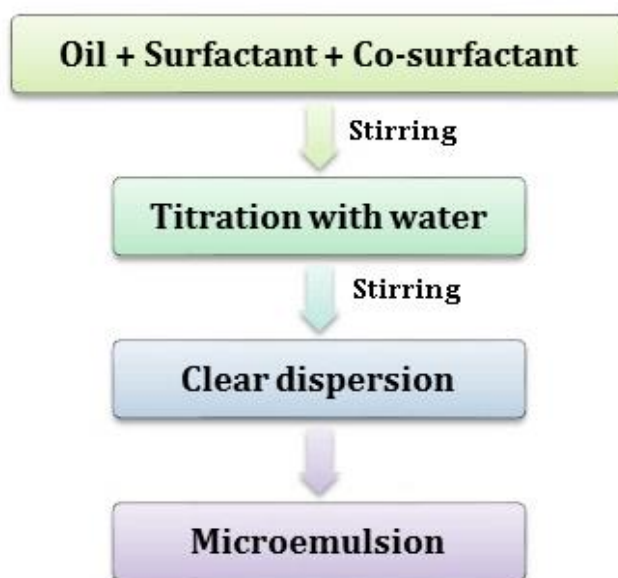


Figure 8 : Aqueous Phase Titration Method.

### 1.2.6.2 Phase inversion method

This method occurs by addition excess of the dispersed phase or by changing the temperature. The phase of microemulsion inverse by changing the temperature from oil in water (o/w) at low temperatures to water in oil (w/o) at higher

temperatures. As well as, these methods make use of changing the spontaneous curvature of the surfactant. *(Kumar et al. 2011)*

### **1.2.7 Factors affecting microemulsion**

Microemulsion is affected by different factors such as:

#### ***1.2.7.1 Temperature:***

Temperature is extremely important in determining the effective head group size of nonionic surfactants. At low temperature, they are hydrophilic and form normal (o/w) system.

At higher temperature, they are lipophilic and form (w/o) systems. At an intermediate temperature, microemulsion coexists with excess water and oil phases and forms bi-continuous structure. *(Muzaffar, Singh, and Chauhan 2013)*

#### ***1.2.7.2 Packing ratio:***

The type of microemulsion determine by The HLB of surfactant through its influence on molecular packing and film curvature.

#### ***1.2.7.3 Nature of surfactant and co-surfactant***

The type of microemulsion depends on the nature of surfactant. Surfactant contains lipophilic tail group and hydrophilic head group. The areas of these groups, which are a measure of the differential tendency of oil to swell the tail area and water to swell head group are important for specific formulation when

estimating the surfactant HLB in a particular system. *(Muzaffar, Singh, and Chauhan 2013)*

#### **1.2.7.4 Chain length**

Longer chain co-surfactant favors (w/o), while shorter chain co-surfactant becomes more hydrophilic and favors (o/w) because it gives positive curvature effect and swells the head region more than tail region. *(Bhattacharya, and Mukhopadhyay 2016)*

#### **1.2.7.5 Property of oil phase**

The oil component has ability to penetrate and swell the tail group region of the surfactant monolayer so it influences curvature.

Short chains oils increase the negative curvature by penetrating the lipophilic group region to a great extent. *(Muzaffar, Singh, and Chauhan 2013)*

#### **1.2.7.6 Water content**

Diluting the mixture of microemulsion with water may increase dissociation and leads to an (o/w) system. *(Muzaffar, Singh, and Chauhan 2013)*

#### **1.2.7.7 pH**

The pH sensitive surfactants such as alkaline or acidic surfactants are influenced by the change in the pH. The phase behavior can be seen from w/o to o/w by increasing the pH when the carboxylic acids and the amines are present. *(Bhattacharya, and Mukhopadhyay 2016)*

### ***1.2.7.8 Salinity***

The droplet size increases when the salinity is less in the case of o/w microemulsion and causes the oil to solubilize more. (*Bhattacharya, and Mukhopadhyay 2016*)

## **1.2.8 Characterization of microemulsion**

The viscosity, droplet size, density, turbidity, pH, refractive index and phase separation measurements shall be performed to characterize the microemulsion using different methods as electron microscopy, scattering techniques, rheology, and conductivity.

### ***1.2.8.1 Electron microscopy (EM)***

Electron microscopy (EM) techniques were instrumental in the description of microemulsions by Schulman in 1959. Electron microscopy can be used to differentiate microemulsions and macroemulsions. (*Oberdisse and Hellweg 2017*)

Clear isotropic one-phase systems are identified as microemulsions while opaque systems showing bi-phase system by using:

- a) Scanning electron microscope (SEM)
- b) Transmission electron microscopy (TEM)

### ***1.2.8.2 Scattering techniques***

Scattering techniques used to measure the droplet size of microemulsion. It have found applications in studies of microemulsion structure, particularly in case of dilute mono-disperse spheres such as *(Oberdisse and Hellweg 2017)* :

#### **a) Dynamic light scattering (DLS)**

Dynamic light scattering (DLS) is the widespread technique used to measure particle size of emulsion and microemulsion between 3 and 5000 nm. *(Julian McClements and Dungan 1995)*

This technique measures the particle size based on the frequency shift of light scattered by particles of sample in solution during their random motion. This means the size of a particle is related to its velocity via the diffusion coefficient and calculated by measuring the frequency shift. *(Julian McClements and Dungan 1995)*

#### **b) Static light scattering (SLS)**

#### **c) Small angle X-ray scattering (SAXS)**

#### **d) Small angle neutron scattering (SANS)**

### ***1.2.8.3 Rheology***

Rheological behavior of the microemulsion can be observed by viscometer. Changes in the rheological characteristics determine the microemulsion region and its separation from another region.

#### ***1.2.8.4 Conductivity***

The electrical conductivity of microemulsion can be measured using a conductometer.

### **1.2.9 Accelerated stability studies for microemulsion**

#### ***1.2.9.1 Freeze-thaw cycle (FTC)***

The microemulsion is stored at (25°C) for 24 hours then stored at (-15°C) for 24 hours. This procedure is repeated 3 times to notice the change in the stability parameters. *(Kumar et al. 2011)*

#### ***1.2.9.2 Centrifugation stress testing***

To check the physical instabilities of microemulsion such as creaming, phase inversion, cracking, phase separation, and the aggregation of the formulation, centrifugation of the microemulsion is done for 30 minutes at the speed of 5000-10,000 rpm. *(Bhattacharya, and Mukhopadhyay 2016)*

### **1.2.10 Long term stability studies for microemulsion**

Based on the ICH guidelines, the stability of microemulsion can be examined for 6 months. By storing the microemulsions under ambient conditions and testing after 1, 3, and 6 months. *(Bhattacharya, and Mukhopadhyay 2016)*

#### **1.2.10.1 Determination of the globule size**

The size of the globules is very important and can be determined by the light scattering method such as photomicroscope method or by light dynamic scattering analytical instrument.

#### **1.2.10.2 Determination of thermal stability**

20 ml of the microemulsion loaded with drugs were stored in a 25 ml transparent volumetric container at three different temperatures, i.e. 4°C, 25°C, and 40°C for 1 month (*Bhattacharya, and Mukhopadhyay 2016*). Then the samples were taken out at definite intervals of time to inspect visually to check any physical changes such as turbidity, coalescence, the loss of clarity and to determine the loss of the aqueous phase which is an important aspect of the stability of the microemulsion. (*Bhattacharya, and Mukhopadhyay 2016*)

#### **1.2.10.3 Determination of pH of the microemulsion**

Different samples of the microemulsions are taken in the sample tubes to check the pH of each sample using a micro pH meter. The pH of the formulation affects the stability and the bioavailability of the microemulsion and determines its permeation site. (*Bhattacharya, and Mukhopadhyay 2016*)



### 1.2.11 In vitro skin permeation studies

To check the permeation of the drug through the skin, skin penetration studies are conducted using Franz diffusion cell and synthetic or natural skin. *(Salamanca et al. 2018)*

## 1.3 Mebendazole

### 1.3.1 Description

Mebendazole or methyl (5-benzoyl-1H-benzimidazol-2-yl) carbamate is a benzimidazole anthelmintic with molecular mass 295.293 g/mol, its chemical formula is  $C_{16}H_{13}N_3O_3$ . *(Popović et al. 2017)*

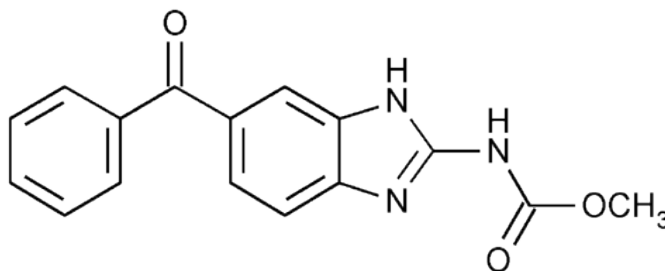


Figure 9: Chemical structure of mebendazole. *(USP 23)*

#### 1.3.1.1 Solubility

Mebendazole is white to slightly yellow powder with a pleasant taste. It is practically insoluble in water (35.4 mg/L at 25°C), ether, ethanol, and chloroform. on the other hand, MBZ is soluble in formic acid. *(Hamilton and Rath 2017)*

### **1.3.1.2 Polymorphs**

Mebendazole has three polymorphs A, B and C with different properties. For instance, polymorph C is the pharmaceutically preferred, while polymorph B has higher toxicity between the three polymorphs, and polymorph A has low solubility and doesn't present the required effect. *(da Silva et al. 2019)*

### **1.3.1.3 Octanol/ water partition coefficient and dissociation constant**

Mebendazole is highly lipophilic (Log p 2.83), and the dissociation constant (pKa) for it is 3.6. *(Poturcu and Demiralay 2019)*

### **1.3.1.4 Melting point**

The melting point for MBZ is about 288.5 °C. *(Popović et al. 2017)*

### **1.3.1.5 Biopharmaceutical Classification System (BCS)**

Mebendazole considered as either class II BCS (low solubility / high permeability) or class IV BCS (low solubility / low permeability). *(Ghafil et al. 2017)*

### **1.3.1.6 Method of manufacturing**

Mebendazole is synthesized by the reaction of 3,4-diaminobenzophenone hydrochloride with N-carboxymethyl-S-methylisothiourea. *(O'Neil, M.J 2001)*

### **1.3.1.7 Mode of action**

The WHO listed orally administered mebendazole as an essential drug against worms; roundworms and hookworms. Mebendazole has a low bioavailability of

2-10 % because it's poorly absorbed into the bloodstream (*Luder PJ 1986*). Moreover, the biological half-life of this drug is 3-6 hours in patient with normal hepatic functions, and the metabolism is primarily hepatic with 5-10 % appearing in the urine. (*Hamilton and Rath 2017*)

### **1.3.2 Mebendazole as anti-cancer**

In recent years, anticancer activities of mebendazole have been reported, and preclinical studies showed that mebendazole prevents the growth of metastatic and malignant tumors such as melanoma, carcinoma and acute myeloid leukemia. Mebendazole can induce the depolymerization of microtubules in neoplasms and newly formed vasculature and hence stopping tumor growth. (*Popović et al. 2017*)

#### **1.3.2.1 Treating melanoma with mebendazole**

The most aggressive form of skin cancer is Melanoma, with a high propensity to metastasize. In the last 20 years, the lifetime risk of an individual in the USA developing melanoma has doubled. Because of the risk of developing melanoma increases with UV exposure. (*Doudican et al. 2013*)

Before 10 years, the in vitro activity of mebendazole against chemo-resistant melanoma cell lines was assessed. From ten compounds, mebendazole had the greatest inhibitory effect against the melanoma and was selected for more detailed analysis based on its relative lack of toxicity and well characterized pharmacokinetics. (*Pantziarka et al. 2014*)

## Chapter 2

### Problem, Objectives and work plan

#### 2.1 Problem

The low toxicity of mebendazole and its potent anticancer effect have promoted us to develop it in a new dosage form. However, the low water solubility of mebendazole makes it difficult to develop an oral dosage form due to its very low bioavailability that may fail to achieve the required therapeutical effects. (*Yulan Qi 2008*)

The other choice is parenteral dosage form that does not have the problem of mebendazole absorptivity in the GI tract, but the low water solubility of mebendazole requires co-solvent vehicles which may cause severe toxicity and which is not acceptable for clinical use.

So, we will investigate delivering mebendazole topically as nano-formulation because it is significantly enhanced the solubility of poorly water-soluble drugs by reducing the particle sizes of drug particles and then increasing the total surface area of particles.

In addition, microemulsion formulations of mebendazole can improve drug solubility by incorporating oil and surfactants in the formulations, and it would be beneficial as a topical anticancer drug for many types of cancer, especially Melanoma.

In our experiment, we are going to formulate mebendazole in a new topically formulation as microemulsion and we will try to optimize its permeation rate using Franz diffusion cells.

## **2.2 Objectives**

1. Application and development of HPLC analysis method to determine the content of mebendazole in topical dosage form and solution.
2. Studying the solubility of mebendazole in different oils, surfactants, and co-surfactants.
3. Preparation and evaluation of different mebendazole topical microemulsion formulations to select the appropriate ones for further testing in terms of stability and physicochemical properties.
4. Studying the permeability of topical mebendazole formulations by using Franz diffusion cell through synthetic membranes.
5. Analysis of data to determine the amount of mebendazole that penetrated the synthetic membranes during previous permeability experiments.

## 2.3 Work plan

The diagram below describes each step in the work plan of this thesis.

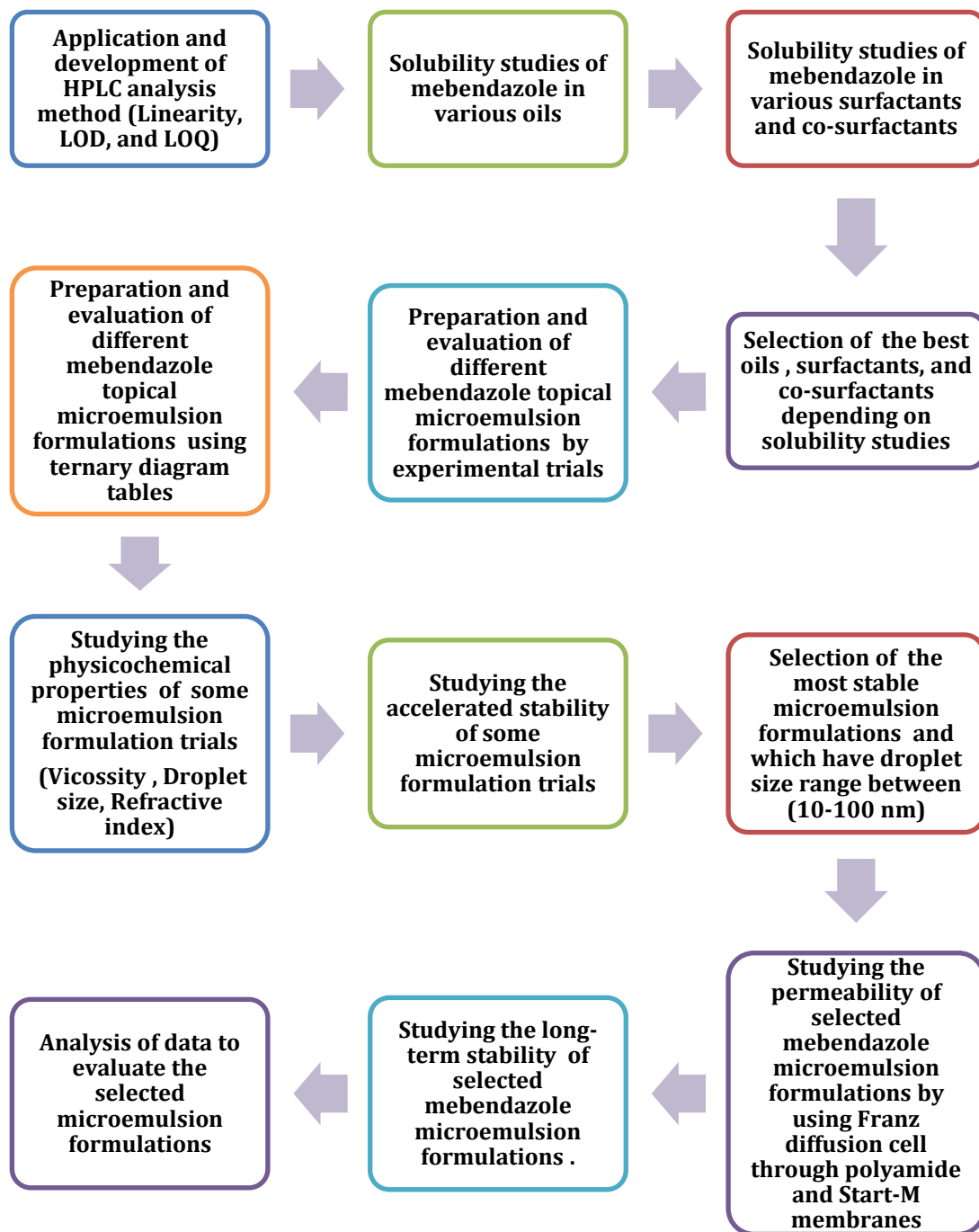


Figure 10: Thesis work plan.

## Chapter 3

### Methodology

#### 3.1 Materials

The reagents and materials used for this study were:

##### 3.1.1 Materials for formulation

Materials used in the study for formulation purposes are depicted in Table #1.

**Table 2: Materials for formulation and their function.**

<b>Material</b>	<b>Function</b>	<b>Grade</b>
Mebendazole	API	USP
Distilled water	Aqueous phase	USP
Kolliphor® RH 40	Surfactant	USP
Tween 80	Surfactant	USP
Oleic acid	Oil phase	USP
Isopropyl myristate	Oil phase	USP
Medium chain triglycerides (M.C.T)	Oil phase	USP
Isopropyl palmitate (IPP)	Oil phase	USP
(R)-(+)-Limonene	Oil phase	USP
PEG 400	Co-surfactant	USP
Ethanol	Co-surfactant	USP
Isopropyl alcohol	Co-surfactant	USP
Benzyl alcohol	Co-surfactant	USP
N-methyl pyrrolidone	Co-surfactant	USP
Diethyleneglycol -mono ethylether (DEGME)	Co-surfactant	USP

### 3.1.2 Materials for analysis

The following materials were used for analysis in this study

**Table 3:Materials used for analysis.**

<b>Material</b>	<b>Grade</b>
Sodium phosphate dibasic	Analytical grade
Acetonitrile	Analytical grade
Phosphoric acid	Analytical grade
Sodium hydroxide	Analytical grade
Formic acid	Analytical grade
Isopropyl alcohol	Analytical grade
Distilled water	Analytical grade
Potassium phosphate monobasic	Analytical grade
Methanol	Analytical grade

### 3.1.3 Membranes

Table 3 describes the synthetic membranes used in the permeation studies of microemulsion formulation trials.

**Table 4:Description of synthetic membranes.**

<b>Synthetic membrane</b>	<b>Polymer type</b>	<b>Thickness</b>	<b>Pore size</b>	<b>Diameter</b>	<b>Manufacturer</b>
Nylon 66	Polyamide	100 $\mu\text{m}$	0.45 $\mu\text{m}$	47 mm	SUPELCO, Bellefonte
Start-M <sup>®</sup>	Polyethersulfone and Polyolefin	300 $\mu\text{m}$	-	47 mm	Merck Millipore, Ireland



### 3.2 Equipment and tools

The equipment and tools used in the study are illustrated in Table 4.

**Table 5: Equipment and tools**

<b>Equipment</b>	<b>Type</b>
UV spectrophotometry	PerkinElmer, Lambda 25
HPLC/UV detector	Agilent Technologies (1200 Series)
Franz diffusion cell	Orchid Science, Model no. FDC-06
Vacuum filter	KNF lab, Laboport
Analytical balance	OHAUS, PIONEER no. ANB002)
Zetasizer DLS	Brookhaven Instrument
PH meter	HANNA instruments (PH/ORP meter)
Stop watch	Digital stop watch
Centrifuge with (BRK5424) Rotor	Centurion Science, Model: K2015R
Bath Sonicator	Elma, S 300H, Elmasonic
Refractometer	KRUSS Optronic GmbH, Model no. DR6000-T
Refrigerator	Beko (BER036)
Multi magnetic stirrer	VELP Scientifica no. MST019
Hot plate with magnetic stirrer	Thermo scientific
Micropipette	Multi-Volume Single Channel Micropipette

### **3.3 Methods**

#### **3.3.1 High performance liquid chromatography (HPLC) analysis**

Mebendazole quantification was performed using HPLC from Agilent Technologies (1200 Series), coupled to a UV detector. MBZ in samples was quantified using a modified U. S. Pharmacopeia method.

Chromatographic separation was achieved isocratically at room temperature with a Dr. Maisch 100 Å C8 column (125 mm x 4.6 mm, 5µm). The mobile phase consisted of 40% 0.05 M Disodium hydrogen phosphate + 60 % Acetonitrile (pH 5.2 with 1 N Phosphoric acid) and, was run at a flow rate of 1.0 mL/min. The ultraviolet-visible detection at 300 nm, the injection volume equal 20 µl and the run time was about 4 minutes.

#### **3.3.2 Preparation method for linearity, LOD, and LOQ**

To evaluate the linearity and range of HPLC method, different standard solutions were prepared by diluting the standard stock solution with the mobile phase in deferent concentrations of mebendazole: 5 ,10 ,20, 40, 60 ,80, and 100 µg/ml. Three injections from each concentration were analyzed under the same conditions.

Linear regression analysis was used to evaluate the linearity of the calibration curve by using the least square linear regression method

After that, seven serial dilutions were prepared (0.005 ,0.01 ,0.02, 0.04, 0.06 ,0.08, and 0.10 µg/ml) to construct calibration curve for LOQ and LOD.

Then all samples were assayed by the HPLC method for MBZ quantification, according to the methodology described in section (3.3.1).

### **3.3.3 Preparation method for solubility tests**

#### **3.3.3.1 The Saturation solubility of MBZ in oils**

An excess amount of mebendazole powder was added to 15 ml of various oils with shaken at 25° C ± 1 on a magnetic stirrer for 24 hours. Then the previous mixtures were centrifuged at 5000 rpm for 20 minutes at 25° C and filtered through a 0.45 µm nylon filter.

#### **3.3.3.2 The Saturation solubility of MBZ in surfactants and co-surfactant**

An excess amount of mebendazole powder was added to 15 ml of various surfactant and co-surfactant and shaken at room temperature on a magnetic stirrer for 24 hours. Then the previous mixture was centrifuged at 5000 rpm for 20 minutes at 25° C and filtered through a 0.45 µm nylon filter.

### **3.3.4 Analysis method for solubility tests**

- **Stock solution:** 100 mg of mebendazole was transferred to 100 ml volumetric flask and dissolved in 20 ml of formic acid then sonicated for about 3 min. Finally, the volume was made up to the mark by isopropyl alcohol.

After that, seven serial dilutions were prepared (0.005 ,0.01 ,0.02, 0.04, 0.06 ,0.08, and 0.10 mg/ml) to construct calibration curve.

- **Sample solutions:** About 4 g of the supernatant of each prepared solution was transferred to a 100 ml volumetric flask and diluted up to mark by the mobile phase.

Then all samples were assayed by the HPLC method for MBZ quantification, according to the methodology described in section (3.3.1).

### **3.3.5 Preparation method for microemulsion**

All microemulsion formulation trials were prepared according to the phase titration method into two stages, the first stage is an experimental stage that was used as an indicator for the best microemulsion formulations, while the microemulsion in the second stage was prepared using ternary diagram tables.

In the previous two stages, the oil phase was first combined with surfactant and co-surfactant, then water was added gradually using a micropipette with magnetic stirring at 1000-1500 rpm at room temperature until the system was transparent. These formulations were stirred for a sufficient time and the endpoint (onset of turbidity or phase separation) was visually monitored against a dark background. Finally, different quantities of mebendazole powder were added to the microemulsions with continuous stirring at 1000 – 1500 rpm for at least two hours.

The volume percent composition of the components of the microemulsion formulation trials (oil, surfactant /co-surfactant, and water) was calculated and plotted on triangular coordinates to construct pseudo-ternary phase diagrams. Then different formulations were selected from the microemulsion regions in the pseudo-ternary phase diagram.

### **3.3.6 Characterization and stability of microemulsion formulation trials**

The following tests were used to characterize the formulation trials:

#### **3.3.6.1 Type of microemulsion**

A dye solubility test using a water-soluble dye (Methylene Blue) and an oil-soluble dye (Sudan Red) were used to determine the type of microemulsion as oil in water (O/W) or water in oil (W/O) microemulsion.

Two drops of each dye were dropped into 2 ml microemulsion formulations. If an oil-soluble dye (Sudan Red) spreads faster than a water-soluble dye (Methylene Blue), it is water in oil (W/O) microemulsion. Contrariwise, if a water-soluble dye diffuses faster, it is oil in water (O/W) microemulsion. (*Xu et al. 2010*)

#### **3.3.6.2 Viscosity measurement**

The dynamic viscosities of microemulsion formulation trials were measured by a house-made viscometer using a 25 ml burette setup with PEG 400 as a

reference. The temperature was maintained at  $25 \pm 1$  °C throughout the experiments.

All microemulsion formulation trials were analyzed in triplicate. Where the viscosity values were calculated depending on flow time of each microemulsion formulation and referred to values of PEG 400 using equation (7).

$$\frac{h1}{h2} = \frac{d1 t1}{d2 t2} \text{-----(7)}$$

Where:

**h1:** Viscosity of PEG400 (cP)

**d1:** Density of PEG 400 (g/ml)

**t1:** Mean flow time of PEG 400 in seconds

**h2:** Viscosity of microemulsion sample (cP)

**d2:** Density of microemulsion sample (g/ml)

**t2:** Mean flow time of microemulsion sample in seconds

### 3.3.6.3 Refractive index measurement

The refractive index of each microemulsion formulation trial was determined using a refractometer (KRUSS Optronic GmbH, Model no. DR6000-T). The refractive index values prove the transparency of the microemulsion formulation trials.

#### **3.3.6.4 Droplet size and size distribution**

Dynamic light scattering technique (DLS) was used to determine the mean droplet size and size distribution of microemulsion formulation trials. Using a Particle Sizer and Zeta Potential Analyzer - NanoBrook Omni (Brookhaven instruments), which had a measuring range of 0.3 nm – 10  $\mu$ m.

The refractive index of each microemulsion formulation trial was used to determine the particle size of each microemulsion formulation trial. The size measurements of all formulations were carried out in triplicate, and the mean particle size of it was reported as volume mean diameter.

#### **3.3.6.5 Centrifugation stress test**

To check the physical instabilities of microemulsion such as creaming, cracking, phase separation, and the aggregation of the formulation, centrifugation of the microemulsion formulation trials was carried out at 25°C for 30 minutes at 5000 rpm using the centrifuge (Centurion Science, Model: K2015R).

#### **3.3.6.6 Freeze thaw cycle**

The microemulsion is stored at (25°C) for 24 hours then stored in the freezer at temperature about -15°C for 24 hours. This procedure is repeated 3 times to notice the change in the stability parameters such as mean droplet size and phase separation.

### 3.3.7 Permeation study of various microemulsion formulations of mebendazole using Franz diffusion cells

#### 3.3.7.1 Description of Franz diffusion cell apparatus

Vertical Franz diffusion cell apparatus (ORCHD science) with 6 cells was used in this permeation study of microemulsion samples. Each diffusion cell is made of two separated glass compartments, the upper glass part is a donor compartment with 20 mm mouth diameter, while the lower glass part is a water-jacketed receiver compartment with volume of 20 ml. Stainless steel clips were used to adjust the apparatus.

The apparatus equipped with circulating water pump to control the temperature in the range of (0°C – 60°C) with controller accuracy  $\pm 0.1^\circ\text{C}$ .

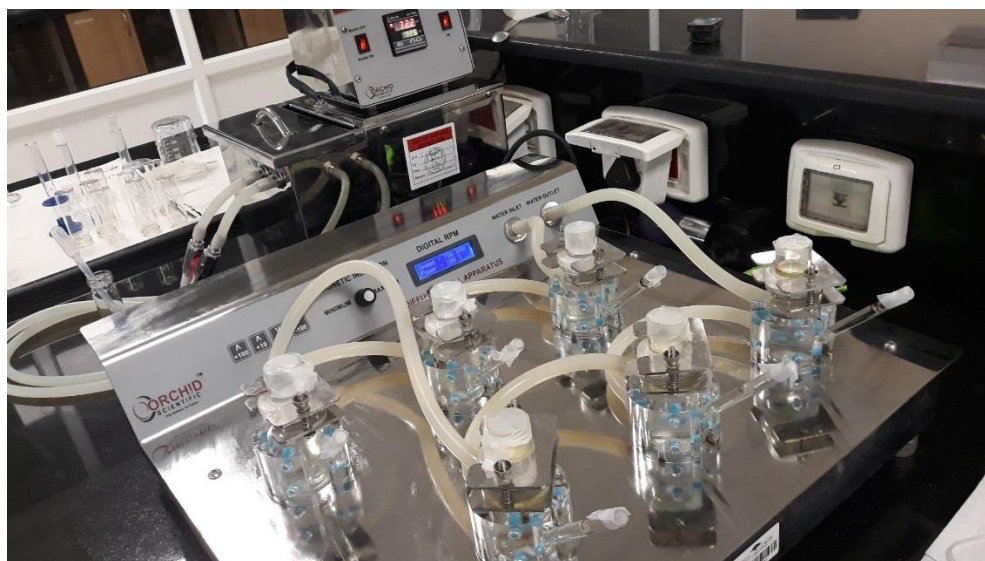


Figure 11: Vertical Franz diffusion cell apparatus (ORCHD science)



### 3.3.7.2 Preparation of receptor medium

Phosphate buffer was prepared by adding the substances presented in Table 5 and diluting with distilled water to 2 liters. The solution was stirred on a magnetic stirrer for 15 minutes.

The pH of the phosphate buffer was adjusted to 7.4 using a pH meter and it was kept at room temperature until use.

**Table 6 : chemicals used for phosphate buffer preparation.**

<b>Chemical</b>	<b>Weight (g)</b>
Potassium phosphate monobasic (99.0-100.5%, Lot no.: V6H654206N, Carlo Erba)	13.6177 g
Sodium hydroxide, pellets (≥ 98%, Lot no.S018807, Daejung)	3.1307 g

The receptor medium was phosphate buffer pH 7.4 with 20% v/v PEG 400. It was prepared by adding 60 ml of PEG 400 to 240 ml of phosphate buffer and stirred on a magnetic stirrer for 10 minutes.

Before placing the receptor medium in the receiver compartments, it was degassed to remove any bubble in it. Degassing step was done by heating the receptor medium to 45°C on the hot plate and degassing it using the sonicator.

### **3.3.7.3 Preparation of membrane**

In this study, two different synthetic membranes were used. The first membrane is 0.45  $\mu\text{m}$  polyamide membrane and the other is the 300  $\mu\text{m}$  Start-M membrane. A piece of the membrane of appropriate size was cut. Polyamide membrane and Start-M membrane were soaked for about 30 minutes in phosphate buffer pH 7.4 with 20% v/v PEG 400 before the experiment.

### **3.3.7.4 In vitro skin permeation studies procedures**

Before the experiment, the water bath was heated and the water pump was run to adjust the temperature of  $32 \pm 1$  °C for the receptor chamber of each cell of the Franz diffusion apparatus.

In each cell of the Franz diffusion apparatus, the receiver chamber was filled to the top with a degassed receptor medium. A membrane was mounted on the flat flange of the Franz diffusion cells and making sure that no air bubbles stick under it.

The donor compartments were attached using stainless-steel clips. After attaching the donor compartment, 3 ml of microemulsion formulation under test was poured into the donor compartment using a micropipette. Every 3 cells of the Franz diffusion apparatus were contained the same formulation of the microemulsion.

The orifice of the sampling arm of each receptor chamber and the mouth of the donor chamber were covered tightly using parafilm to prevent any evaporation of contents with time. All cells had a final receptor medium volume of 20 ml and it was marked on the sampling arm.

At the beginning and through of the diffusion experiment, the speed of the stirrer in FDC was 700 rpm, and the power activated to maximum (100%).

The concentration of mebendazole in each formulation was determined using HPLC. After 30 minutes, 1 ml of each sample was pulled from the middle of the receptor chamber using a syringe through the sampling port.

The sampled quantity was replaced by an equal amount (1 ml) of phosphate buffer pH 7.4 with 20% v/v PEG 400 to keep the volume of buffer in the receiver chamber constant. Six samples were pulled from each cell of FDC at times 30 minutes, 1 hour, 2 hours, 3 hours, 4 hours, and 5 hours.

Samples taken were analyzed by HPLC according to test methods (see section 3.3.1) and every experiment was done in triplicates.

The cumulative amount of the penetrant is calculated according to the following equation:

$$\text{Cumulative amount of penetrant at time (t)} = C_t \times V + \sum_{t=0}^{t-1} C_t \text{ -----(8)}$$

Where,

**C<sub>t</sub>**: is the measured concentration of the Mebendazole at time **t** in the receptor compartment in mg/ml.

**V:** is the volume of the solution in the receiver chamber.

### 3.3.7.5 Calculation of permeation membrane parameters

At every sampling time a sample is withdrawn and the amount of mebendazole is determined by HPLC analysis. A cumulative amount of mebendazole through time is drawn, and the diffusion parameters are calculated.

The curve is extrapolated using Excel 2016 to find the steady state line. The **x**-intercept of the line will be the lag time. According to equation (9):

$$\frac{dM}{dt} = \frac{DSK C_d}{h} = PSC_d \text{-----(9)}$$

Where,

**S:** is the area

**P:** is the permeability coefficient

**C<sub>d</sub>:** is the concentration in the donor compartment.

The slope =  $PSC_d$

The thickness of the membrane (h) equals 0.45 μm for polyamide membrane and 300 μm for Start-M® membrane. Area of membrane (S) equals 3.14 cm<sup>2</sup>, and the volume of the receiver compartment is 20 ml.

The permeability coefficient can be calculated as the slope. The area of membrane and concentration in donor compartment are known.

According to equation (10):

$$T_L = \frac{h^2}{6D} \text{-----} \quad (10)$$

Where **h** is thickness of membrane that was measured during the experiment, the lag time (**T<sub>L</sub>**) was calculated from the plot so the diffusion coefficient (**D**) is calculated.

According to equation (11), the permeability coefficient equal:

$$P = \frac{DK}{h} \text{-----} \quad (11)$$

Where **h** is thickness of membrane that was measured during the experiment, **P** is the permeability coefficient that was calculated previously and thus the partition coefficient **K** is calculated.

A summary of the diffusion parameters and their method of calculation are seen in table (6).

**Table 7: Summary of diffusion parameters and their method of calculation.**

Slope	Lag Time (TL)	Diffusion Coefficient (D)	Permeability Coefficient (P)	Partition coefficient (K)	Steady state flux (J <sub>ss</sub> )
Calculated from the plot	Intercept with x axes	$\frac{h^2}{6TL}$	Slope/C <sub>d</sub>	$\frac{P \cdot h}{D}$	P · C <sub>d</sub>

### **3.3.8 Mebendazole solubility in receptor medium**

Mebendazole solubility was determined in phosphate buffer pH 7.4 + 20% v/v PEG 400 at 25° C ± 1. The solubility study was carried out by adding an excess of MBZ in a beaker containing 15 mL of receptor medium to obtain a saturated solution. The solutions were kept for 24 h under constant magnetic stirring at 1500 rpm. After that, the solutions were centrifuged (Centurion Science, Model: K2015R) at a speed of 5000 rpm for 20 min. The supernatant was filtered through a 0.45 µm Nylon membrane, and the filtrate was assayed by the HPLC method for mebendazole quantification. This test was carried out in triplicate.

### **3.3.9 Statistical analysis**

Microsoft Office Excel 2016 was used for all calculations and to determine in vitro permeation data. It is also used to plot all graphs in this study.

Pseudo-ternary phase diagrams for all microemulsion formulation trials were plotted using the software SigmaPlot (version 14.0).

## Chapter 4

### Results and discussion

#### 4.1 Linearity, LOD, and LOQ for HPLC method

Analytical method linearity is defined as the ability of the method to obtain test results that are directly proportional to the analyte concentration, within a specific range. The mean peak area obtained from the HPLC was plotted against corresponding concentrations to obtain the calibration graph. The results of linearity study (Figure 12) gave a linear relationship over the concentration range of (5–100 µg/ml) for mebendazole. From the regression analysis, a linear equation was obtained:  $y = 54.9x + 30.892$ , and the  $R^2$  was found to be 0.9998, indicating a linear relationship between the concentration of analyte and area under the peak.

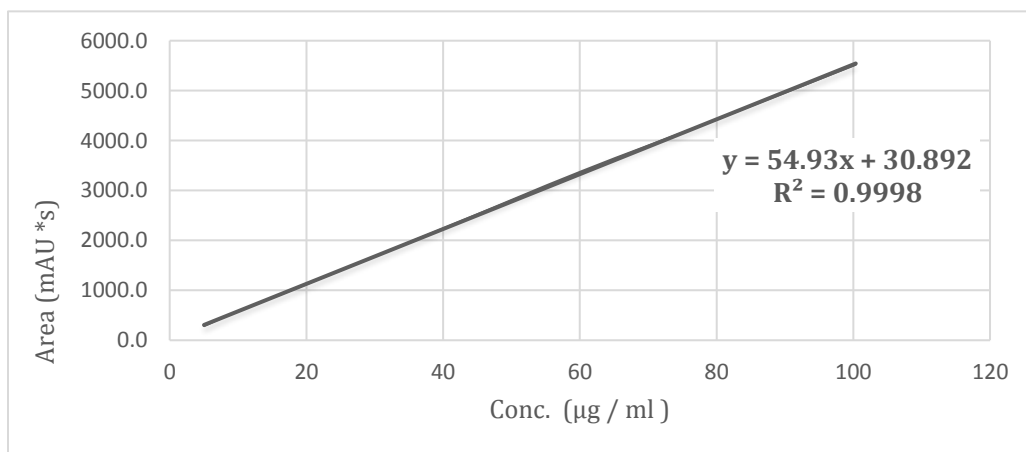
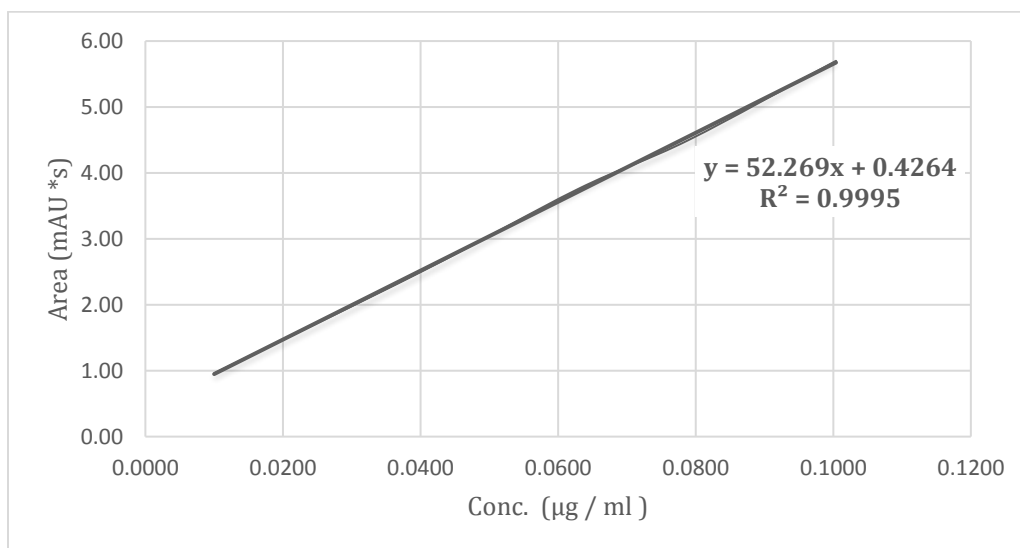


Figure 12: Standard calibration curve of mebendazole.

The LOQ and LOD were calculated from calibration curve in (Figure 13) based on the equations:  $LOD = 3.3 * (SD / \text{slope})$  and  $LOQ = 10 * (SD / \text{slope})$  where SD is the standard deviation of intercept. The calculations of LOD and LOQ were done by regression analysis using Microsoft Office Excel 2016.



**Figure 13: Standard calibration curve using small concentrations of mebendazole**

The results of LOD and LOQ for mebendazole are shown in Table 7.

**Table 8: Statistical analysis of the HPLC method validation**

Validation parameters	Results
<b>LOD</b>	0.013 (µg/ml)
<b>LOQ</b>	0.038 (µg/ml)



## 4.2 Solubility studies of mebendazole in various oils

From the calibration curve in Figure 14, the solubility of mebendazole in various oils was calculated and listed in Table 8.

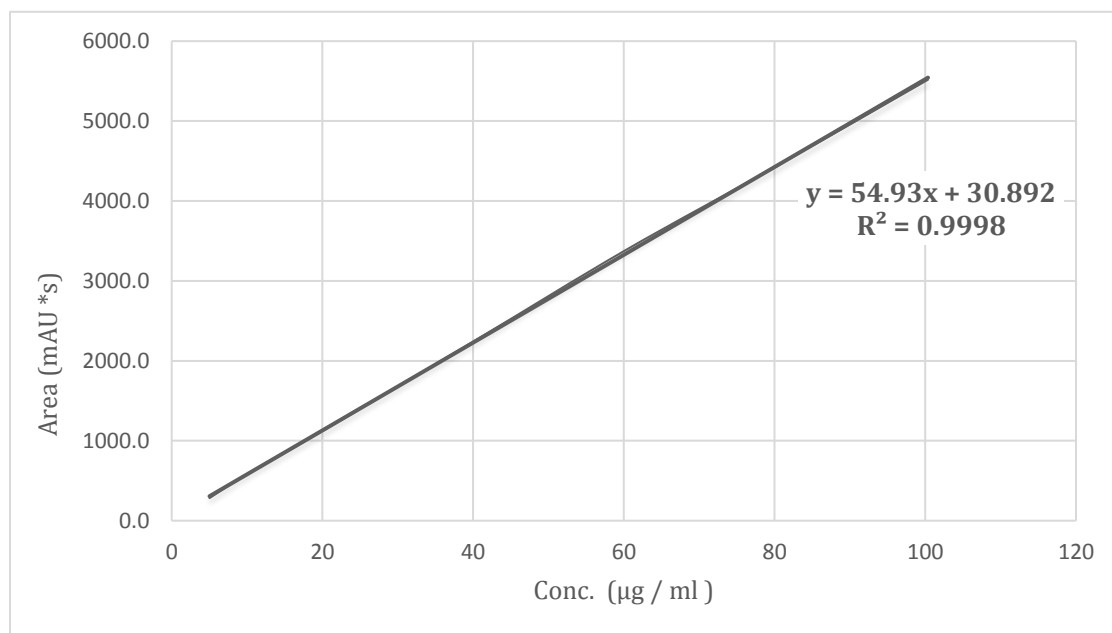


**Figure 14: Standard calibration curve of mebendazole**

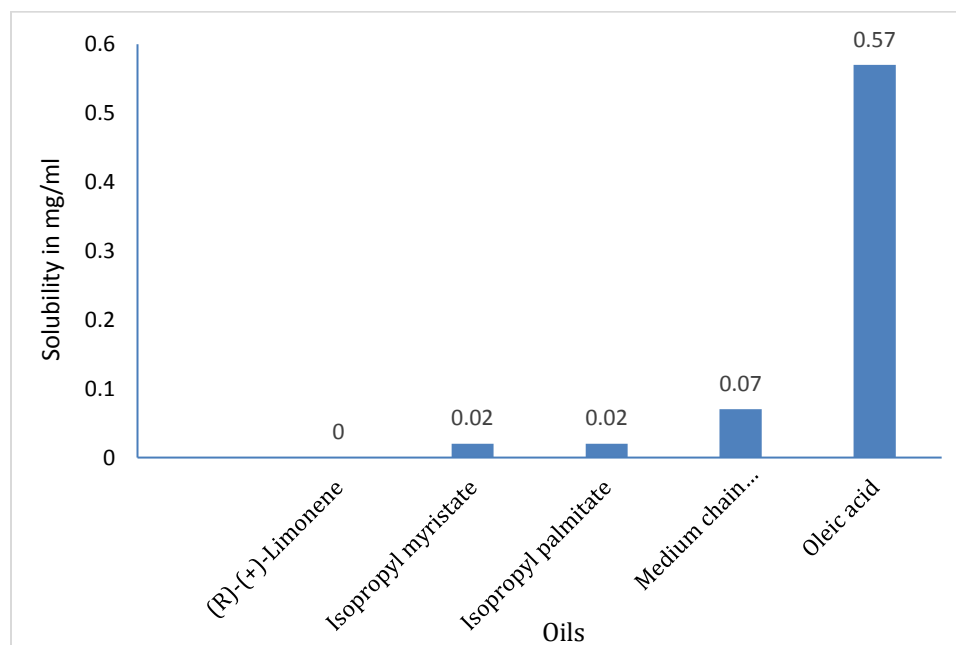
As shown in Table 8 and Figure 15, oleic acid shows the highest solubilisation capacity than other oils for mebendazole (0.57 mg/ml) followed by low solubilisation capacity for Medium chain triglycerides (M.C.T) (0.07 mg/ml), Isopropyl myristate (0.02 mg/ml), and Isopropyl palmitate (0.02 mg/ml).

Depending on the above results, Oleic acid was chosen as the main oil phase in the microemulsion formulation trials.

**Table 9 :Saturation solubility of MBZ in various oils**

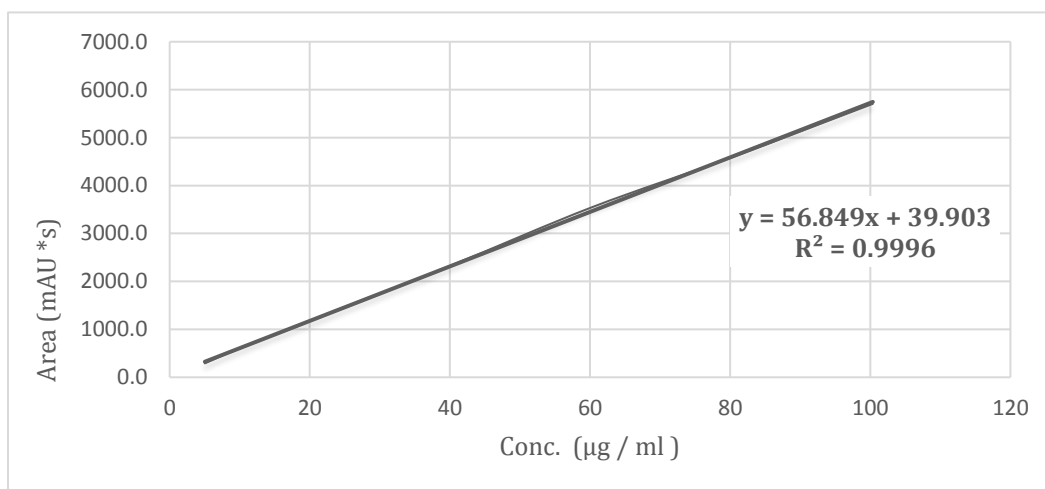
Sample	Solubility of MBZ (mg / ml)
(R)-(+)-Limonene	Not detected
Isopropyl myristate	0.02 ± 0.007
Isopropyl palmitate	0.02 ± 0.005
Medium chain triglycerides (M.C.T)	0.07 ± 0.02
Oleic acid	0.57 ± 0.04

Figure 15 below shows the most and the less effective oils to dissolve mebendazole.

**Figure 15: Saturation solubility of mebendazole in oils.**

### 4.3 Solubility studies of mebendazole in various surfactants and co-surfactants

From the calibration curve in Figure 16, the solubility of mebendazole in various surfactants and co-surfactants was calculated and listed in Table 9.



**Figure 16. Standard calibration curve of mebendazole.**

From the above calibration curve, N-methyl pyrrolidone shows the highest solubilization capacity than other co-surfactants for mebendazole (11.39 mg/ml) followed by Benzyl alcohol (3.09 mg/ml). The solubility of mebendazole in DEGME, PEG 400 and PEG 300 (2.61 mg/ml, 2.61 mg/ml, 2.51 mg/ml) respectively, while PG and ethanol show low solubilization capacity (0.57 mg/ml, 0.28 mg/ml) respectively.

Besides, the surfactant Kolliphor® RH 40 shows the highest solubilization capacity than Tween 80 for mebendazole (5.07 mg/ml and 1.63 mg/ml) respectively.

Depending on the above results, Tween 80 and Kolliphor® RH 40 were used as surfactants in this study, while N-methyl pyrrolidone, benzyl alcohol, DEGME, and PEG 400 were used as co-surfactants in different microemulsion formulation trials.

**Table 10 :Saturation solubility of MBZ in various surfactants and co-surfactants.**

Sample	Function	Solubility of MBZ (mg / ml)
Ethanol	Co-surfactant	0.28 ± 0.05
PG	Co-surfactant	0.57 ± 0.09
PEG 300	Co-surfactant	2.51 ± 0.15
PEG 400	Co-surfactant	2.61 ± 0.24
DEGME	Co-surfactant	2.61 ± 0.44
Benzyl alcohol	Co-surfactant	3.09 ± 0.91
N-methyl pyrrolidone	Co-surfactant	11.39 ± 0.95
Kolliphor® RH 40	Surfactant	5.07 ± 0.87
Tween 80	Surfactant	1.63 ± 0.66

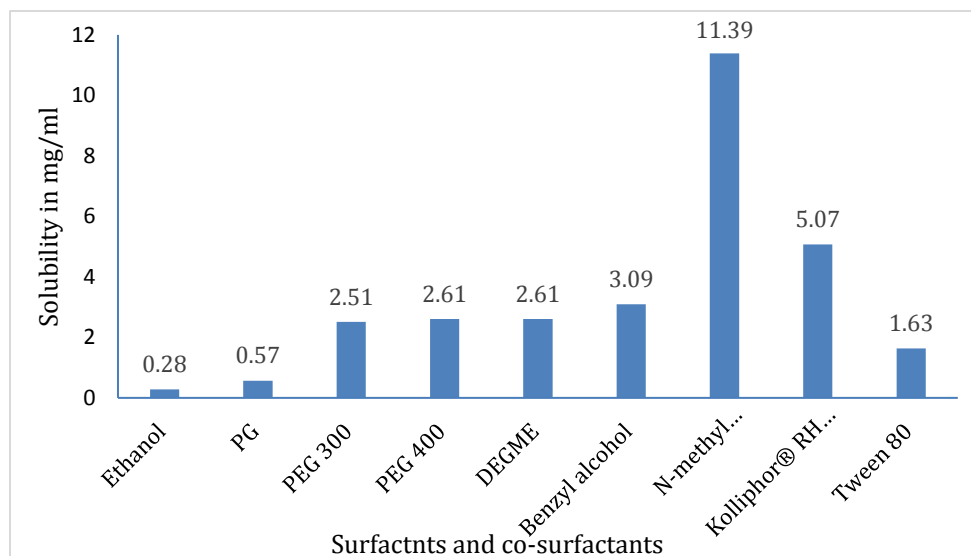


**Figure 17:Saturation solubility of mebendazole in surfactants and co-surfactants.**

## 4.4 Microemulsion formulations trials

### 4.4.1 Stage1: By Experimental Trials

This stage was used as a primary indicator for the microemulsion formulation. Table 10 describes the composition, volume %, and some physical properties of microemulsion formulation trials prepared in this stage.

**Table 11: Microemulsion Formulations by experimental trials.**

Sample code	Composition	Water %	Oil %	Surf. %	co-surf. %	Appearance	Type of ME	Viscosity
ME#1	Oleic acid: T80 / Bl	25	17	29	29	Turbid	*	Low
ME#2	Oleic acid: T80 / Bl	11	20	34	35	Clear	O/W	Low
ME#3	Oleic acid: T80/ Pyrrol	25	17	29	29	Clear	O/W	like gel
ME#4	Oleic acid: T80/ Pyrrol	15	19	33	33	Clear	O/W	low
ME#5	Oleic acid: RH 40 / PEG 400	8	21	37	34	Turbid	*	low
ME#6	Oleic acid: RH 40 / PEG 400	6	22	38	34	Clear	O/W	low
ME#7	Oleic acid: RH 40 /Bl: Pyrrol	21	17	31	31	Clear	O/W	low
ME#8	Oleic acid: RH 40 / Pyrrol	22	17	30	31	Clear	O/W	High
ME#9	Oleic acid: T80 / Ethanol	23	23	23	31	Clear	O/W	low

While: **T80**: Tween 80, **Bl**: Benzyl alcohol, **Pyrrol**: N-methyl pyrrolidone, and **RH40**: Kolliphor® RH 40

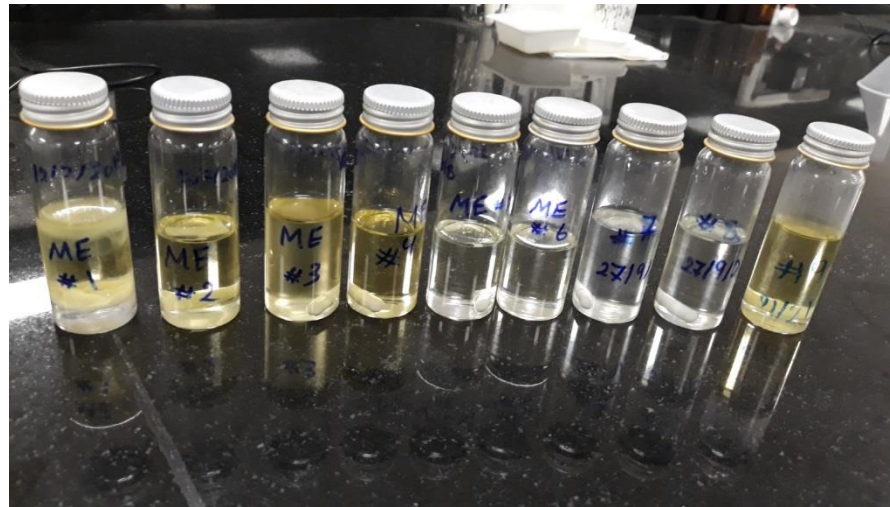


**Figure 18: Formulations by experimental trials after one year. ME#1 and ME#5 were separated while other formulations were clear and monophasic.**

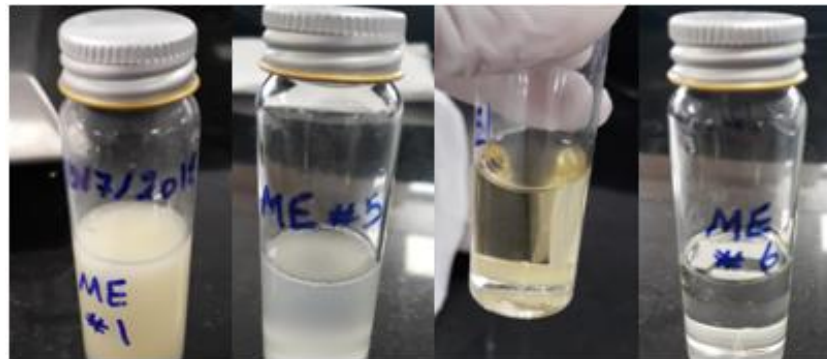


**Figure 19: Some formulations after prepared. ME#1 and ME#5 were turbid while ME#4 and ME#6 were clear.**

#### 4.4.2 Stage 2: Using ternary diagram tables

In this stage, various formulation trials of microemulsion were prepared by using the phase titration method and pseudo-ternary diagram tables as shown in tables 11 and 12. The endpoint for each formulation was determined, then the volume percent composition of the microemulsion formulation trial components (oil, surfactant /co-surfactant, and water) was calculated and plotted on triangular coordinates to construct pseudo-ternary phase diagrams. After that different formulations were selected from the microemulsion regions in the phase diagram.

**Table 12: Microemulsion formulation ratios using titration method and pseudo-ternary diagram tables.**

<b>Oil: (surf. + co-surf. ) ratio</b>	<b>Surfactant: Co-surfactant ratio</b>	<b>% Water</b>
<b>1:1</b>	1:1 , 1:2 , 2:1 , 1:3 , 3:1	5% -70%
<b>2:1</b>	1:1 , 1:2 , 2:1 , 1:3 , 3:1	5% -70%
<b>1:4</b>	1:1 , 1:2 , 2:1 , 1:3 , 3:1	5% -70%
<b>1:9</b>	1:1 , 1:2 , 2:1 , 1:3 , 3:1	5% -70%
<b>2:8</b>	1:1 , 1:2 , 2:1 , 1:3 , 3:1	5% -70%
<b>3:7</b>	1:1 , 1:2 , 2:1 , 1:3 , 3:1	5% -70%
<b>4:6</b>	1:1 , 1:2 , 2:1 , 1:3 , 3:1	5% -70%
<b>5:5</b>	1:1 , 1:2 , 2:1 , 1:3 , 3:1	5% -70%
<b>6:4</b>	1:1 , 1:2 , 2:1 , 1:3 , 3:1	5% -70%
<b>7:3</b>	1:1 , 1:2 , 2:1 , 1:3 , 3:1	5% -70%
<b>8:2</b>	1:1 , 1:2 , 2:1 , 1:3 , 3:1	5% -70%
<b>9:1</b>	1:1 , 1:2 , 2:1 , 1:3 , 3:1	5% -70%

Table 13: Pseudo-ternary diagram table.

<b>water (µl)</b>	<b>132</b>	<b>146</b>	<b>163</b>	<b>184</b>	<b>208</b>	<b>238</b>	<b>275</b>	<b>321</b>	<b>379</b>	<b>455</b>	<b>556</b>	<b>694</b>	<b>893</b>	<b>1190</b>
<b>oil %</b>	<b>9.50</b>	<b>9.00</b>	<b>8.50</b>	<b>8.00</b>	<b>7.50</b>	<b>7.00</b>	<b>6.50</b>	<b>6.00</b>	<b>5.50</b>	<b>5.00</b>	<b>4.50</b>	<b>4.00</b>	<b>3.50</b>	<b>3.00</b>
<b>1:9</b>														
<b>oil %</b>	<b>19.00</b>	<b>18.00</b>	<b>17.00</b>	<b>16.00</b>	<b>15.00</b>	<b>14.00</b>	<b>13.00</b>	<b>12.00</b>	<b>11.00</b>	<b>10.00</b>	<b>9.00</b>	<b>8.00</b>	<b>7.00</b>	<b>6.00</b>
<b>2:8</b>														
<b>oil %</b>	<b>28.50</b>	<b>27.00</b>	<b>25.50</b>	<b>24.00</b>	<b>22.50</b>	<b>21.00</b>	<b>19.50</b>	<b>18.00</b>	<b>16.50</b>	<b>15.00</b>	<b>13.50</b>	<b>12.00</b>	<b>10.50</b>	<b>9.00</b>
<b>3:7</b>														
<b>oil %</b>	<b>37.99</b>	<b>36.00</b>	<b>34.00</b>	<b>32.00</b>	<b>30.00</b>	<b>28.00</b>	<b>26.02</b>	<b>24.00</b>	<b>22.00</b>	<b>20.00</b>	<b>18.00</b>	<b>16.00</b>	<b>14.00</b>	<b>12.00</b>
<b>4:6</b>														
<b>oil %</b>	<b>47.49</b>	<b>45.00</b>	<b>42.50</b>	<b>40.00</b>	<b>37.51</b>	<b>35.01</b>	<b>32.51</b>	<b>30.01</b>	<b>27.52</b>	<b>25.02</b>	<b>22.52</b>	<b>20.03</b>	<b>17.53</b>	<b>15.03</b>
<b>5:5</b>														
<b>oil %</b>	<b>56.99</b>	<b>54.00</b>	<b>51.00</b>	<b>48.00</b>	<b>45.01</b>	<b>42.01</b>	<b>39.01</b>	<b>36.01</b>	<b>33.02</b>	<b>30.02</b>	<b>27.02</b>	<b>24.03</b>	<b>21.03</b>	<b>18.03</b>
<b>6:4</b>														
<b>oil %</b>	<b>66.49</b>	<b>62.99</b>	<b>59.50</b>	<b>56.00</b>	<b>52.51</b>	<b>49.01</b>	<b>45.51</b>	<b>42.02</b>	<b>38.52</b>	<b>35.03</b>	<b>31.53</b>	<b>28.03</b>	<b>24.54</b>	<b>21.04</b>
<b>7:3</b>														
<b>oil %</b>	<b>75.99</b>	<b>71.99</b>	<b>68.00</b>	<b>64.00</b>	<b>60.01</b>	<b>56.01</b>	<b>52.02</b>	<b>48.02</b>	<b>44.03</b>	<b>40.03</b>	<b>36.04</b>	<b>32.04</b>	<b>28.05</b>	<b>24.05</b>
<b>8:2</b>														
<b>oil %</b>	<b>85.49</b>	<b>80.99</b>	<b>76.50</b>	<b>72.00</b>	<b>67.51</b>	<b>63.01</b>	<b>58.52</b>	<b>54.02</b>	<b>49.53</b>	<b>45.03</b>	<b>40.54</b>	<b>36.04</b>	<b>31.55</b>	<b>27.05</b>
<b>9:1</b>														

In the following tables (Table 13 – Table 16) the symbol ☑ means that the formulation was clear and monophasic while the symbol ✖ means that the formulation was turbid or separated.

The pseudo-ternary phase diagrams for the selected microemulsion formulations are shown in Figures 20 to 23.











#### 4.4.2.1 Pseudo-ternary phase diagrams

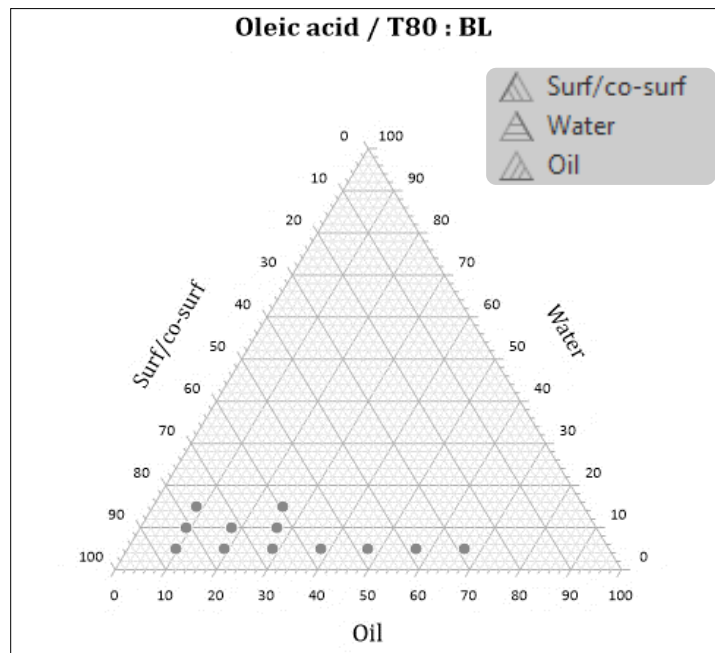


Figure 20 : Ternary phase diagram for Oleic acid/T80: BL

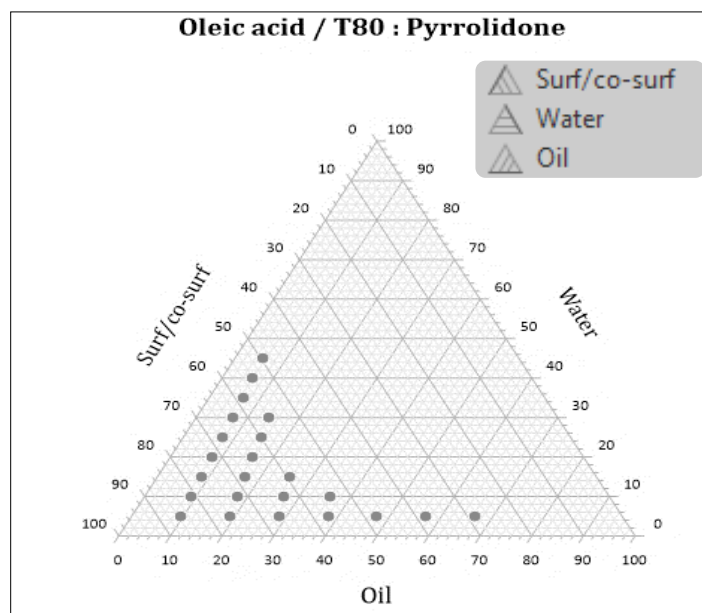
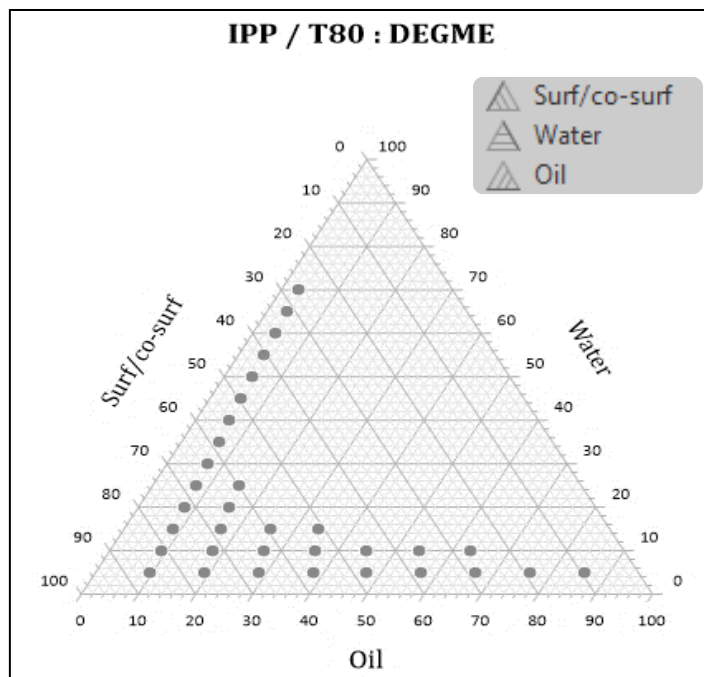
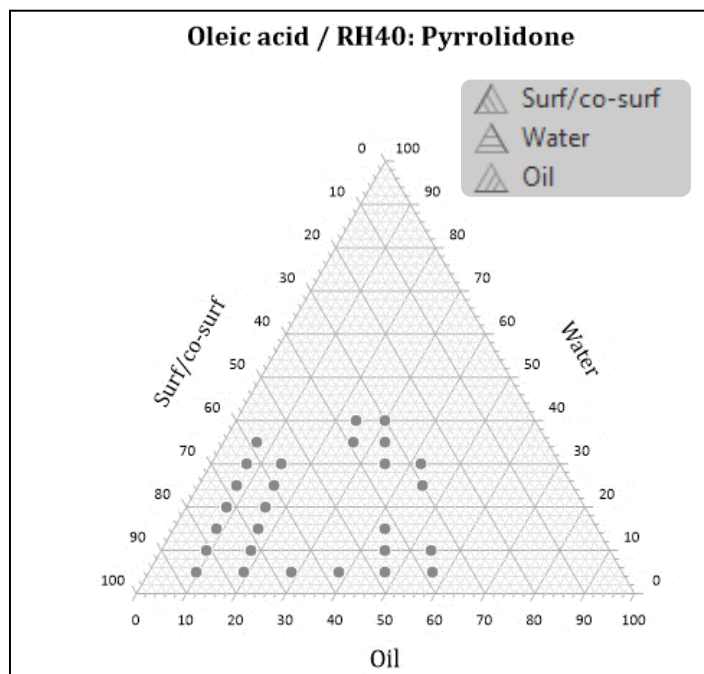


Figure 21: Ternary phase diagram for Oleic acid/T80: N-methyl pyrrolidone.



**Figure 22: Ternary phase diagram for IPP/T80: DEGME.**



**Figure 23: Ternary phase diagram for Oleic acid/RH40: N-methyl pyrrolidone.**

#### 4.5 Solubility studies of mebendazole in various formulations of microemulsion

The table below shows the saturation solubility of mebendazole in various microemulsion formulations.

**Table 18: Saturation solubility of MBZ in various microemulsion formulation trials.**

Formulation trial	Ratio Oil: surf. /co-surf.	Solubility of MBZ (mg / ml)
Oleic acid: T80/ IPA	3:7	0.86 ± 0.27
IPP: T80/ DEGME	3:7	1.49 ±0.20
Oleic acid: RH40/ Pyrrol	3:7	1.50 ± 0.60
Oleic acid: T80/ Pyrrol	3:7	1.51± 0.14
Oleic acid: T80/ BL	3:7	1.80 ± 0.13

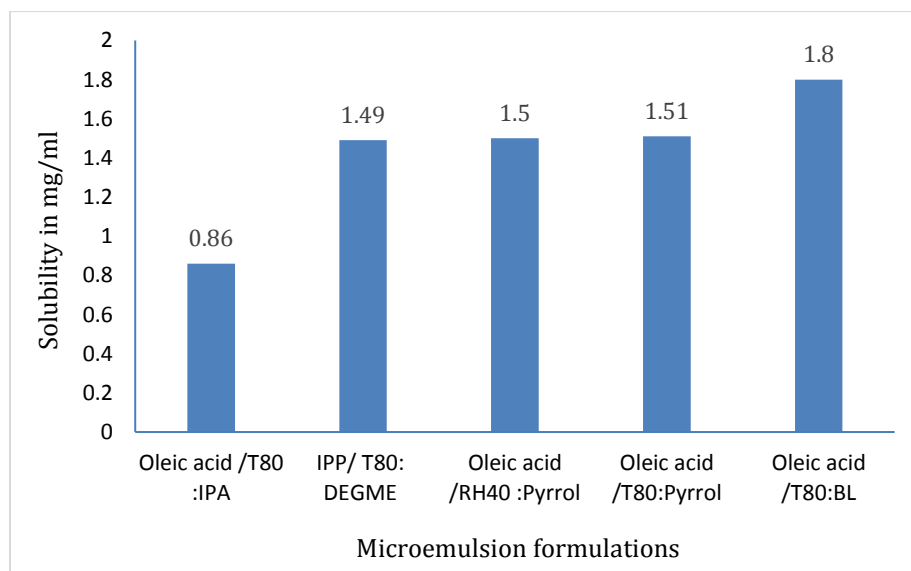


**Figure 24: Saturation solubility of mebendazole in various microemulsion formulation trials.**

The results show that formulation of (Oleic acid :T80/BL) has the highest solubilization capacity (1.81 mg/ml) than other microemulsion formulation trials for mebendazole , followed by formulations of (Oleic acid: T80/Pyrrrol) (1.51 mg/ml) , (Oleic acid: RH40 /Pyrrrol) (1.50 mg/ml) then ( IPP: T80/ DEGME) (1.49 mg/ml) .Finally the formulation of (Oleic acid: T80 /IPA) with low solubilization capacity ( 0.86 mg/ml).

Depending on the above solubility study results, (Oleic acid: T80/BL), (Oleic acid: T80/Pyrrrol), (Oleic acid: RH40 /Pyrrrol) and (IPP: T80/ DEGME) were chosen in various ratios as selected microemulsion formulations to study their physical properties and permeation behavior.

#### **4.6 Type and composition of the selected microemulsion formulations trials**

From the solubility studies results, the oils, surfactants, and co-surfactants which given the highest solubility of mebendazole were selected to prepare various formulations of microemulsion. After that, the formulations of microemulsion that given the highest solubility of mebendazole were prepared in different ratios and test their physical properties.

The selected formulation trials of microemulsion are illustrated in Table 18.



**Table 19: Selected formulation trials of microemulsion with (v/v%) using ternary diagram tables.**

<b>ME #</b>	<b>Composition</b>	<b>Ratio</b> Oil: surf. /co-surf.	<b>Water %</b>	<b>Oil %</b>	<b>Surf. %</b>	<b>co-surf. %</b>	<b>Type of ME</b>
#1	Oleic acid: T80/ BL	1:9	15	9	38	38	O/W
#2	Oleic acid: T80/ BL	3:7	15	26	29	30	O/W
#3	Oleic acid: T80/ Pyrrol	1:9	40	6	27	27	O/W
#4	Oleic acid: T80/ Pyrrol	3:7	15	25	30	30	O/W
#5	IPP: T80/ DEGME	1:9	50	5	22	23	O/W
#6	IPP: T80/DEGME	3:7	5	29	28	28	O/W
#7	Oleic acid: RH40/Pyrrol	1:9	25	8	33	34	O/W
#8	Oleic acid: RH40/Pyrrol	3:7	20	24	28	28	O/W
#9	Oleic acid: Pyrrol /RH40: Ethanol	1:9	25	11	32	32	O/W
#10	Oleic acid: Pyrol /RH40: Ethanol	4:6	25	31	22	22	O/W
#11	Oleic acid: Pyrol /T80: Ethanol	1:9	25	8	34	33	O/W
#12	Oleic acid: Pyrol /T80: Ethanol	4:6	25	31	22	22	O/W

The above table contains the composition with ratios and type of selected microemulsion formulation trials. The visual appearance for all formulations in the above table was clear and monophasic. Therefore, these formulations were chosen to study their properties to determine which one of them has the droplet size of microemulsion (10 – 100 nm).

The ratio of water in the selected formulations was (5% - 50%). The type of all microemulsion formulations was oil in water (O/W), and it was determined using the dye solubility test that was described in section (3.3.6.1).

#### 4.7 Viscosity of selected formulations of microemulsion

The viscosity of all microemulsion formulation trials was measured using a house-made viscometer that was described in section (3.3.6.2) and the results are illustrated in Table 19 below.

**Table 20 : Viscosity of the selected microemulsion formulation trials.**

ME #	Sample	Ratio Oil: surf. /co-surf.	Viscosity (cP)
#1	Oleic acid: T80/ BL	1:9	52.77 ± 0.67
#2	Oleic acid: T80/ BL	3:7	50.84 ± 0.21
#3	Oleic acid: T80/ Pyrrol	1:9	52.06 ± 0.78
#4	Oleic acid: T80/ Pyrrol	3:7	40.11 ± 0.54
#5	IPP: T80/ DEGME	1:9	97.66 ± 0.22
#6	IPP: T80/DEGME	3:7	45.43 ± 0.24
#7	Oleic acid: RH40/Pyrrol	1:9	78.10 ± 0.47
#8	Oleic acid: RH40/Pyrrol	3:7	73.20 ± 0.41
#9	Oleic acid: Pyrrol /RH40: Ethanol	1:9	35.79 ± 0.28
#10	Oleic acid: Pyrol /RH40: Ethanol	4:6	36.66 ± 0.39
#11	Oleic acid: Pyrol /T80: Ethanol	1:9	24.70 ± 0.59
#12	Oleic acid: Pyrol /T80: Ethanol	4:6	25.30 ± 0.33

Viscosity values ranging between (24.70 to 97.66 cP). These values used to determine the droplet size of each microemulsion formulation trial by DLS instrument.

#### 4.8 Refractive index of the selected microemulsion formulation trials

Table 20 shows the refractive index value for each microemulsion formulation trial that measured as mentioned in section (3.3.6.3).

The refractive index of microemulsion was almost same to the refractive index of water. The refractive index values prove the transparency of the microemulsion formulation trials, and used to determine the droplet size of each microemulsion formulation trial by DLS instrument. *(Desai et al. 2015)*

**Table 21:Refractive index of the selected microemulsion formulation trials.**

<b>ME #</b>	<b>Sample</b>	<b>Ratio</b> Oil: surf. /co-surf.	<b>Refractive Index</b> <b>(RI)</b>
#1	Oleic acid: T80/ BL	1:9	1.4819
#2	Oleic acid: T80/ BL	3:7	1.4861
#3	Oleic acid: T80/ Pyrrol	1:9	1.4473
#4	Oleic acid: T80/ Pyrrol	3:7	1.4581
#5	IPP: T80/ DEGME	1:9	1.4297
#6	IPP: T80/DEGME	3:7	1.441
#7	Oleic acid: RH40/Pyrrol	1:9	1.4516
#8	Oleic acid: RH40/Pyrrol	3:7	1.4611
#9	Oleic acid: Pyrrol /RH40: Ethanol	1:9	1.4027
#10	Oleic acid: Pyrol /RH40: Ethanol	4:6	1.4150
#11	Oleic acid: Pyrol /T80: Ethanol	1:9	1.4067
#12	Oleic acid: Pyrol /T80: Ethanol	4:6	1.4151
-	Distilled water	-	1.3316

The refractive index values prove the transparency of the microemulsion formulation trials as shown in Table 20.

#### 4.9 Droplet size of the selected microemulsion formulation trials

Table 21 shows the droplet size of each microemulsion formulation trial. The results were obtained from DLS as mentioned in section (3.3.6.4)

**Table 22 : Droplet size of the selected microemulsion formulation trials.**

<b>ME #</b>	<b>Sample</b>	<b>Ratio</b> Oil: surf. /co-surf.	<b>Average droplet size (nm)</b>	<b>Polydispersity</b>
#1	Oleic acid: T80/ BL	1:9	85.70 ± 1.71	0.326 ± 0.056
#2	Oleic acid: T80/ BL	3:7	0.16 ± 0.05	0.160 ± 0.017
#3	Oleic acid: T80/ Pyrrol	1:9	2.64 ± 0.17	0.315 ± 0.019
#4	Oleic acid: T80/ Pyrrol	3:7	74.25 ± 4.81	0.515 ± 0.062
#5	IPP: T80/ DEGME	1:9	5.39 ± 0.88	0.131 ± 0.012
#6	IPP: T80/DEGME	3:7	27.21 ± 1.91	0.196 ± 0.066
#7	Oleic acid: RH40/ Pyrrol	1:9	12.04 ± 0.40	0.196 ± 0.040
#8	Oleic acid: RH40/ Pyrrol	3:7	53.39 ± 1.92	0.552 ± 0.046
#9	Oleic acid: Pyrrol /RH40: Ethanol	1:9	1.72 ± 0.06	0.265 ± 0.011
#10	Oleic acid: Pyrrol /RH40: Ethanol	4:6	3.32 ± 0.03	0.310 ± 0.020
#11	Oleic acid: Pyrrol /T80: Ethanol	1:9	0.96 ± 0.09	0.198 ± 0.008
#12	Oleic acid: Pyrrol /T80: Ethanol	4:6	2.62 ± 0.06	0.230 ± 0.021

The microemulsion droplet size range is 10-100 nm. Thus, from the above results, formulations ME#1 (Oleic acid/T80: BL 1:9), ME#4 (Oleic acid/T80: Pyrol 3:7), ME#6 (IPP/ T80: DEGME 3:7), ME#7 (Oleic acid /RH40: Pyrol 1:9), and ME#8 (Oleic acid /RH40: Pyrol 3:7) considered as a microemulsion and chosen for stability and permeation studies.

The polydispersity index (PDI) is used to describe the degree of non-uniformity of a size distribution of particles. Also known as the heterogeneity index, PDI is a number calculated from a two-parameter fit to the correlation data. This index is dimensionless and scaled such that values smaller than 0.05 are mainly seen with highly monodisperse standards, while values bigger than 0.7 indicate that the sample has a very broad particle size distribution and is probably not suitable to be analyzed by the dynamic light scattering (DLS) technique. (*Danaei et al. 2018*)

As shown in Table 21, polydispersity index values ranging between 0.131 and 0.552. This indicated a uniform microemulsion with a narrow size distribution.

➤ **Summary of physical properties of the selected microemulsion formulation trials.**

Table 22 below shows the values of different parameters for 12 selected microemulsion formulation trials.

**Table 23 : Summary of physical properties for the selected microemulsion formulation trials.**

#	Composition	Ratio Oil: surf. /co-surf.	Visual appearance	Viscosity (cp)	RI	Droplet size (nm)
1	Oleic acid: T80/ BL	1:9	Monophasic	52.77	1.48	85.70 ± 1.71
2	Oleic acid: T80/ BL	3:7	Monophasic	50.84	1.49	0.16 ± 0.05
3	Oleic acid: T80/ Pyrrol	1:9	Monophasic	52.06	1.45	2.64 ± 0.17
4	Oleic acid: T80/ Pyrrol	3:7	Monophasic	40.11	1.46	74.25 ± 4.81
5	IPP: T80/ DEGME	1:9	Monophasic	97.66	1.43	5.39 ± 0.88
6	IPP: T80/DEGME	3:7	Monophasic	45.43	1.44	27.21 ± 3.91
7	Oleic acid: RH40/Pyrrol	1:9	Monophasic	78.10	1.45	12.04 ± 0.40
8	Oleic acid: RH40/Pyrrol	3:7	Monophasic	73.20	1.46	53.39 ± 3.92
9	Oleic acid: Pyrrol /RH40: Ethanol	1:9	Monophasic	35.80	1.40	1.72 ± 0.06
10	Oleic acid: Pyrrol /RH40: Ethanol	4:6	Monophasic	36.66	1.41	3.32 ± 0.03
11	Oleic acid: Pyrrol /T80: Ethanol	1:9	Monophasic	24.70	1.40	0.96 ± 0.09
12	Oleic acid: Pyrrol /T80: Ethanol	4:6	Monophasic	25.30	1.41	2.62 ± 0.06

Depending on the results in Table 22, microemulsion formulations ME#1, ME#4, ME#6, ME#7, and ME#8 were chosen to determine the accelerated stability for it.

**4.10 Stability studies for formulations of microemulsion without mebendazole**

This step was conducted to determine the stability of selected microemulsion formulations (ME#1, ME#4, ME#6, ME#7, and ME#8) before adding mebendazole to these formulations. The droplet size of each microemulsion formulation was measured after freeze-thaw cycle and after one week at room temperature as illustrated in table 23.

**Table 24: Stability studies for formulations of microemulsion without mebendazole.**

<b>Formula Code</b>	<b>Composition</b>	<b>Ratio</b> Oil: surf. /co-surf.	<b>Water %</b>	<b>Oil %</b>	<b>Surf. %</b>	<b>co-surf %</b>	<b>Droplet size (nm) at time zero</b>	<b>Droplet size (nm) after freeze-thaw cycle</b>	<b>Droplet size (nm) after one week at room temp.</b>
<b>ME#1</b>	Oleic acid: T80/ BL	1:9	15	9	38	38	85.70 ± 1.71	22.58 ± 3.50	18.22 ± 2.73
<b>ME#4</b>	Oleic acid: T80/ Pyrrol	3:7	15	25	30	30	74.25 ± 4.81	78.39 ± 5.06	72.75 ± 4.60
<b>ME#6</b>	IPP: T80/DEGME	3:7	5	29	33	33	23.47 ± 1.76	25.98 ± 2.13	17.02 ± 1.36
<b>ME#7</b>	Oleic acid: RH 40/ Pyrrol	1:9	25	8	33	34	12.04 ± 0.40	7.33 ± 0.82	9.30 ± 2.10
<b>ME#8</b>	Oleic acid: RH 40 / Pyrrol	3:7	20	24	28	28	57.77 ± 2.45	50.25 ± 3.38	55.31 ± 1.24

All the selected formulations of microemulsion were stable and the droplet size of each formulation was within the range of (10 – 100 nm) except formulation ME#7. In addition, all formulations were not separated (monophasic) after the centrifugation stress test (that mentioned in section 3.3.6.5).

Depending on the results in Table 23 formulations ME#1 (Oleic acid: T80/ BL 1:9), ME#4 (Oleic acid: T80/ Pyrrol 3:7), ME#6 (IPP: T80/DEGME 3:7), ME#7 (Oleic acid: RH 40/ Pyrrol 1:9), and ME#8 (Oleic acid: RH 40 / Pyrrol 3:7) were chosen to study their stability after adding mebendazole to each formulation and to conduct permeation study on each one of it.

#### **4.11 Stability studies of the selected formulations of microemulsion with MBZ**

##### **4.11.1 Stability study of the selected microemulsion formulations with MBZ at room temperature**

Stability studies of the selected microemulsion formulations were conducted at room temperature for two weeks. At time zero and each week, the droplet size for each microemulsion formulation was measured using DLS and the assay% of mebendazole in each formulation was determined using HPLC.



The results of stability studies at room temperate are illustrated in the following tables (Table 24, Table 25, and Table 26).

**Table 25: Assay % and droplet size of the selected formulations of microemulsion with MBZ at Time Zero.**

<b>Formula Code</b>	<b>Composition</b>	<b>Ratio</b> Oil: surf. /co-surf.	<b>Water %</b>	<b>Oil %</b>	<b>Surf. %</b>	<b>co-surf %</b>	<b>Assay %</b>	<b>Particle size (nm)</b>	<b>Polydispersity</b>
<b>ME#1</b>	Oleic acid: T80/ BL	1:9	15	9	38	38	97.49	75.23 ± 1.51	0.521 ± 0.171
<b>ME#4</b>	Oleic acid: T80/ Pyrrol	3:7	15	25	30	30	99.84	49.10 ± 3.60	0.369 ± 0.062
<b>ME#6</b>	IPP: T80/DEGME	3:7	5	29	33	33	98.59	27.24 ± 2.76	0.332 ± 0.018
<b>ME#7</b>	Oleic acid: RH 40/ Pyrrol	1:9	25	8	33	34	97.78	16.51 ± 1.75	0.283 ± 0.019
<b>ME#8</b>	Oleic acid: RH 40 / Pyrrol	3:7	20	24	28	28	99.39	53.25 ± 2.78	0.533 ± 0.186

**Table 26: Assay % and droplet size of the selected formulations of microemulsion with MBZ after one week at room temperature.**

<b>Formula Code</b>	<b>Composition</b>	<b>Ratio</b> Oil: surf. /co-surf.	<b>Visual appearance</b>	<b>Assay %</b>	<b>Particle size (nm)</b>	<b>Polydispersity</b>
<b>ME#1</b>	Oleic acid: T80/ BL	1:9	MBZ precipitation	-	-	-
<b>ME#4</b>	Oleic acid: T80/ Pyrrol	3:7	Clear	98.39	51.22 ± 9.01	0.398 ± 0.110
<b>ME#6</b>	IPP: T80/DEGME	3:7	Clear	98.51	20.21 ± 1.35	0.271 ± 0.013
<b>ME#7</b>	Oleic acid: RH 40/ Pyrrol	1:9	Clear	96.04	13.52 ± 1.23	0.236 ± 0.024
<b>ME#8</b>	Oleic acid: RH 40 / Pyrrol	3:7	Clear	98.2	55.30 ± 5.22	0.602 ± 0.031

**Table 27: Assay % and droplet size of the selected formulations of microemulsion with MBZ after 2 weeks at room temperature.**

<b>Formula Code</b>	<b>Composition</b>	<b>Ratio</b> Oil: surf. /co-surf.	<b>Visual appearance</b>	<b>Assay %</b>	<b>Particle size (nm)</b>	<b>Polydispersity</b>
<b>ME#4</b>	Oleic acid: T80/ Pyrrol	3:7	Clear	97.46	57.07 ± 10.08	0.412 ± 0.114
<b>ME#6</b>	IPP: T80/DEGME	3:7	Clear	98.07	15.13 ± 2.55	0.181 ± 0.021
<b>ME#7</b>	Oleic acid: RH 40/ Pyrrol	1:9	Clear	95.91	10.69 ± 1.79	0.196 ± 0.029
<b>ME#8</b>	Oleic acid: RH 40 / Pyrrol	3:7	Clear	97.95	58.70 ± 7.63	0.704 ± 0.056

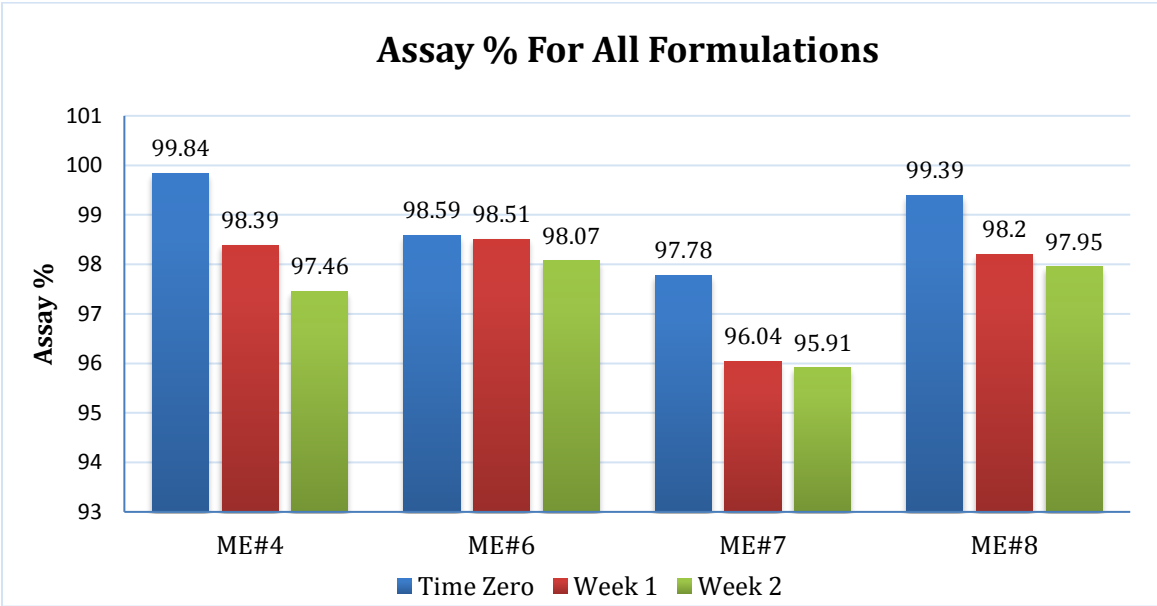


**Figure 25: Assay % of the selected formulations of microemulsion with MBZ at room temperature.**

As shown in Figure 25 and Tables 24, 25, and 26, all the selected formulations (except ME#1) of microemulsion were stable and the droplet size of each formulation was within the range of (10 – 100 nm). In addition, all formulations (except ME#1) were not separated after 2 weeks. The assay % was within the range of (95-105 %) during the two weeks.

**4.11.2 Accelerated Stability study for selected formulations of microemulsion with MBZ**

Freeze-thaw cycle and centrifugation stress test (were mentioned in section 3.3.6.6 and 3.3.6.5 respectively) were conducted for the selected microemulsion formulations to test the accelerated stability of each formulation. Tables 27 and 28 show the results of the accelerated stability study.

**Table 28 : The Assay % and visual appearance of the selected microemulsion formulations after Freeze-thaw cycle.**

<b>Formula Code</b>	<b>Composition</b>	<b>Ratio</b> Oil: surf. /co-surf.	<b>Visual appearance</b>	<b>MBZ precipitation</b>	<b>Assay %</b>
<b>ME#4</b>	Oleic acid: T80/ Pyrrol	3:7	Clear monophasic	No	93.40
<b>ME#6</b>	IPP: T80/DEGME	3:7	Clear monophasic	No	97.40
<b>ME#7</b>	Oleic acid: RH 40/ Pyrrol	1:9	Clear monophasic	No	87.16
<b>ME#8</b>	Oleic acid: RH 40 / Pyrrol	3:7	Clear monophasic	No	98.45

After freeze-thaw cycle test, all microemulsion formulations were monophasic and without any MBZ precipitation as shown in Table 27. In addition, assay % for ME#4 and ME#7 were out of the acceptance range (95-105%).

**Table 29: The visual appearance of the selected microemulsion formulations after centrifugation stress test.**

<b>Formula code</b>	<b>Composition</b>	<b>Ratio</b> Oil: surf. /co-surf.	<b>Visual appearance</b>	<b>MBZ precipitation</b>
<b>ME#4</b>	Oleic acid: T80/ Pyrrol	3:7	Clear monophasic	No
<b>ME#6</b>	IPP: T80/DEGME	3:7	Clear monophasic	No
<b>ME#7</b>	Oleic acid: RH 40/ Pyrrol	1:9	Clear monophasic	No
<b>ME#8</b>	Oleic acid: RH 40 / Pyrrol	3:7	Clear monophasic	No

Table 28 shows that all formulations were not separated and stilled monophasic without any MBZ precipitation after the centrifugation stress test.

**4.12 Permeation study using Franz diffusion cells**

The cumulative amount of mebendazole permeated (mg/cm<sup>2</sup>) was calculated and displayed as a function of time. The slope of the linear portion of this plot showed the steady-state flux of mebendazole (mg/cm<sup>2</sup>/h) through the polyamide and Start-M membranes. In addition, the other permeation parameters such as Diffusion coefficient

(D), Permeability coefficient (P), Lag time ( $T_L$ ), and Partition coefficient (K) were calculated depending on the plot of the cumulative amount of mebendazole permeated with time for each formulation as shown in the following tables and plots.

**4.12.1 Permeation study using nylon (polyamide) 100  $\mu$ m membrane**

*a) For formulation ME#4 (Oleic acid: T80/Pyrrol) (3:7)*

**Table 30: Data obtained from Franz diffusion cells for formulation ME#4 (Oleic acid: T80/Pyrrol) using polyamide membrane.**

<b>Time (hr.)</b>	<b>Avg. area 1</b>	<b>Avg. area 2</b>	<b>Avg. area 3</b>	<b>Conc. 1 (mg/ml)</b>	<b>Conc. 2 (mg/ml)</b>	<b>Conc. 3 (mg/ml)</b>
0.5	4.40	4.63	4.63	0.0015	0.0016	0.0016
1	14.90	14.90	14.98	0.0055	0.0055	0.0056
2	31.17	29.60	30.50	0.0118	0.0112	0.0117
3	43.37	41.30	42.41	0.0164	0.0156	0.016
4	52.17	49.03	51.87	0.0198	0.0186	0.0191
5	55.27	50.70	55.21	0.021	0.0192	0.02

**Table 31:Data obtained from Franz diffusion cells for formulation ME#4 (Oleic acid: T80/Pyrrrol) using polyamide membrane.**

<b>Time (hr.)</b>	<b>Q: cumulative amount released 1 (mg)</b>	<b>Q: cumulative amount released 2 (mg)</b>	<b>Q: cumulative amount released 3 (mg)</b>	<b>m: cumulative amount released 1 (mg/cm<sup>2</sup>)</b>	<b>m cumulative amount released 2 (mg/cm<sup>2</sup>)</b>	<b>m: cumulative amount released 3 (mg/cm<sup>2</sup>)</b>	<b>Mean</b>	<b>SD</b>	<b>%RSD</b>
<b>0.5</b>	0.0015	0.0016	0.0016	0.000	0.001	0.001	0.000	0.000	3.685
<b>1</b>	0.007	0.0071	0.0072	0.002	0.002	0.002	0.002	0.000	1.408
<b>2</b>	0.0188	0.0183	0.0189	0.006	0.006	0.006	0.006	0.000	1.722
<b>3</b>	0.0352	0.0339	0.0349	0.011	0.011	0.011	0.011	0.000	1.964
<b>4</b>	0.055	0.0525	0.054	0.018	0.017	0.017	0.017	0.000	2.337
<b>5</b>	0.076	0.0717	0.074	0.024	0.023	0.024	0.024	0.001	2.912

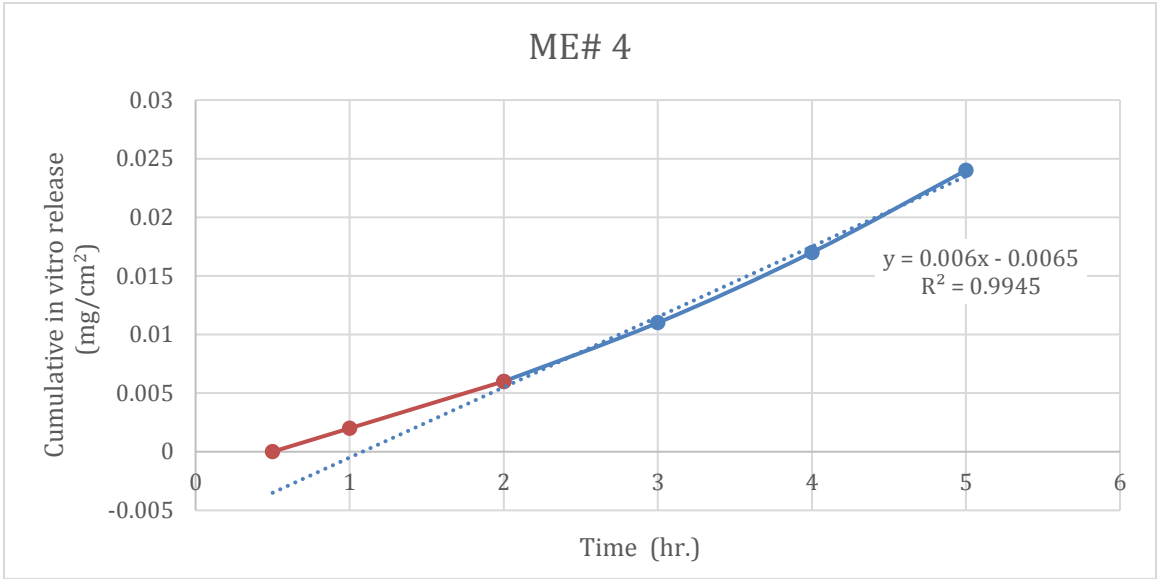


Figure 26: In vitro cumulative permeation profile of formulation ME#4 obtained from studies in Franz Diffusion Cells using polyamide membrane.

Table 32: Diffusion parameters for formulation ME#4:

Formulation #	Slope	y-intercept	TL	D	P	K
ME#4	0.0060	0.0065	1.083	0.0015	0.0093	0.6028

**b) For formulation ME#6 (IPP: T80/DEGME) (3:7)**

**Table 33:Data obtained from Franz diffusion cells for formulation ME#6 (IPP: T80/DEGME) using polyamide membrane.**

<b>Time (hr.)</b>	<b>Avg. area 1</b>	<b>Avg. area 2</b>	<b>Avg. area 3</b>	<b>Conc. 1 (mg/ml)</b>	<b>Conc. 2 (mg/ml)</b>	<b>Conc. 3 (mg/ml)</b>
0.5	3.57	6.70	5.27	0.0012	0.0024	0.0019
1	17.27	31.67	19.20	0.0064	0.012	0.0072
2	38.67	59.07	45.90	0.0146	0.0224	0.0174
3	58.17	83.23	59.40	0.0221	0.0317	0.0226
4	79.97	115.67	85.80	0.0304	0.0441	0.0327
5	104.57	124.77	86.70	0.0398	0.0476	0.033



**Table 34 :Data obtained from Franz diffusion cells for formulation ME#6 (IPP: T80/DEGME) using polyamide membrane.**

<b>Time (hr.)</b>	<b>Q: cumulative amount released 1 (mg)</b>	<b>Q: cumulative amount released 2 (mg)</b>	<b>Q: cumulative amount released 3 (mg)</b>	<b>m: cumulative amount released 1 (mg/cm<sup>2</sup>)</b>	<b>m cumulative amount released 2 (mg/cm<sup>2</sup>)</b>	<b>m: cumulative amount released 3 (mg/cm<sup>2</sup>)</b>	<b>mean</b>	<b>SD</b>	<b>%RSD</b>
<b>0.5</b>	0.0012	0.0024	0.0019	0.000	0.001	0.001	0.001	0.000	32.878
<b>1</b>	0.0076	0.0144	0.0091	0.002	0.005	0.003	0.003	0.001	34.462
<b>2</b>	0.0222	0.0368	0.0265	0.007	0.012	0.008	0.009	0.002	26.325
<b>3</b>	0.0443	0.0685	0.0491	0.014	0.022	0.016	0.017	0.004	23.742
<b>4</b>	0.0747	0.1126	0.0818	0.024	0.036	0.026	0.029	0.006	22.461
<b>5</b>	0.1145	0.1602	0.1148	0.036	0.051	0.037	0.041	0.008	20.256

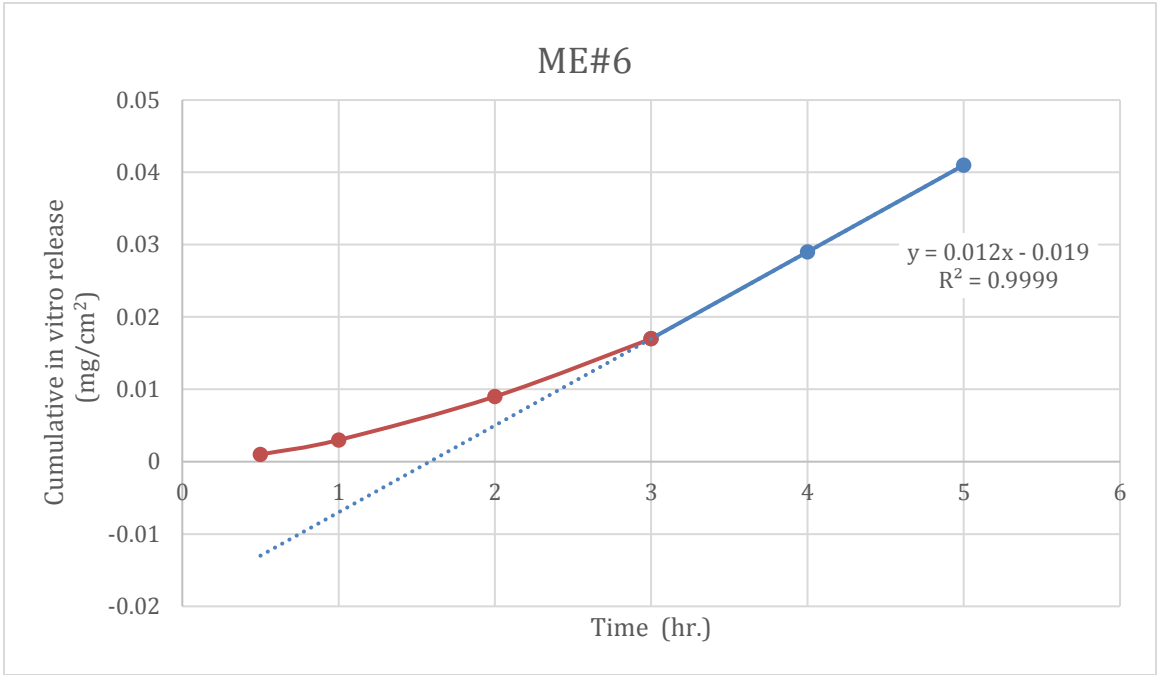


Figure 27::In vitro cumulative permeation profile of formulation ME#6 obtained from studies in Franz Diffusion Cells using polyamide membrane.

Table 35:Diffusion parameters for formulation ME#6.

Formulation #	Slope	y-intercept	TL	D	P	K
ME#6	0.0120	0.0190	1.583	0.0011	0.0172	1.633

**c) For formulation ME#7 (Oleic: RH40/Pyrrrol) (1:9)**

**Table 36 : Data obtained from Franz diffusion cells for formulation ME#7 (Oleic: RH40/Pyrrrol) using polyamide membrane.**

<b>Time (hr.)</b>	<b>Avg. area 1</b>	<b>Avg. area 2</b>	<b>Avg. area 3</b>	<b>Conc. 1 (mg/ml)</b>	<b>Conc. 2 (mg/ml)</b>	<b>Conc. 3 (mg/ml)</b>
<b>0.5</b>	16.97	21.23	17.1	0.0063	0.008	0.0066
<b>1</b>	46.80	52.90	51.72	0.0177	0.0201	0.019
<b>2</b>	91.93	95.60	95.5	0.035	0.0364	0.036
<b>3</b>	138.57	126.30	136.12	0.0529	0.0482	0.051
<b>4</b>	164.63	151.90	160.4	0.0628	0.058	0.0601
<b>5</b>	165.13	159.17	164.97	0.063	0.0607	0.0628

**Table 37 : Data obtained from Franz diffusion cells for formulation ME#7 (Oleic: RH40/Pyrrrol) using polyamide membrane.**

<b>Time (hr.)</b>	<b>Q: cumulative amount released 1 (mg)</b>	<b>Q: cumulative amount released 2 (mg)</b>	<b>Q: cumulative amount released 3 (mg)</b>	<b>m: cumulative amount released 1 (mg/cm<sup>2</sup>)</b>	<b>m cumulative amount released 2 (mg/cm<sup>2</sup>)</b>	<b>m: cumulative amount released 3 (mg/cm<sup>2</sup>)</b>	<b>mean</b>	<b>SD</b>	<b>%RSD</b>
<b>0.5</b>	0.0063	0.008	0.0066	0.002	0.003	0.002	0.002	0.000	13.025
<b>1</b>	0.024	0.0281	0.0256	0.008	0.009	0.008	0.008	0.001	7.978
<b>2</b>	0.059	0.0645	0.0616	0.019	0.021	0.020	0.020	0.001	4.459
<b>3</b>	0.1119	0.1127	0.1126	0.036	0.036	0.036	0.036	0.000	0.388
<b>4</b>	0.1747	0.1707	0.1727	0.056	0.054	0.055	0.055	0.001	1.158
<b>5</b>	0.2377	0.2314	0.2355	0.076	0.074	0.075	0.075	0.001	1.361

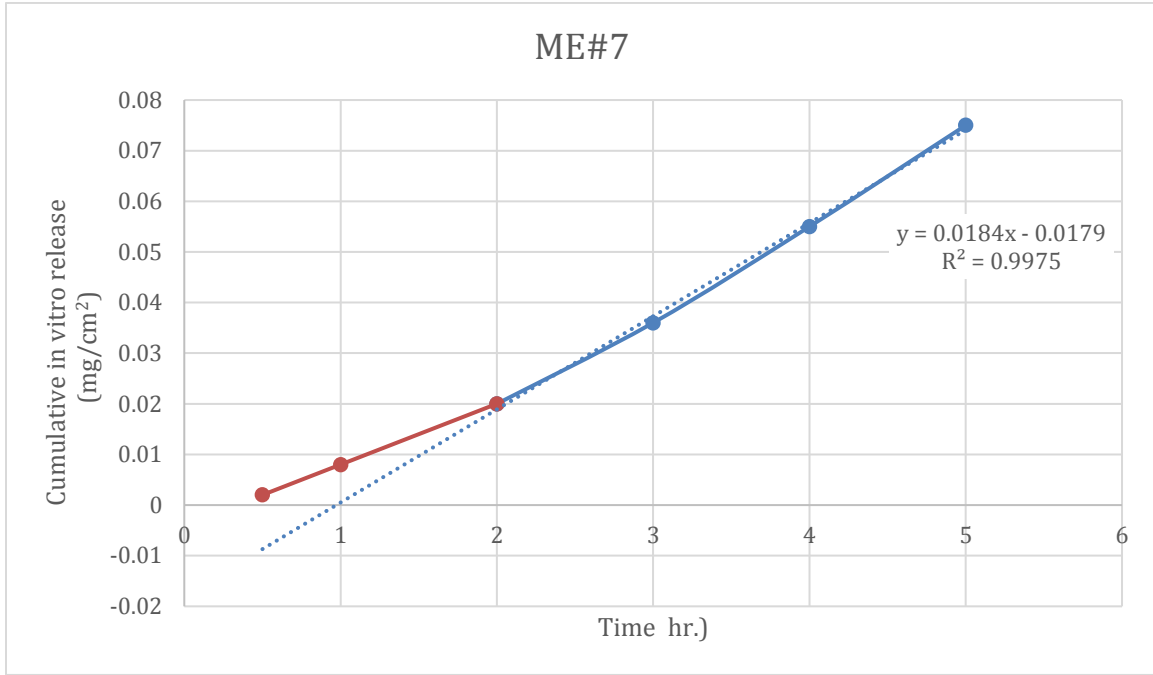


**Figure 28:**In vitro cumulative permeation profile of formulation ME#7 obtained from studies in Franz Diffusion Cells using polyamide membranes.

**Table 38:**Diffusion parameters for formulation ME#7.

Formulation #	Slope	y-intercept	TL	D	P	K
ME#7	0.0184	0.0179	0.973	0.0017	0.0362	2.114

**d) For formulation ME#8 (Oleic: RH40/Pyrrrol) (3:7)**

**Table 39: Data obtained from Franz diffusion cells for formulation ME#8 (Oleic: RH40/Pyrrrol) using polyamide membrane.**

<b>Time (hr.)</b>	<b>Avg. area 1</b>	<b>Avg. area 2</b>	<b>Avg. area 3</b>	<b>Conc. 1 (mg/ml)</b>	<b>Conc. 2 (mg/ml)</b>	<b>Conc. 3 (mg/ml)</b>
<b>0.5</b>	4.97	5.23	13.40	0.0017	0.0018	0.005
<b>1</b>	11.10	12.17	36.10	0.0041	0.0045	0.0137
<b>2</b>	14.37	27.77	74.07	0.0053	0.0105	0.0282
<b>3</b>	35.60	43.20	112.77	0.0135	0.0164	0.043
<b>4</b>	43.70	60.67	145.13	0.0166	0.0231	0.0554
<b>5</b>	60.23	75.00	193.53	0.0229	0.0285	0.0739

**Table 40 : Data obtained from Franz diffusion cells for formulation ME#8 (Oleic: RH40/Pyrrrol) using polyamide membrane.**

<b>Time (hr.)</b>	<b>Q: cumulative amount released 1 (mg)</b>	<b>Q: cumulative amount released 2 (mg)</b>	<b>Q: cumulative amount released 3 (mg)</b>	<b>m: cumulative amount released 1 (mg/cm<sup>2</sup>)</b>	<b>m cumulative amount released 2 (mg/cm<sup>2</sup>)</b>	<b>m: cumulative amount released 3 (mg/cm<sup>2</sup>)</b>	<b>mean</b>	<b>SD</b>	<b>%RSD</b>
<b>0.5</b>	0.0017	0.0018	0.005	0.001	0.001	0.002	0.001	0.001	66.249
<b>1</b>	0.0058	0.0063	0.0187	0.002	0.002	0.006	0.003	0.002	71.179
<b>2</b>	0.0111	0.0168	0.0469	0.004	0.005	0.015	0.008	0.006	77.150
<b>3</b>	0.0246	0.0332	0.0899	0.008	0.011	0.029	0.016	0.011	72.065
<b>4</b>	0.0412	0.0563	0.1453	0.013	0.018	0.046	0.026	0.018	69.504
<b>5</b>	0.0641	0.0848	0.2192	0.020	0.027	0.070	0.039	0.027	68.631

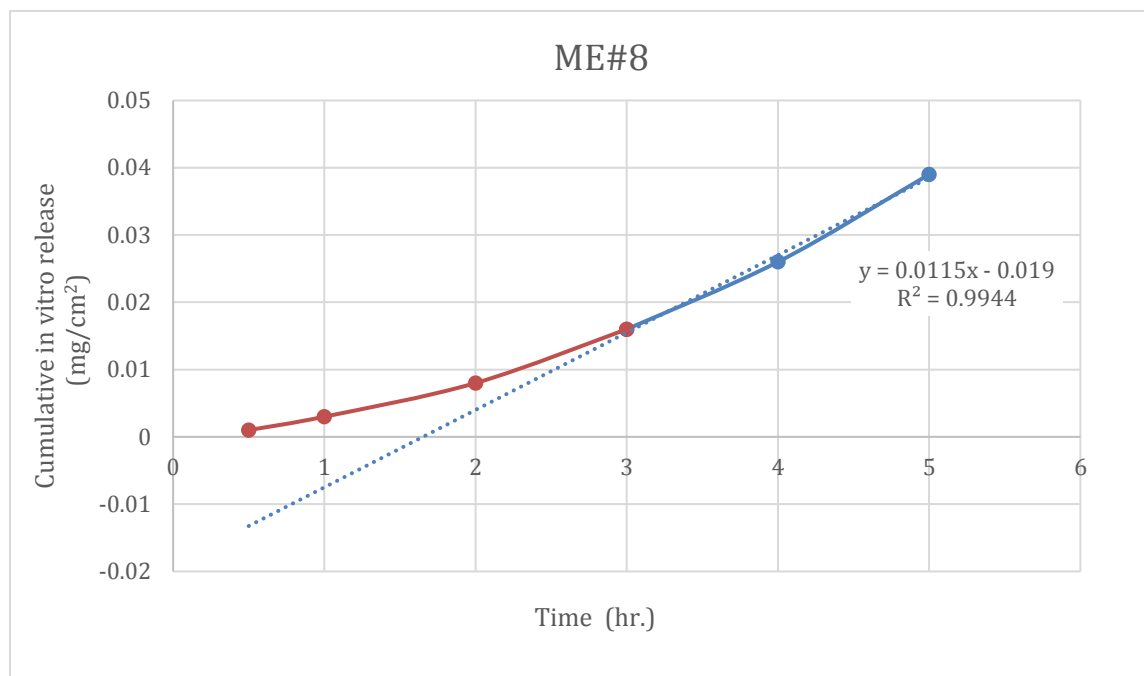


Figure 29: In vitro cumulative permeation profile of formulation ME#8 obtained from studies in Franz Diffusion Cells using polyamide membranes.

Table 41: Diffusion parameters for formulation ME#8.

Formulation #	Slope	y-intercept	TL	D	P	K
ME#8	0.0115	0.0190	1.652	0.0010	0.0155	1.538



e) In vitro cumulative permeation profile of all Formulations

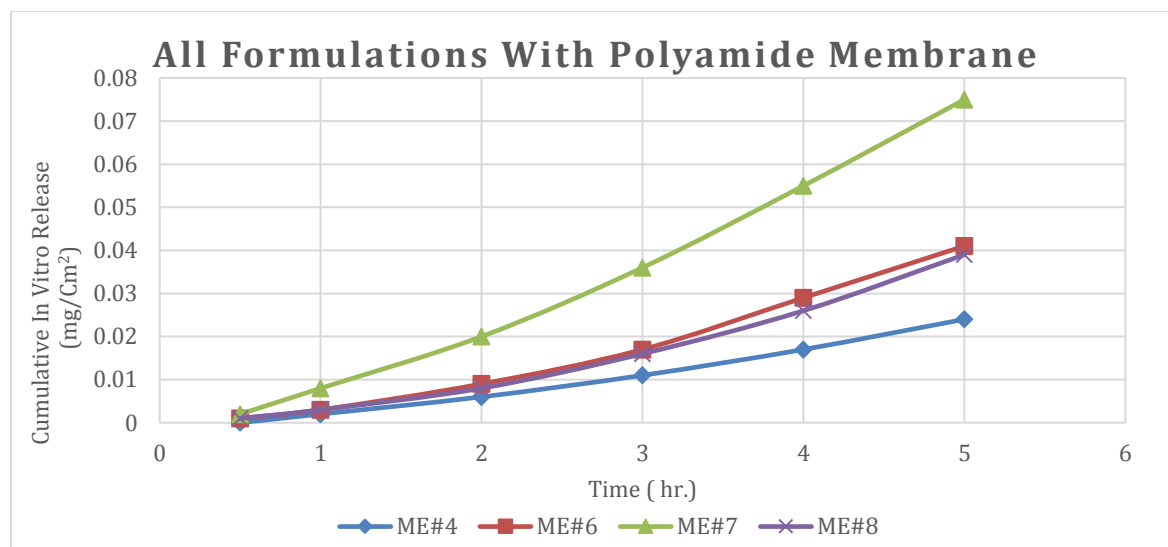


Figure 30: In vitro cumulative permeation profile of formulations ME#4, ME#6, ME#7 and ME#8 obtained from studies in Franz Diffusion Cells using polyamide membrane.

Table 42: Steady state flux for microemulsion formulations (with polyamide membrane).

Formulation	$J_{ss}$ (mg/cm <sup>2</sup> /h)
ME#4	0.0068
ME#6	0.0119
ME#7	0.0212
ME#8	0.0119

In vitro cumulative permeation profiles of all microemulsion formulations are shown in Figure 30, and the steady-state flux of mebendazole in the microemulsion formulations are shown in Table 41. The steady-state flux was calculated from the linear portion observed during this period (from 2 or 3 to 5 hours).

Among all formulations, ME#7 showed the highest permeation flux of mebendazole (0.0212 mg/cm<sup>2</sup>/h) at 5 hours, followed by ME#6 and ME#8, then ME#7 which has the lowest permeation flux of mebendazole.

#### 4.12.2 Permeation study using Start-M membrane 300 $\mu\text{m}$

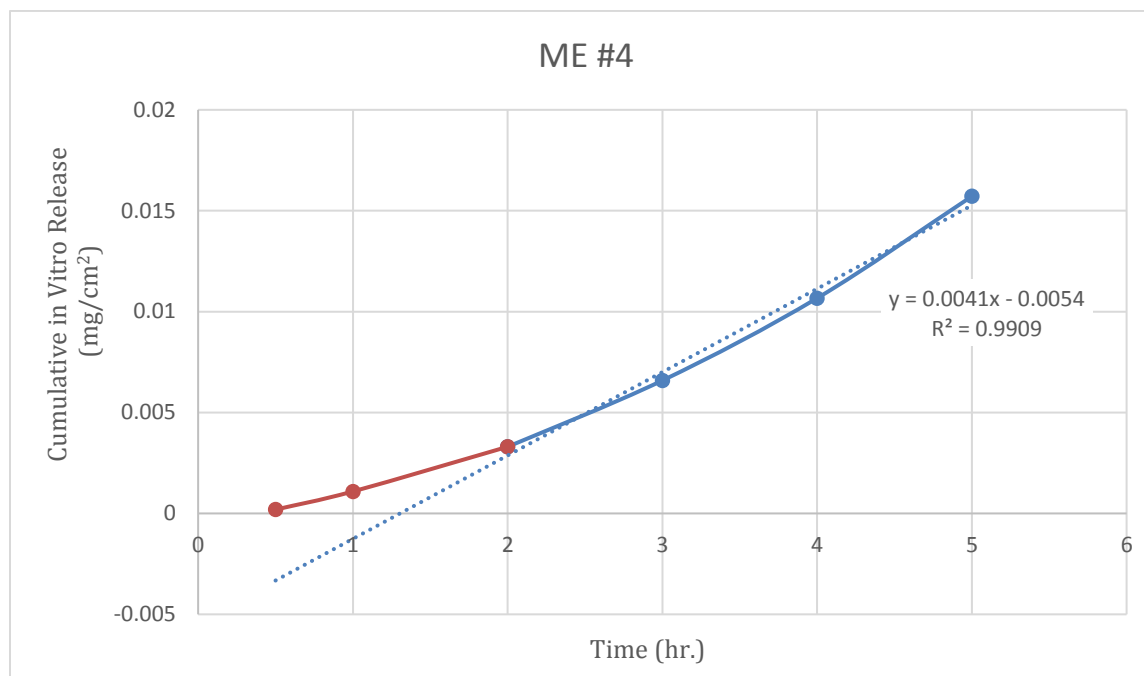
a) For formulation ME#4 (Oleic acid: T80/Pyrrrol) (3:7)

Table 43: Data obtained from Franz diffusion cells for formulations trial ME#4 (Oleic acid: T80/Pyrrrol) using Start-M membrane.

Time (hr.)	Avg. area 1	Avg. area 2	Avg. area 3	Conc. 1 (mg/ml)	Conc. 2 (mg/ml)	Conc. 3 (mg/ml)
0.5	1.87	3.10	0.99	0.0006	0.0010	0.0002
1	4.27	16.73	2.43	0.0015	0.0062	0.0008
2	9.50	39.60	6.70	0.0035	0.0150	0.0024
3	14.87	55.43	11.80	0.0055	0.0210	0.0044
4	20.43	65.03	16.23	0.0077	0.0247	0.0060
5	25.37	80.00	20.17	0.0095	0.0304	0.0076

**Table 44: Data obtained from Franz diffusion cells for formulation ME#4 (Oleic acid: T80/Pyrrrol) using Start-M membrane.**

Time (hr.)	Q: cumulative amount released 1 (mg)	Q: cumulative amount released 2 (mg)	Q: cumulative amount released 3 (mg)	m: cumulative amount released 1 (mg/cm <sup>2</sup> )	m cumulative amount released 2 (mg/cm <sup>2</sup> )	m: cumulative amount released 3 (mg/cm <sup>2</sup> )	mean	SD	%RSD
0.5	0.0006	0.0010	0.0002	0.0002	0.0003	0.0001	0.0002	0.0001	66.67
1	0.0020	0.0073	0.0010	0.0006	0.0023	0.0003	0.0011	0.0011	98.38
2	0.0055	0.0223	0.0034	0.0017	0.0071	0.0011	0.0033	0.0033	99.65
3	0.0110	0.0433	0.0077	0.0035	0.0138	0.0025	0.0066	0.0063	95.02
4	0.0187	0.0680	0.0138	0.0059	0.0217	0.0044	0.0107	0.0096	89.58
5	0.0282	0.0985	0.0213	0.0090	0.0314	0.0068	0.0157	0.0136	86.51



**Figure 31:** In vitro cumulative permeation profile of formulation ME#4 obtained from studies in Franz Cell using Start-M membranes.

**Table 45:** Diffusion parameters for formulation ME#4:

Formulation #	Slope	y-intercept	TL	D	P	K
ME#4	0.0041	0.0054	1.317	0.0114	0.0059	0.2331

***b) For formulation ME#6 (IPP: T80/DEGME) (3:7)***

**Table 46: Data obtained from Franz diffusion cells for formulation ME#6 (IPP: T80/DEGME) using Start-M membrane.**

<b>Time (hr.)</b>	<b>Avg. area 1</b>	<b>Avg. area 2</b>	<b>Avg. area 3</b>	<b>Conc. 1 (mg/ml)</b>	<b>Conc. 2 (mg/ml)</b>	<b>Conc. 3 (mg/ml)</b>
<b>0.5</b>	2.20	2.57	3.93	0.0007	0.0008	0.0013
<b>1</b>	4.97	5.83	42.77	0.0017	0.0021	0.0162
<b>2</b>	11.77	13.00	83.33	0.0043	0.0048	0.0317
<b>3</b>	18.50	19.83	118.90	0.0069	0.0074	0.0453
<b>4</b>	23.60	24.40	272.57	0.0089	0.0092	0.1041
<b>5</b>	29.73	29.77	388.53	0.0112	0.0112	0.1485

**Table 47: Data obtained from Franz diffusion cells for formulation ME#6 (IPP: T80/DEGME) using Start-M membrane.**

<b>Time (hr.)</b>	<b>Q: cumulative amount released 1 (mg)</b>	<b>Q: cumulative amount released 2 (mg)</b>	<b>Q: cumulative amount released 3 (mg)</b>	<b>m: cumulative amount released 1 (mg/cm<sup>2</sup>)</b>	<b>m: cumulative amount released 2 (mg/cm<sup>2</sup>)</b>	<b>m: cumulative amount released 3 (mg/cm<sup>2</sup>)</b>	<b>mean</b>	<b>SD</b>	<b>%RSD</b>
<b>0.5</b>	0.0007	0.0008	0.0013	0.0002	0.0003	0.0004	0.0002	0.0000	9.43
<b>1</b>	0.0024	0.0029	0.0175	0.0008	0.0009	0.0056	0.0008	0.0001	13.34
<b>2</b>	0.0067	0.0077	0.0492	0.0021	0.0025	0.0157	0.0023	0.0002	9.82
<b>3</b>	0.0136	0.0151	0.0945	0.0043	0.0048	0.0301	0.0046	0.0003	7.39
<b>4</b>	0.0225	0.0243	0.1986	0.0072	0.0077	0.0632	0.0075	0.0004	5.44
<b>5</b>	0.0337	0.0355	0.3471	0.0107	0.0113	0.1105	0.0110	0.0004	3.68

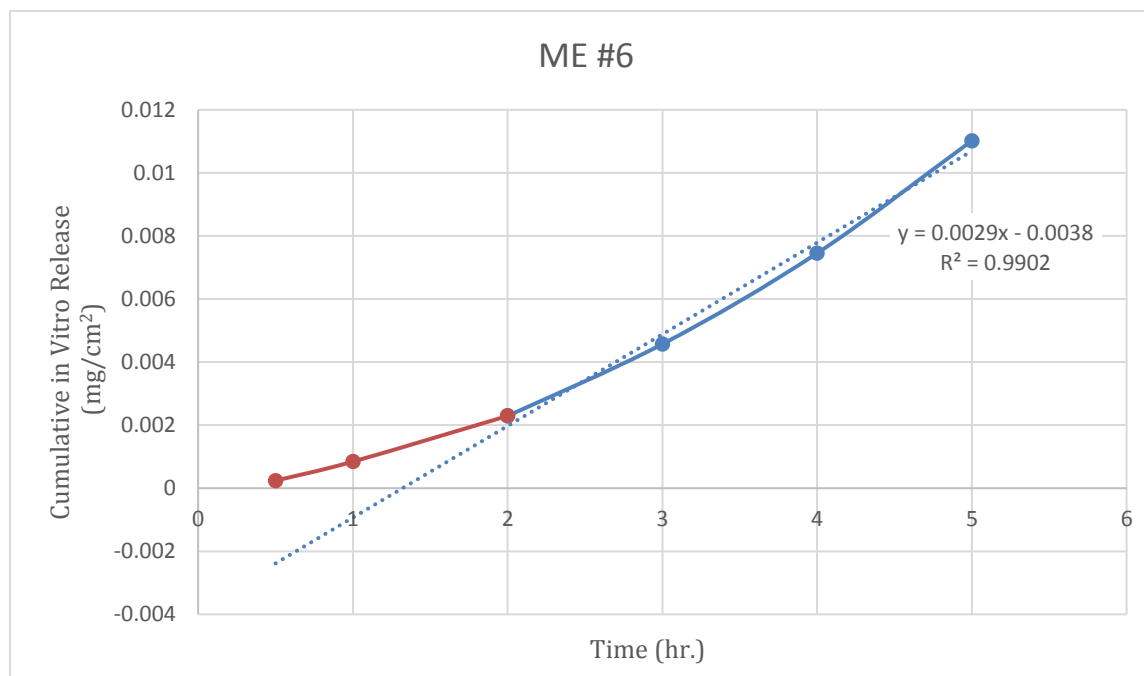


**Figure 32:**In vitro cumulative permeation profile of formulation ME#6 obtained from studies in Franz Cell using Start-M membranes.

**Table 48:** Diffusion parameters for formulation ME#6:

Formulation #	Slope	y-intercept	TL	D	P	K
ME#6	0.0029	0.0038	1.310	0.0115	0.0039	0.1557



**c) For formulation ME#7 (Oleic: RH 40/Pyrrrol) (1:9)**

**Table 49: Data obtained from Franz diffusion cells for formulation ME#7 (Oleic: RH 40/Pyrrrol) using Start-M membrane.**

<b>Time (hr.)</b>	<b>Avg. area 1</b>	<b>Avg. area 2</b>	<b>Avg. area 3</b>	<b>Conc. 1 (mg/ml)</b>	<b>Conc. 2 (mg/ml)</b>	<b>Conc. 3 (mg/ml)</b>
<b>0.5</b>	0.75	1.23	0.60	0.0001	0.0003	0.0001
<b>1</b>	1.80	3.43	1.70	0.0005	0.0012	0.0005
<b>2</b>	5.60	9.87	5.30	0.0020	0.0036	0.0019
<b>3</b>	10.20	16.97	9.53	0.0037	0.0063	0.0035
<b>4</b>	14.07	22.70	13.63	0.0052	0.0085	0.0051
<b>5</b>	17.80	28.40	17.77	0.0066	0.0107	0.0066

**Table 50: Data obtained from Franz diffusion cells for formulation ME#7 (Oleic: RH 40/Pyrrrol) using Start-M membrane.**

Time (hr.)	Q: cumulative amount released 1 (mg)	Q: cumulative amount released 2 (mg)	Q: cumulative amount released 3 (mg)	m: cumulative amount released 1 (mg/cm <sup>2</sup> )	m cumulative amount released 2 (mg/cm <sup>2</sup> )	m: cumulative amount released 3 (mg/cm <sup>2</sup> )	Mean	SD	%RSD
0.5	0.0001	0.0003	0.0001	0.0000	0.0001	0.0000	0.0001	0.0000	69.28
1	0.0006	0.0015	0.0006	0.0002	0.0005	0.0002	0.0003	0.0002	57.74
2	0.0026	0.0051	0.0025	0.0008	0.0016	0.0008	0.0011	0.0005	43.33
3	0.0063	0.0114	0.0060	0.0020	0.0036	0.0019	0.0025	0.0010	38.42
4	0.0115	0.0199	0.0111	0.0037	0.0063	0.0035	0.0045	0.0016	35.08
5	0.0181	0.0306	0.0177	0.0058	0.0097	0.0056	0.0070	0.0023	33.14

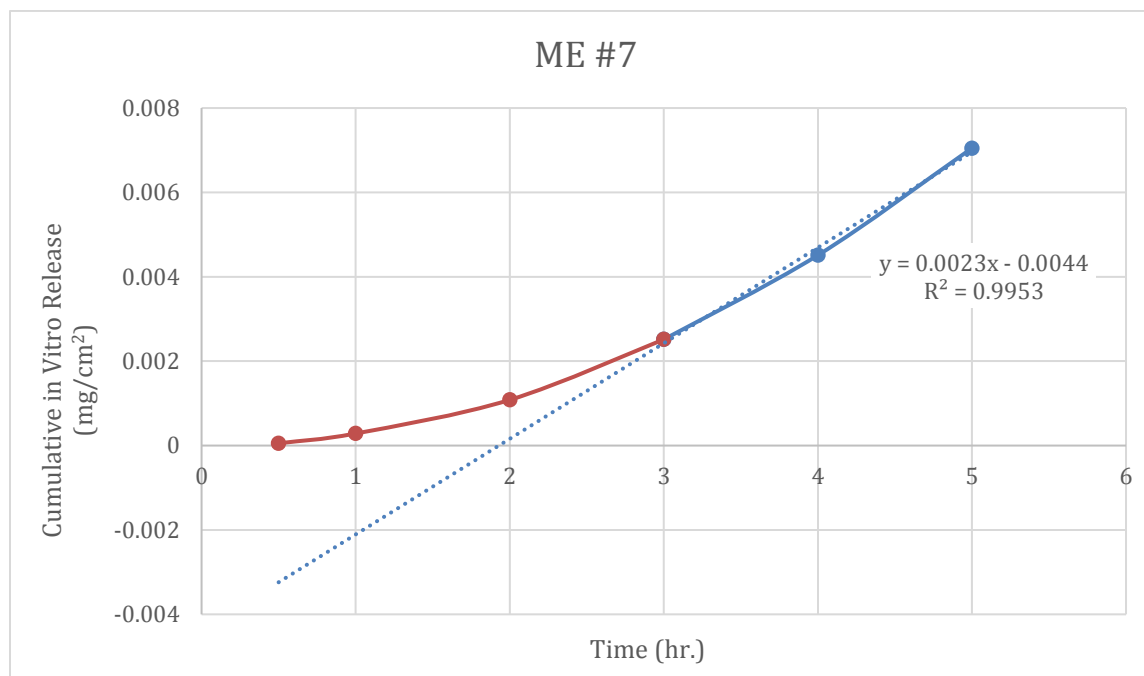


**Figure 33:**In vitro cumulative permeation profile of formulation ME#7 obtained from studies in Franz Cell using Start-M membranes.

**Table 51:**Diffusion parameters for formulation ME#7.

Formulation #	Slope	y-intercept	TL	D	P	K
ME#7	0.0023	0.0044	1.913	0.0078	0.0036	0.2082

**d) For formulation ME#8 (Oleic: RH 40/ Pyrrol) (3:7)**

**Table 52: Data obtained from Franz diffusion cells for formulation ME#8 (Oleic: RH 40/Pyrrol) using Start-M membrane.**

<b>Time (hr.)</b>	<b>Avg. area 1</b>	<b>Avg. area 2</b>	<b>Avg. area 3</b>	<b>Conc. 1 (mg/ml)</b>	<b>Conc. 2 (mg/ml)</b>	<b>Conc. 3 (mg/ml)</b>
<b>0.5</b>	0.54	0.86	0.26	0.0000	0.0002	0.0000
<b>1</b>	1.23	1.97	5.37	0.0003	0.0006	0.0019
<b>2</b>	3.70	5.00	13.90	0.0013	0.0018	0.0052
<b>3</b>	8.63	8.30	24.07	0.0031	0.0030	0.0090
<b>4</b>	12.73	9.60	31.40	0.0047	0.0035	0.0119
<b>5</b>	18.20	13.10	38.07	0.0068	0.0048	0.0144

**Table 53: Data obtained from Franz diffusion cells for formulation ME#8 (Oleic: RH 40/Pyrrrol) using Start-M membrane.**

<b>Time (hr.)</b>	<b>Q: cumulative amount released 1 (mg)</b>	<b>Q: cumulative amount released 2 (mg)</b>	<b>Q: cumulative amount released 3 (mg)</b>	<b>m: cumulative amount released 1 (mg/cm<sup>2</sup>)</b>	<b>m: cumulative amount released 2 (mg/cm<sup>2</sup>)</b>	<b>m: cumulative amount released 3 (mg/cm<sup>2</sup>)</b>	<b>Mean</b>	<b>SD</b>	<b>%RSD</b>
<b>0.5</b>	0.0000	0.0002	0.0000	0.0000	0.0001	0.0000	0.0000	0.0000	173.21
<b>1</b>	0.0003	0.0008	0.0019	0.0001	0.0003	0.0006	0.0003	0.0003	81.85
<b>2</b>	0.0016	0.0026	0.0071	0.0005	0.0008	0.0023	0.0012	0.0009	77.78
<b>3</b>	0.0047	0.0056	0.0161	0.0015	0.0018	0.0051	0.0028	0.0020	72.02
<b>4</b>	0.0094	0.0091	0.0280	0.0030	0.0029	0.0089	0.0049	0.0034	69.85
<b>5</b>	0.0162	0.0139	0.0424	0.0052	0.0044	0.0135	0.0077	0.0050	65.51

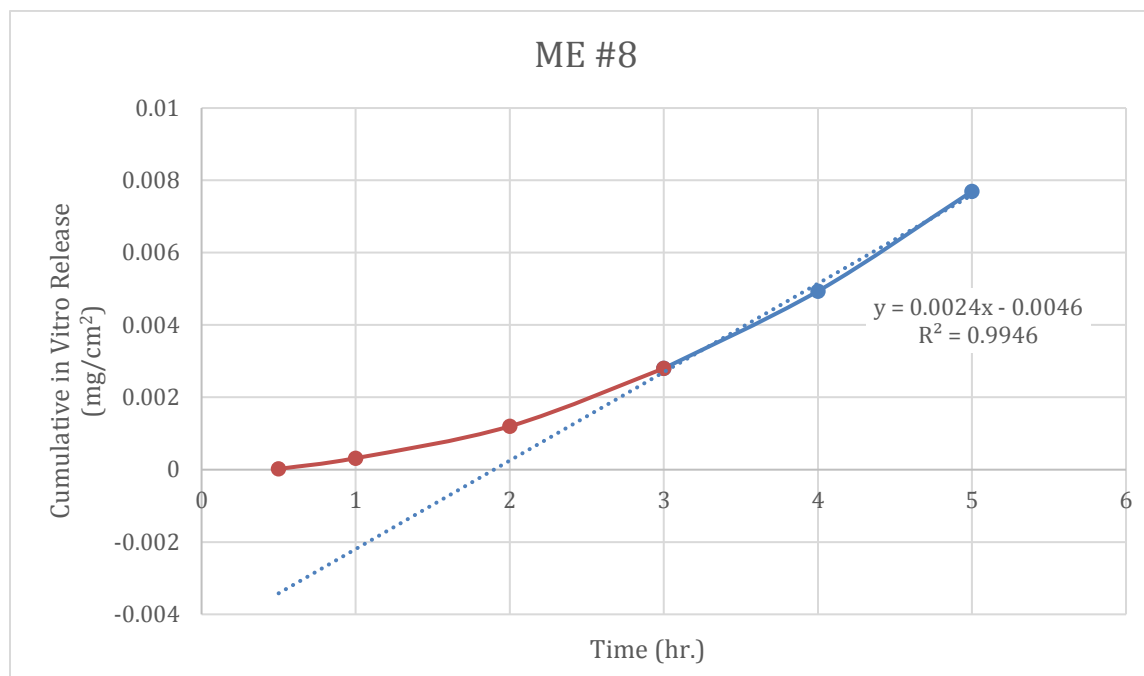


**Figure 34:** In vitro cumulative permeation profile of formulation ME#8 obtained from studies in Franz Cell using Start-M membranes.

**Table 54:** Diffusion parameters for formulation ME#8:

Formulation #	Slope	y-intercept	TL	D	P	K
<b>ME#8</b>	0.0024	0.0046	1.917	0.0078	0.0038	0.2177

e) All formulations

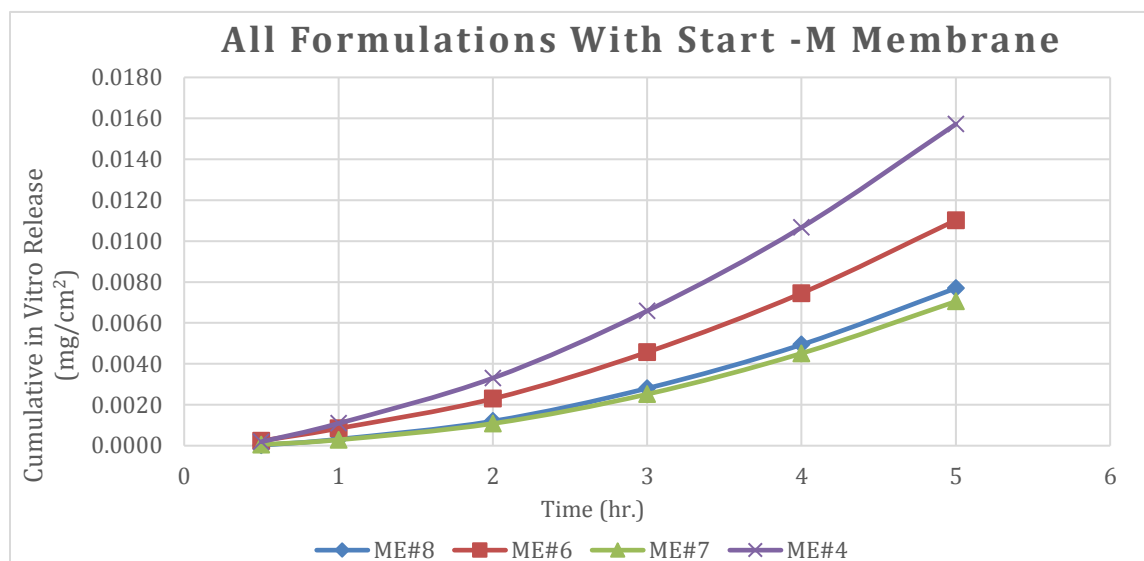


Figure 35: In vitro cumulative permeation profile of formulations ME#4, ME#6, ME#7 and ME#8 obtained from studies in Franz Diffusion Cells using Start-M membrane.

Table 52: Steady state flux for microemulsion formulations (with Start-M membrane).

Formulation	$J_{ss}$ (mg/cm <sup>2</sup> /h)
ME#4	0.0042
ME#6	0.0029
ME#7	0.0023
ME#8	0.0024

In vitro cumulative permeation profiles of all microemulsion formulations are shown in Figure 35, and the steady-state flux of mebendazole in the microemulsion formulations are shown in Table 52. The steady-state flux was calculated from the linear portion that observed during this period (from 2 or 3 to 5 hours).

As the ratio of oleic acid increases , the permeation flux of drug through biological membranes increases. (*Jafri et al. 2019*) Among all formulations, ME#4 which has the highest ratio of oleic acid as oily phase showed the highest permeation flux of mebendazole (0.0042 mg/cm<sup>2</sup>/h) at 5 hours, followed by ME#6 which has a high ratio of isopropyl palmitate as oily phase, then ME#8 which contains less ratio of oleic acid than ME#4, and ME#7 which has the lowest ratio of oleic acid.

➤ ***Summary of permeation study results using polyamide and Start-M membrane***

As describes in Table 54, polyamide membrane showed better permeation results than Start-M<sup>®</sup> membrane. That refers to the difference between the thickness and physical properties of the two membranes. Besides, the composition and properties of the Start-M<sup>®</sup> membrane make it very similar to the properties of human skin layers.



**Table 55: Permeation parameters for microemulsion formulations using polyamide and Start-M membranes.**

<b>Formulation</b>	<b>Polyamide membrane</b>			<b>Start- M® membrane</b>		
	R <sup>2</sup>	<i>P</i> value	J <sub>ss</sub> (mg/cm <sup>2</sup> /h)	R <sup>2</sup>	<i>P</i> value	J <sub>ss</sub> (mg/cm <sup>2</sup> /h)
<b>ME#4</b>	0.9945	0.0093	0.0068	0.9909	0.0059	0.0042
<b>ME#6</b>	0.9999	0.0172	0.0119	0.9902	0.0039	0.0029
<b>ME#7</b>	0.9975	0.0362	0.0212	0.9953	0.0036	0.0023
<b>ME#8</b>	0.9944	0.0155	0.0119	0.9946	0.0038	0.0024

## Chapter 5

### Conclusion

In this study, different microemulsion formulations for mebendazole were designed using pseudo-ternary phase diagrams. pharmaceutical development, physical and chemical characterization, stability, and in vitro permeation studies using synthetic membranes were performed for four O/W microemulsion formulations.

The four selected microemulsion formulations were ME#4 (Oleic acid: T80/ Pyrrol 3:7), ME#6 (IPP: T80/DEGME 3:7), ME#7 (Oleic acid: RH 40/ Pyrrol 1:9), and ME#8 (Oleic acid: RH 40 / Pyrrol 3:7). The stability in terms of the droplet size, visual appearance, and assay was conducted and the four microemulsion formulations were stable over the period of study.

The permeation experiments were performed with polyamide and Strat-M® membranes in phosphate buffer pH7.4 +20% v/v PEG 400. The mebendazole permeation flux of microemulsion formulations through polyamide membrane was comparatively greater than the mebendazole permeation flux of microemulsion formulations through the Start-M membrane using Franz diffusion cells for 5 hours. That refers to the difference between the thickness and

physical properties of the two membranes. Where the composition and properties of Start-M<sup>®</sup> membrane make it very similar to the properties of human skin layers.

In permeation experiments using Start-M<sup>®</sup> membrane, ME#4 which has the highest ratio of oleic acid as oily phase showed the highest permeation flux of mebendazole (0.0042 mg/cm<sup>2</sup>/h) at 5 hours, followed by ME#6 which has a high ratio of isopropyl palmitate as oily phase, then ME#8 which contains less ratio of oleic acid than ME#4, and ME#7 which has the lowest ratio of oleic acid.

Since formulation ME#4 (Oleic acid: T80/ Pyrrol 3:7) containing the highest oleic acid revealed a good in vitro release and permeation of mebendazole, ME#4 was known to be the best-suited formulation amongst all for delivery of mebendazole across the skin safely and thus can be possibly used as an alternative delivery route for administration of mebendazole.

## **Future work**

1. Long-term stability study for the microemulsion formulations.
2. Compatibility study of mebendazole with different surfactants, co-surfactants, and oils.
3. Full validation HPLC method.
4. Evaluate the permeation of mebendazole on FDC at pH around 5 (similar to the skin).
5. Evaluate the permeation of mebendazole on FDC using animal skin.
6. Study the effect of microemulsion formulations of mebendazole on different types of cancer cells.

## References

- Acharya, Durga P., and Patrick G. Hartley. 2012. "Progress in Microemulsion Characterization." *Current Opinion in Colloid and Interface Science* 17 (5): 274–80.
- Alkilani, Ahlam Zaid, Maelíosa T C Mccrudden, and Ryan F Donnelly. 2015. "Transdermal Drug Delivery: Innovative Pharmaceutical Developments Based on Disruption of the Barrier Properties of the Stratum Corneum," 438–70.
- Aminpour, Shohreh, Abdollah Rafiei, Ali Jelowdar, and Maryam Kouchak. 2019. "Evaluation of the Protoscolicidal Effects of Albendazole and Albendazole Loaded Solid Lipid Nanoparticles." *Iranian Journal of Parasitology* 14 (1): 127–35.
- Anil, Landge, and Krishnamoorthy Kannan. 2018. "Microemulsion as Drug Delivery System for Peptides and Proteins." *Journal of Pharmaceutical Sciences and Research* 10 (1): 16–25.
- Arce, Florencio Jr, Narumi Asano, Gerard Lee See, Shoko Itakura, Hiroaki Todo, and Kenji Sugibayashi. 2020. "Usefulness of Artificial Membrane, Strat-M®, in the Assessment of Drug Permeation from Complex Vehicles in Finite Dose Conditions." *Pharmaceutics* 12 (2).
- Article, Review, Rohit Bhattacharya, and Sayantan Mukhopadhyay. 2016. "REVIEW ON MICROEMULSION- AS A POTENTIAL NOVEL DRUG" 5 (6): 700–729.
- Article, Review, Greater Noida, and Uttar Pradesh. 2014. "Futuristic Drug Delivery System Microemulsions : A Review" 2 (3): 54–60.
- Arun Desai, Sujit, Rishikesh Ajit Mohite, and Ashok A Hajare. 2015. "Screening of Safflower Oil Microemulsion for Enhancing Bioavailability of Lovastatin." *International Journal of Pharma Sciences and Research* 6 (1): 28–49.
- Ashok, J, S Lakshmana, and V Gopal. 2010. "TRANSDERMAL DRUG DELIVERY SYSTEM : AN OVERVIEW" 3 (2): 49–54.

Badawi, Alia A., Samia A. Nour, Wedad S. Sakran, and Shereen Mohamed Sameh El-Mancy. 2009. "Preparation and Evaluation of Microemulsion Systems Containing Salicylic Acid." *AAPS PharmSciTech* 10 (4): 1081–84.

Barkat Ali Khan,. 2011. "Basics of Pharmaceutical Emulsions: A Review." *African Journal of Pharmacy and Pharmacology* 5 (25).

Bartosova, L., and J. Bajgar. 2012. "Transdermal Drug Delivery In Vitro Using Diffusion Cells." *Current Medicinal Chemistry* 19 (27): 4671–77.

Basheer, Hussam S., Mohamed Ibrahim Noordin, and Mowafaq M. Ghareeb. 2013. "Characterization of Microemulsions Prepared Using Isopropyl Palmitate with Various Surfactants and Cosurfactants." *Tropical Journal of Pharmaceutical Research* 12 (3): 305–10.

Benigni, Marta, Silvia Pescina, Maria Aurora Grimaudo, Cristina Padula, Patrizia Santi, and Sara Nicoli. 2018. "Development of Microemulsions of Suitable Viscosity for Cyclosporine Skin Delivery." *International Journal of Pharmaceutics* 545 (1–2): 197–205.

Boer, Magdalena, Ewa Duchnik, Romuald Maleszka, and Mariola Marchlewicz. 2016. "Structural and Biophysical Characteristics of Human Skin in Maintaining Proper Epidermal Barrier Function," 1–5.

Brown, Marc B., Gary P. Martin, Stuart A. Jones, and Franklin K. Akomeah. 2006. "Dermal and Transdermal Drug Delivery Systems: Current and Future Prospects." *Drug Delivery: Journal of Delivery and Targeting of Therapeutic Agents* 13 (3): 175–87.

Buchter, Valentin, Josefina Priotti, Darío Leonardi, María C. Lamas, and Jennifer Keiser. 2020. "Activity of Novel Oral Formulations of Albendazole and Mebendazole against Heligmosomoides Polygyrus in Vitro and in Vivo." *Journal of Pharmaceutical Sciences*.

Callender, Shannon P., Jessica A. Mathews, Katherine Kobernyk, and Shawn D. Wettig. 2017. "Microemulsion Utility in Pharmaceuticals: Implications for Multi-Drug Delivery." *International Journal of Pharmaceutics* 526 (1–2): 425–42.

Chen, Liangmei, Fengping Tan, Jinfeng Wang, and Feng Liu. 2012a. "Assessment of the Percutaneous Penetration of Indomethacin from Soybean Oil Microemulsion : Effects of the HLB Value of Mixed Surfactants," 31–36.

Chen, Yang, Peng Quan, Xiaochang Liu, Manli Wang, and Liang Fang. 2014. "ScienceDirect Novel Chemical Permeation Enhancers for Transdermal Drug Delivery." *Asian Journal of Pharmaceutical Sciences* 9 (2): 51–64.

Cheng, Nelson, Honoris Causa, Patrick Moe, B Sc Grad Diploma, and M Sc. 2017. "Simplification Process of Determining the Mixing Oil Ratio for Ascertaining the Kinematic Viscosity Oil Mixtures Blended from 2 or More Based Oils with Different Viscosity . Kinetic Theory Approach to Viscosity Blending Calculations," no. 65.

Clément, Pascale, Cécile Laugel, and Jean Paul Marty. 2000. "Influence of Three Synthetic Membranes on the Release of Caffeine from Concentrated W/O Emulsions." *Journal of Controlled Release* 66 (2–3): 243–54.

CM, Jadhav. 2014. "Stability Study of Griseofulvin in Non Aqueous Microemulsion System." *Asian Journal of Biomedical and Pharmaceutical Sciences* 4 (35): 71–75.

Danaei, M., M. Dehghankhold, S. Ataei, F. Hasanzadeh Davarani, R. Javanmard, A. Dokhani, S. Khorasani, and M. R. Mozafari. 2018. "Impact of Particle Size and Polydispersity Index on the Clinical Applications of Lipidic Nanocarrier Systems." *Pharmaceutics* 10 (2): 1–17.

Doudican, Nicole A, Sara A Byron, Pamela M Pollock, and Seth J Orlow. n.d. "XIAP Downregulation Accompanies Mebendazole Growth Inhibition in Melanoma Xenografts" 2: 181–88.

Doudican, Nicole, Adrianna Rodriguez, Iman Osman, and Seth J Orlow. 2008. "Mebendazole Induces Apoptosis via Bcl-2 Inactivation in Chemoresistant Melanoma Cells" 6 (August): 1308–16.

Fanun, Monzer. 2012. "Microemulsion as Delivery Systems." *Current Opinion in Colloid & Interface Science* 17 (5): 306–13.

Fern, Shio Fern, Jennifer Rouse, Dominic Sanderson, and Gillian Eccleston. 2010. "A Comparative Study of Transmembrane Diffusion and Permeation of Ibuprofen across Synthetic Membranes Using Franz Diffusion Cells." *Pharmaceutics* 2 (2): 209–23.

Fonseca-Santos, Bruno, Maria Palmira Daflon Gremião, and Marlus Chorilli. 2015. "Nanotechnology-Based Drug Delivery Systems for the Treatment of Alzheimer's Disease." *International Journal of Nanomedicine* 10 (August).

Formulations, Ketoconazole K Z. 2013. "Artificial Membrane Selection for Franz Cell Diffusion Testing of Semi-Solid," no. October: 1–2.

Gaddam, Praveen, P Muthuprasanna, K Suriyaprabha, J Manojkumar, Bharghav Bhushan Rao, and Raju. Jukanti. 2009. "Diffusion Cells for Measuring Skin Permeation in Vitro." *Materials Science: An Indian Journal* 5 (3): 277–87.

Gadhve, Ashish D, and Jyotsna T Waghmare. 2014. "A SHORT REVIEW ON MICROEMULSION AND ITS APPLICATION IN EXTRACTION OF VEGETABLE OIL," 147–58.

Garbuio, A. AL, Fábio Ferreira Perazzo, and Paulo Cesar Pires Rosa. 2014. "Evaluation and Study of Mebendazole Polymorphs Present in Raw Materials and Tablets Available in the Brazilian Pharmaceutical Market." *Journal of Applied Pharmaceutical Science* 4 (11): 1–7.

Ghafil, Firas, Valentina Anuta, Iulian Sarbu, Corina Dalia Toderescu, and Ion Mircioiu. 2017. "Increasing the Bioavalilability of Mebendazole I. Influence of Croscarmellose on Dissolution Rate, Extent and Mechanism in Simulated Gastric Medium." *Studia Universitatis Vasile Goldis Arad, Seria Stiintele Vietii* 27 (1): 69–78.



Grande, Fedora, Gaetano Ragno, Rita Muzzalupo, Maria Antonietta Occhiuzzi, Elisabetta Mazzotta, Michele De Luca, Antonio Garofalo, and Giuseppina Ioele. 2020. "Gel Formulation of Nabumetone and a Newly Synthesized Analog: Microemulsion as a Photoprotective Topical Delivery System." *Pharmaceutics* 12 (5).

Griffin, William C, Ricardo C Pasquali, Natalia Sacco, and Carlos Bregni. 2016. "The Studies on Hydrophilic-Lipophilic Balance (HLB): Sixty Years after The Studies on Hydrophilic-Lipophilic Balance (HLB): Sixty Years after William C. Griffin's Pioneer Work (1949-2009)," no. January 2009.

Guerini, Andrea Emanuele, Luca Triggiani, Marta Maddalo, Marco Lorenzo, Francesco Frassine, Anna Baiguini, Alessandro Alghisi, et al. 2019. "Mebendazole as a Candidate for Drug Repurposing in Oncology: An Extensive Review of Current Literature," 1-22.

Guo, Jiun-wen, Yu-pin Cheng, Chih-yi Liu, Haw-yueh Thong, and Chi-jung Huang. n.d. "Salvianolic Acid B in Microemulsion Formulation Provided Sufficient Hydration for Dry Skin and Ameliorated the Severity of Imiquimod-Induced Psoriasis-Like Dermatitis in Mice," 1-17.

Hamilton, Gerhard, and Barbara Rath. 2017. "Repurposing of Anthelmintics as Anticancer Drugs" 2: 142-49.

Haq, Anika, Benjamin Goodyear, Dina Ameen, Vivek Joshi, and Bozena Michniak-Kohn. 2018a. "Strat-M® SyntheHaq, A., Goodyear, B., Ameen, D., Joshi, V., & Michniak-Kohn, B. (2018). Strat-M® Synthetic Membrane: Permeability Comparison to Human Cadaver Skin. *International Journal of Pharmaceutics*, 547.

S.O. 2018b. "Strat-M® Synthetic Membrane: Permeability Comparison to Human Cadaver Skin." *International Journal of Pharmaceutics* 547 (1-2): 432-37.

Harunrasheed, Shaik, R Haribabu, J Vineela, and A Raviteja. 2011. "Research Journal of Pharmaceutical, Biological and Chemical Sciences REVIEW ARTICLE Transdermal Drug Delivery System - Simplified Medication Regimen - A Review" 2 (4): 223-38.

Haugen, Thomas A., Espen Tønnessen, and Stephen K. Seiler. 2012. "The Difference Is in the Start: Impact of Timing and Start Procedure on Sprint Running Performance." *Journal of Strength and Conditioning Research* 26 (2): 473–79.

Hou, Wanguo, and Jie Xu. 2016. "Surfactant-Free Microemulsions." *Current Opinion in Colloid and Interface Science* 25: 67–74.

Hussein, Ahmed A. 2014. "Preparation and Evaluation of Liquid and Solid Self-Microemulsifying Drug Delivery System of Mebendazole" 23 (1).

Iddleton, Mark R M, Jane K Elly, Nicholas T Hatcher, Dorothy J D Onnelly, R Stanley M C E Lhinney, T Brian H M C M Urry, Joan E M C C Ormick, and Geoffrey P M Argison. 2000. "O 6 - ( 4-BROMOTHENYL ) GUANINE IMPROVES THE THERAPEUTIC INDEX OF TEMOZOLOMIDE AGAINST A375M MELANOMA XENOGRAFTS" 252 (March 1999): 248–52.

Iqbal, Babar, M Pharm, Javed Ali, M Pharm, Sanjula Baboota, and M Pharm. 2018. "Recent Advances and Development in Epidermal and Dermal Drug Deposition Enhancement Technology."

Iqbal, Mohammad Kashif, and Jamia Hamdard. 2018. "Review Article Microemulsions : Current Trends in Novel Drug Delivery Microemulsions : Current Trends in Novel Drug Delivery Systems," no. March.

Islam, Md Rafiqul, Md Raihan Chowdhury, Rie Wakabayashi, Noriho Kamiya, Muhammad Moniruzzaman, and Masahiro Goto. 2020. "Ionic Liquid-in-Oil Microemulsions Prepared with Biocompatible Choline Carboxylic Acids for Improving the Transdermal Delivery of a Sparingly Soluble Drug." *Pharmaceutics* 12 (4): 1–18.

Jafri, Ifrah, Muhammad Harris, Shoaib Rabia, Ismail Yousuf, and Fatima Ramzan. 2019. "Effect of Permeation Enhancers on in Vitro Release and Transdermal Delivery of Lamotrigine from - Eudragit ® RS100 Polymer Matrix - Type Drug in Adhesive Patches." *Progress in Biomaterials* 8 (2): 91–100.

Jane, E, W Sha, D Ph, and Constance Mitchell. 1983. "DERMAL DRUG DELIVERY SYSTEMS : A REVIEW" 2: 249-66.

Jankowski, A, and R Dyja. 2017. "Dermal and Transdermal Delivery of Active Substances from Semisolid Bases" 79 (August 2016): 488-500.

Jatana, Samreen, Linda M. Callahan, Alice P. Pentland, and Lisa A. DeLouise. 2016. "Impact of Cosmetic Lotions on Nanoparticle Penetration through Ex Vivo C57Bl/6 Hairless Mouse and Human Skin: A Comparison Study." *Cosmetics* 3 (1).

Julian McClements, D., and Stephanie R. Dungan. 1995. "Light Scattering Study of Solubilization of Emulsion Droplets by Non-Ionic Surfactant Solutions." *Colloids and Surfaces A: Physicochemical and Engineering Aspects* 104 (2-3): 127-35.

Jung, Youn Jung, Jeong Hyun Yoon, Nae Gyu Kang, Sun Gyoo Park, and Seong Hoon Jeong. 2012. "Diffusion Properties of Different Compounds across Various Synthetic Membranes Using Franz-Type Diffusion Cells." *Journal of Pharmaceutical Investigation* 42 (5): 271-77.

Kale, Santosh Nemichand, and Sharada Laxman Deore. 2016. "Emulsion Micro Emulsion and Nano Emulsion: A Review." *Systematic Reviews in Pharmacy* 8 (1): 39-47.

Kalra.Rupali, Mulik R. S. A, Badgular.L, Paradkar A. R., Mahadik K.R., Bodhankar S.L., and Sharma. Shekhar. 2010. "Development and Characterization of Microemulsion Formulations for Transdermal Delivery of Aceclofenac: A Research." *International Journal of Drug Formulation & Research* 1 (iii): 32-57.

Klier, John, Christopher J. Tucker, Thomas H. Kalantar, and D. P. Green. 2000. "Properties and Applications of Microemulsions." *Advanced Materials* 12 (23): 1751-57.

Kogan, Anna, and Nissim Garti. 2006. "Microemulsions as Transdermal Drug Delivery Vehicles." *Advances in Colloid and Interface Science* 123-126 (SPEC. ISS.): 369-85.

Kolarsick, Paul A J, Maria Ann Kolarsick, and Carolyn Goodwin. 2006. "Anatomy and Physiology of the Skin."

Kumar, K Senthil, D Dhachinamoorthi, R Saravanan, Udaykumar Gopal, and V Shanmugam. 2011. "Review Article MICROEMULSIONS AS CARRIER FOR NOVEL DRUG DELIVERY : A REVIEW" 10 (2).

Larsson, Jesper. 2009. "Methods for Measurement of Solubility and Dissolution Rate of Sparingly Soluble Drugs.", 25.

Lawrence, M. Jayne, and Gareth D. Rees. 2012. "Microemulsion-Based Media as Novel Drug Delivery Systems." *Advanced Drug Delivery Reviews* 64 (SUPPL.): 175–93.

Li, Yulin, Daniel Thomas, Anja Deutzmann, Ravindra Majeti, Dean W. Felsher, and David L. Dill. 2019. "Mebendazole for Differentiation Therapy of Acute Myeloid Leukemia Identified by a Lineage Maturation Index." *Scientific Reports* 9 (1): 1–9.

Liebenberg, Wilna, Eileen Engelbrecht, Anita Wessels, Bharathi Devarakonda, Wenzhan Yang, and Melgardt M. De Villiers. 2004. "A Comparative Study of the Release of Active Ingredients from Semisolid Cosmeceuticals Measured with Franz, Enhancer or Flow-through Cell Diffusion Apparatus." *Journal of Food and Drug Analysis* 12 (1): 19–28.

Lopes, Luciana B. 2014. "Overcoming the Cutaneous Barrier with Microemulsions." *Pharmaceutics* 6 (1): 52–77.

López-Quintela, M. A., C. Tojo, M. C. Blanco, L. García Rio, and J. R. Leis. 2004. "Microemulsion Dynamics and Reactions in Microemulsions." *Current Opinion in Colloid and Interface Science* 9 (3–4): 264–78.

Luber, Verena, Mathias Lutz, Marianne Abele-Horn, Hermann Einsele, Götz Ulrich Grigoleit, and Stephan Mielke. 2019. "Excretion of *Ascaris Lumbricoides* Following Reduced-intensity Allogeneic Hematopoietic Stem Cell Transplantation and Consecutive Treatment with Mebendazole." *Transplant Infectious Disease*, no. November 2019: 4–7.

Luís, André, Morais Ruela, Aline Gravinez Perissinato, Mônica Esselin, and De Sousa Lino. 2016a. "Evaluation of Skin Absorption of Drugs from Topical and Transdermal Formulations." *Brazilian Journal of Pharmaceutical Sciences* 52.

Malik, Maqsood Ahmad, Mohammad Younus Wani, and Mohd Ali Hashim. 2012. "Microemulsion Method: A Novel Route to Synthesize Organic and Inorganic Nanomaterials. 1st Nano Update." *Arabian Journal of Chemistry* 5 (4): 397–417.

Marwah, Harneet, Tarun Garg, Amit K Goyal, Goutam Rath, Harneet Marwah, Tarun Garg, Amit K Goyal, and Goutam Rath. 2016. "Permeation Enhancer Strategies in Transdermal Drug Delivery" 7544.

Mishra, Amul, Ridhi Panola, and A C Rana. 2014. "Microemulsions : As Drug Delivery System." *Journal of Scientific and Innovative Research* 3 (4): 467–74.

Mujoriya, Rajesh, and Kishor Dhamande. 2014. "A Review on Transdermal Drug Delivery System . A Review on Transdermal Drug Delivery System .," no. June.

Muzaffar, Faizi, U K Singh, and Lalit Chauhan. 2013. "REVIEW ON MICROEMULSION AS FUTURISTIC DRUG DELIVERY" 5 (3).

Naik, Preethi, Sanket M. Shah, John Heaney, Royal Hanson, and Mangal S. Nagarsenker. 2016. "Influence of Test Parameters on Release Rate of Hydrocortisone from Cream: Study Using Vertical Diffusion Cell." *Dissolution Technologies* 23 (3): 14–20.

Nandi, Indranil, Mohammad Bari, and Hemant Joshi. 2003. "Study of Isopropyl Myristate Microemulsion Systems Containing Cyclodextrins to Improve the Solubility of 2 Model Hydrophobic Drugs." *AAPS PharmSciTech* 4 (1).

Neupane, Rabin, Sai H S Boddu, Jwala Renukuntla, and R Jayachandra Babu. n.d. "Alternatives to Biological Skin in Permeation Studies : Current Trends and Possibilities."

Ng, Shiow-Fern, Jennifer J. Rouse, Francis D. Sanderson, Victor Meidan, and Gillian M. Eccleston. 2010. "Validation of a Static Franz Diffusion Cell System for In Vitro Permeation Studies." *AAPS PharmSciTech* 11 (3): 1432–41.

Ng, Shiow Fern, Jennifer J. Rouse, Francis D. Sanderson, Victor Meidan, and Gillian M. Eccleston. 2010. "Validation of a Static Franz Diffusion Cell System for in Vitro Permeation Studies." *AAPS PharmSciTech* 11 (3): 1432–41.

Ngawhirunpat, Tanasait, Narumon Worachun, Praneet Opanasopit, Theerasak Rojanarata, and Suwannee Panomsuk. 2013. "Cremophor RH40-PEG 400 Microemulsions as Transdermal Drug Delivery Carrier for Ketoprofen." *Pharmaceutical Development and Technology* 18 (4): 798–803.

Nygren, Peter, Mårten Fryknäs, Bengt Ågerup, and Rolf Larsson. 2013. "Repositioning of the Anthelmintic Drug Mebendazole for the Treatment for Colon Cancer," 2133–40.

Oberdisse, Julian, and Thomas Hellweg. 2017. "Structure, Interfacial Film Properties, and Thermal Fluctuations of Microemulsions as Seen by Scattering Experiments." *Advances in Colloid and Interface Science* 247 (July): 354–62.

Pantziarka, Pan, Gauthier Bouche, Lydie Meheus, Vidula Sukhatme, and Vikas P Sukhatme. 2014a. "Repurposing Drugs in Oncology ( ReDO )— Mebendazole as an Anti-Cancer Agent." <https://doi.org/10.3332/ecancer.2014.443>.

Paroor, Harsha Mohan. 2012. "Microemulsion: Prediction of the Phase Diagram with a Modified Helfrich Free Energy," no. May: 134.

Part, C F R, and General Chapter. 2017. "VALIDATION OF HPLC METHODS IN PHARMACEUTICAL ANALYSIS," 1–18.

Paul, Bidyut K., and Satya P. Moulik. 2001. "Applications and Use of Microemulsions." *Current Science* 80 (8): 990–1001.

Pawar, Rajendra Prasad, Pooja Mishra, Abhilasha Durgbanshi, Devasish Bose, Jaume Albiol-Chiva, Juan Peris-Vicente, Daniel García-Ferrer, and Josep Esteve-Romero. 2020. "Use of Micellar Liquid Chromatography to Determine Mebendazole in Dairy Products and Breeding Waste from Bovine Animals." *Antibiotics* 9 (2): 1–14.

Pengon, Sirikarn, Chutima Limmatvapirat, and Sontaya Limmatvapirat. 2016. "Factors Affecting Formation of Microemulsions Containing Modified Coconut Oil." *Asian Journal of Pharmaceutical Sciences*.

Plöger, Gerlinde F., Martin A. Hofsäss, and Jennifer B. Dressman. 2018. "Solubility Determination of Active Pharmaceutical Ingredients Which Have Been Recently Added to the List of Essential Medicines in the Context of the Biopharmaceutics Classification System–Biowaiver." *Journal of Pharmaceutical Sciences* 107 (6): 1478–88.

Popović, Dušica J, Mihalj Poša, Kosta J Popović, Jovanka Kolarović, K Popović, and Pavle Z Banović. 2017. "Application of a Widely-Used Tropical Anti-Worm Agent , Mebendazole , in Modern Oncology" 16 (October): 2555–62.

Porwal, Dr Prashant Upadhyay and Mayur. 2012. "Transdermal Drug Delivery System : An Overview Volume 6 / Issue 3 / Jul-Sep 2012." *Asian Journal of Pharmaceutics* 6 (3): 161–70.

Poturcu, Kader, and Ebru C Demiralay. 2019. "Determination of Some Physicochemical Properties of Mebendazole with RPLC Method."

Qurt., Moammal Salah E-deen. 2009. "Preparation of Topical Orphenadrine Citrate and Investigating the Effect of Different Penetration Enhancers on Drug Permeation Rate."

Rahman et al. 2011. "Rahman et Al.," 2 (6): 1379–88.

Reddy, B Venkateswara. 2015. "Transdermal Drug Delivery Systems a Review International Journal of Chemistry and Transdermal Drug Delivery System A Review," no. January 2014.

Rizwan, Mohammad, Mohammad Aqil, Sushama Talegaonkar, Adnan Azeem, Yasmin Sultana, and Asgar Ali. 2009. "Enhanced Transdermal Drug Delivery Techniques : An Extensive Review of Patents," 105–24.

Rosano, Henri L, John L Cavallo, David L Chang, and James H Whittam. 1988. "Microemulsions: A Commentary on Their Preparation." *Journal of the Society of Cosmetic Chemists* 39 (June): 201–9.

Roshdy, Aya, Heba Elmansi, Shereen Shalan, and Amina Elbrashy. 2020. "Use of Eosin for Green Spectroscopic Determination of Mebendazole." *Luminescence*, no. January: 1–9.

Rushworth, Linda K., Al .2019. "Repurposing Screen Identifies Mebendazole as a Clinical Candidate to Synergise with Docetaxel for Prostate Cancer Treatment." *British Journal of Cancer*, no. November.

Ryu, Kyeong A., Phil June Park, Seong Bo Kim, Bum Ho Bin, Dong Jin Jang, and Sung Tae Kim. 2020. "Topical Delivery of Coenzyme Q10-Loaded Microemulsion for Skin Regeneration." *Pharmaceutics* 12 (4).

Salamanca, Constain, Alvaro Barrera-Ocampo, Juan Lasso, Nathalia Camacho, and Cristhian Yarce. 2018. "Franz Diffusion Cell Approach for Pre-Formulation Characterisation of Ketoprofen Semi-Solid Dosage Forms." *Pharmaceutics* 10 (3): 148.

Salerno, Claudia, Susana Gorzalczany, Alicia Arechavala, Silvia L. Scioscia, Adriana M. Carlucci, and Carlos Bregni. 2015. "Novel Gel-like Microemulsion for Topical Delivery of Amphotericin B." *Revista Colombiana de Ciencias Químico Farmacéuticas* 44 (3): 359–81.

Science, Pharmaceutical. 2008. "Impacts of Size on Pharmacokinetics and Biodistributions of Mebendazole Nanoformulations in Mice and Rats Impacts of Size on Pharmacokinetics and Biodistributions of Mebendazole Nanoformulations in Mice and Rats."

Seo, Ji Eun, Sungkyoon Kim, and Bae Hwan Kim. 2017. "In Vitro Skin Absorption Tests of Three Types of Parabens Using a Franz Diffusion Cell." *Journal of Exposure Science and Environmental Epidemiology* 27 (3): 320–25.



Sesto Cabral, Maria Eugenia, Alberto Nicolas Ramos, Carla Agostina Cabrera, Juan Carlos Valdez, and Silvia Nelina González. 2015. "Equipment and Method for in Vitro Release Measurements on Topical Dosage Forms." *Pharmaceutical Development and Technology* 20 (5): 619–25.

Shaaban, Hamdy A., and Amr E. Edris. 2015. "Factors Affecting the Phase Behavior and Antimicrobial Activity of Carvacrol Microemulsions." *Journal of Oleo Science* 64 (4): 393–404.

Sharma, Devender, Hemraj Vashist, and R. B. Sharma. 2015. "Stability-Indicating Spectrophotometric Methods for Determination of Gliclazide in Pure Form and Pharmaceutical Preparation." *European Journal of Biomedical AND Pharmaceutical Sciences* 2 (4): 122–35.

Sharma, Nikhil, Geta Agarwal, A C Rana, and Zulfiqar A L I Bhat. 2011. "A Review : Transdermal Drug Delivery System : A Tool For Novel Drug Delivery System" 3 (3): 70–84.

Simbulan-Rosenthal, Cynthia M., Sivanesan Dakshanamurthy, Anirudh Gaur, You Shin Chen, Hong Bin Fang, Maryam Abdussamad, Hengbo Zhou, et al. 2017. "The Repurposed Anthelmintic Mebendazole in Combination with Trametinib Suppresses Refractory NRASQ61K Melanoma." *Oncotarget* 8 (8): 12576–95.

Simon, Alice, Maria Inês Amaro, Anne Marie Healy, Lucio Mendes Cabral, and Valeria Pereira de Sousa. 2016. "Comparative Evaluation of Rivastigmine Permeation from a Transdermal System in the Franz Cell Using Synthetic Membranes and Pig Ear Skin with in Vivo-in Vitro Correlation." *International Journal of Pharmaceutics* 512 (1): 234–41.

Singh, Pranjal Kumar, Mohd Kashif Iqbal, Vikesh Kumar Shukla, and Mohd Shuaib. 2014. "Microemulsions: Current Trends in Novel Drug Delivery Systems." *Journal of Pharmaceutical, Chemical and Biological Sciences* *Journal of Pharmaceutical, Chemical and Biological Sciences* 1 (11): 39–5139.

Singh, Vinod, S S Bushettii, Appala Raju S, Rizwan Ahmad, Mamta Singh, and Anupam Bisht. 2011. "Microemulsions as Promising Delivery Systems : A Review" 45 (4).

Spornath, Aviram, and Abraham Aserin. 2006. "Microemulsions as Carriers for Drugs and Nutraceuticals." *Advances in Colloid and Interface Science* 128–130 (2006): 47–64. <https://doi.org/10.1016/j.cis.2006.11.016>.

Subongkot, Thirapit, and Tanasait Ngawhirunpat. 2017. "Development of a Novel Microemulsion for Oral Absorption Enhancement of All-Trans Retinoic Acid." *International Journal of Nanomedicine* 12: 5585–99.

Tagavifar, Mohsen, Sumudu Herath, Upali P. Weerasooriya, Kamy Sepehrnoori, and Gary Pope. 2018. "Measurement of Microemulsion Viscosity and Its Implications for Chemical Enhanced Oil Recovery." *SPE Journal* 23 (1): 66–83.

Tan, Zhi, Lu Chen, and Shuxing Zhang. 2016. "Comprehensive Modeling and Discovery of Mebendazole as a Novel TRAF2- and NCK-Interacting Kinase Inhibitor." *Nature Publishing Group*, no. July: 2–11.

Torre-, Paloma Marina De, Juan José García-rodriguez, Guillermo Torrado, Susana Torrado, and Santiago Torrado-santiago. 2014. "Enhanced Bioavailability and Anthelmintic Efficacy of Mebendazole in Redispersible Microparticles with Low-Substituted Hydroxypropylcellulose," 1467–79.

Uchida, Takashi, Wesam R. Kadhum, Sayumi Kanai, Hiroaki Todo, Takeshi Oshizaka, and Kenji Sugibayashi. 2015. "Prediction of Skin Permeation by Chemical Compounds Using the Artificial Membrane, Strat-MTM." *European Journal of Pharmaceutical Sciences* 67: 113–18.

Uchida, Takashi, Wesam R. Kadhum, Sayumi Kanai, Hiroaki Todo, Takeshi Oshizaka, and Kenji Sugibayashi. 2015. "Prediction of Skin Permeation by Chemical Compounds Using the Artificial Membrane, Strat-M™." *European Journal of Pharmaceutical Sciences* 67: 113–18.

Upadhay, M. 2012. "Preparation and Evaluation of Cilnidipine Microemulsion." *Journal of Pharmacy and Bioallied Sciences* 4 (SUPPL.): 114–15.

USP. 2015. "Solution Procedures." USP. (2015c). <1092> The Dissolution Procedure: Development And Validation. In: *The United States Pharmacopeia and National Formulary*. c: 33–38.

Wang, Yue. 2014. "Preparation on Nano- and Microemulsions Using Phase Inversion and Emulsion Titration Methods," 1–133

Yagi, Masayuki, and Yoshikazu Yonei. 2018. "The Figure Is Adapted from Adapted from Ref 1" *5* (1): 50–54.

Y. Isaac, et .al. 2016. "Differential Pulse Voltammetric Determination of Albendazole and Mebendazole in Pharmaceutical Formulations Based on Modified Sonogel Carbon Paste Electrodes with Perovskite-Type LaFeO<sub>3</sub> Nanoparticles" *163* (8): 428–34.

Zimmermann, Sarah C, Jan Va, Alexandra J Gadiano, Ying Wu, and Andrej Janc. 2018. "N - Substituted Prodrugs of Mebendazole Provide Improved Aqueous Solubility and Oral Bioavailability in Mice and Dogs."

Zsikó, Stella, Erzsébet Csányi, Anita Kovács, Mária Budai-Szűcs, Attila Gácsi, and Szilvia Berkó. 2019. "Methods to Evaluate Skin Penetration in Vitro." *Scientia Pharmaceutica* 87 (3).

<https://pubchem.ncbi.nlm.nih.gov/compound/Mebendazole#section=2D-Structure> 11/2/2021

<https://pubchem.ncbi.nlm.nih.gov/compound/Mebendazole#section=Stability-Shelf-Life> 11/2/2021

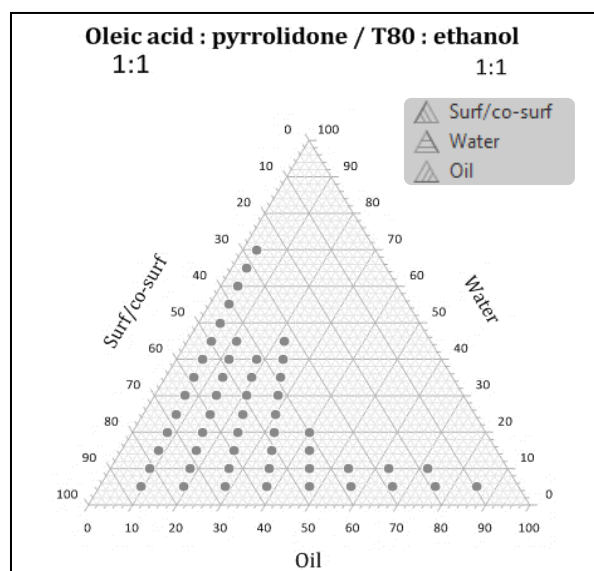
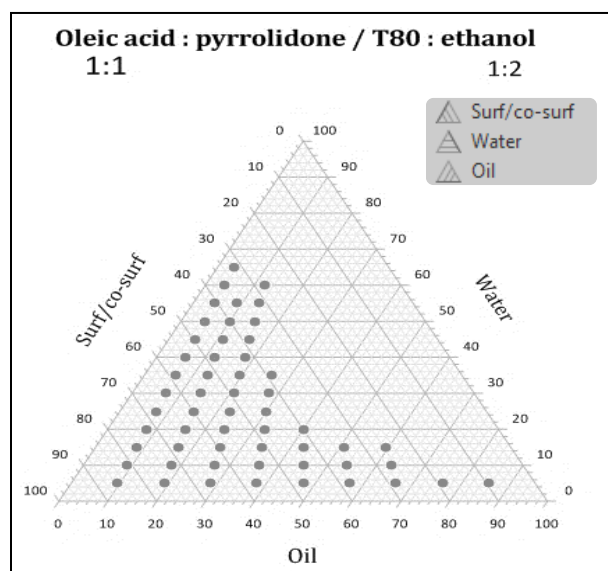
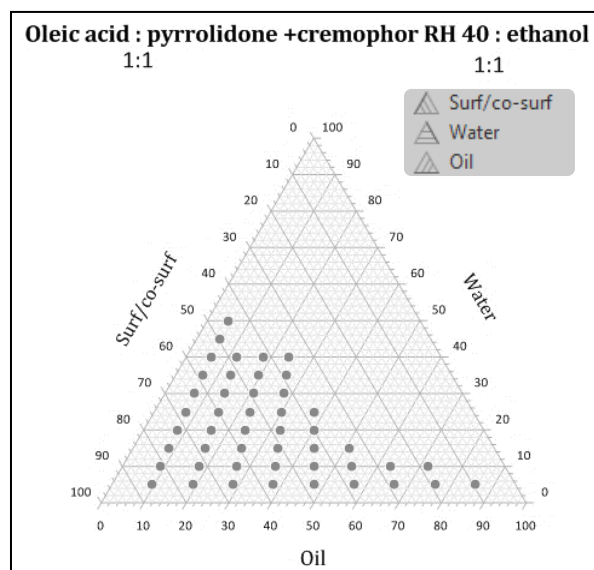
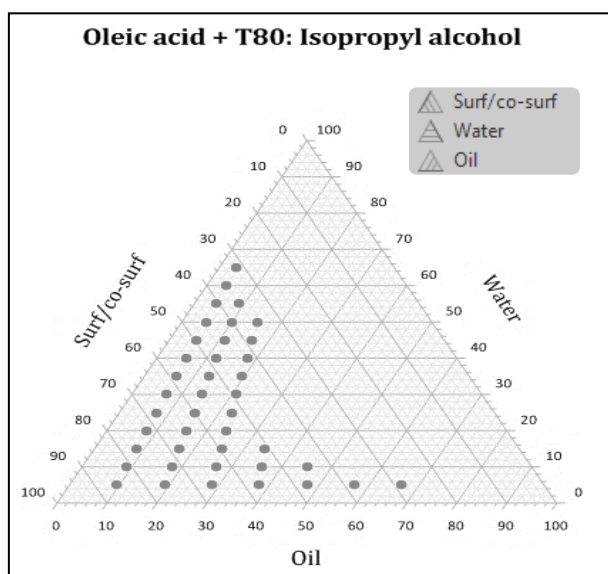
[http://www.uspbpep.com/usp32/pub/data/v32270/usp32nf27s0\\_m47510.html](http://www.uspbpep.com/usp32/pub/data/v32270/usp32nf27s0_m47510.html)  
11/2/2021

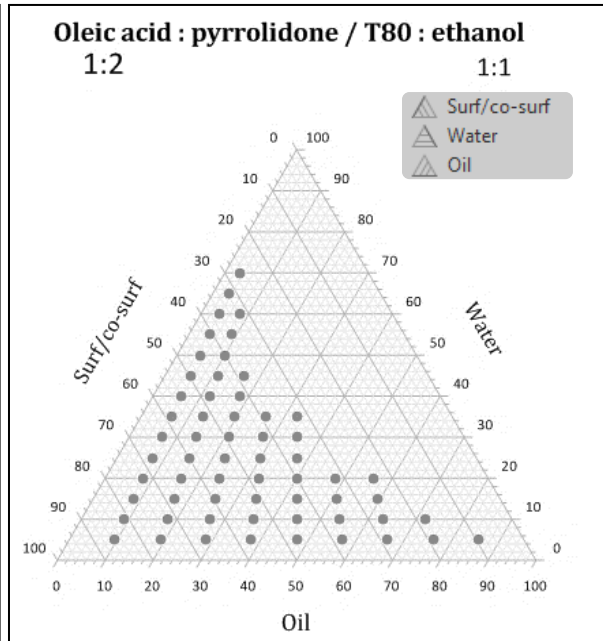
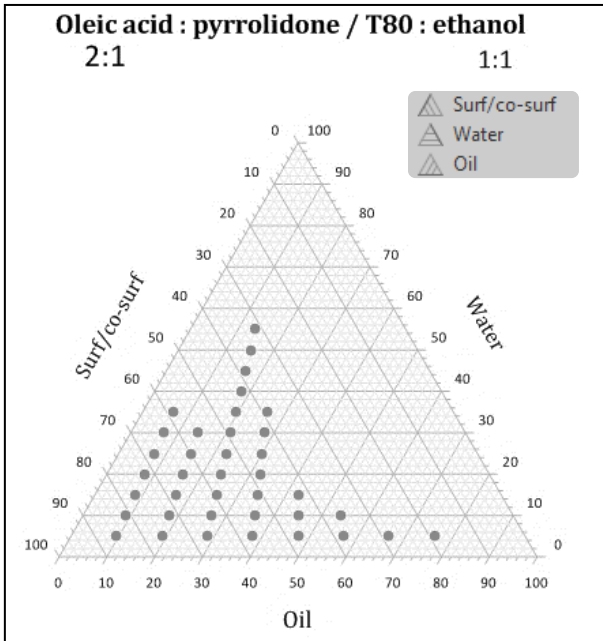
<https://www.merckmillipore.com/INTL/en/life-science-research/drug-discovery->

[development/strat-m-transdermal-diffusion  
membrane/yrOb.qB.rrIAAAE\\_5nsRHeiO.nav?ReferrerURL=https%3A%2F%2Fwww.goo  
gle.com%2F](#) 1/3/2021

## Appendices

### Appendix 1: Pseudo- ternary diagrams for some microemulsion formulations.





## Appendix 2: Chromatograph of mebendazole using HPLC.

Data File: E:\CHEM32\1\DATA\MEBENDAZOLE 2018-07-05 13-35-03\007-0802.D  
 Sample Name: STD7- Mebendazole (0.10 mg/ml)

```

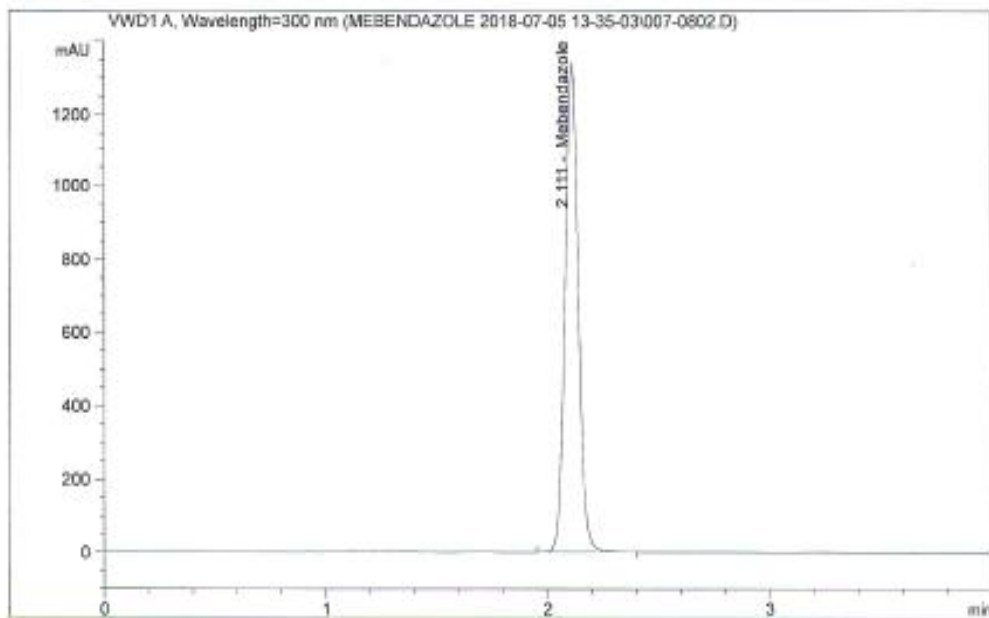
=====
Acq. Operator   :Ramzi Muqedi
Acq. Instrument :Instrument 1
Injection Time  : 04:07:24 pm
Injection Date  : 7/5/2018
Seq. Line      : 8
Location       : Vial 7
Inj            : 2
Inj. Volume    (Method): 20 µl
Act. Inj. Vol. from Sequence: 20 µl
  
```

```

Acq. Method     : E:\Chem32\1\DATA\MEBENDAZOLE 2018-07-05 13-35-03\
                  MEBENDAZOLE.M
  
```

```

Last changed    :7/9/2018 11:44:22
  
```



```

Available Signals:
VWD1 A, Wavelength=300 nm
  
```

```

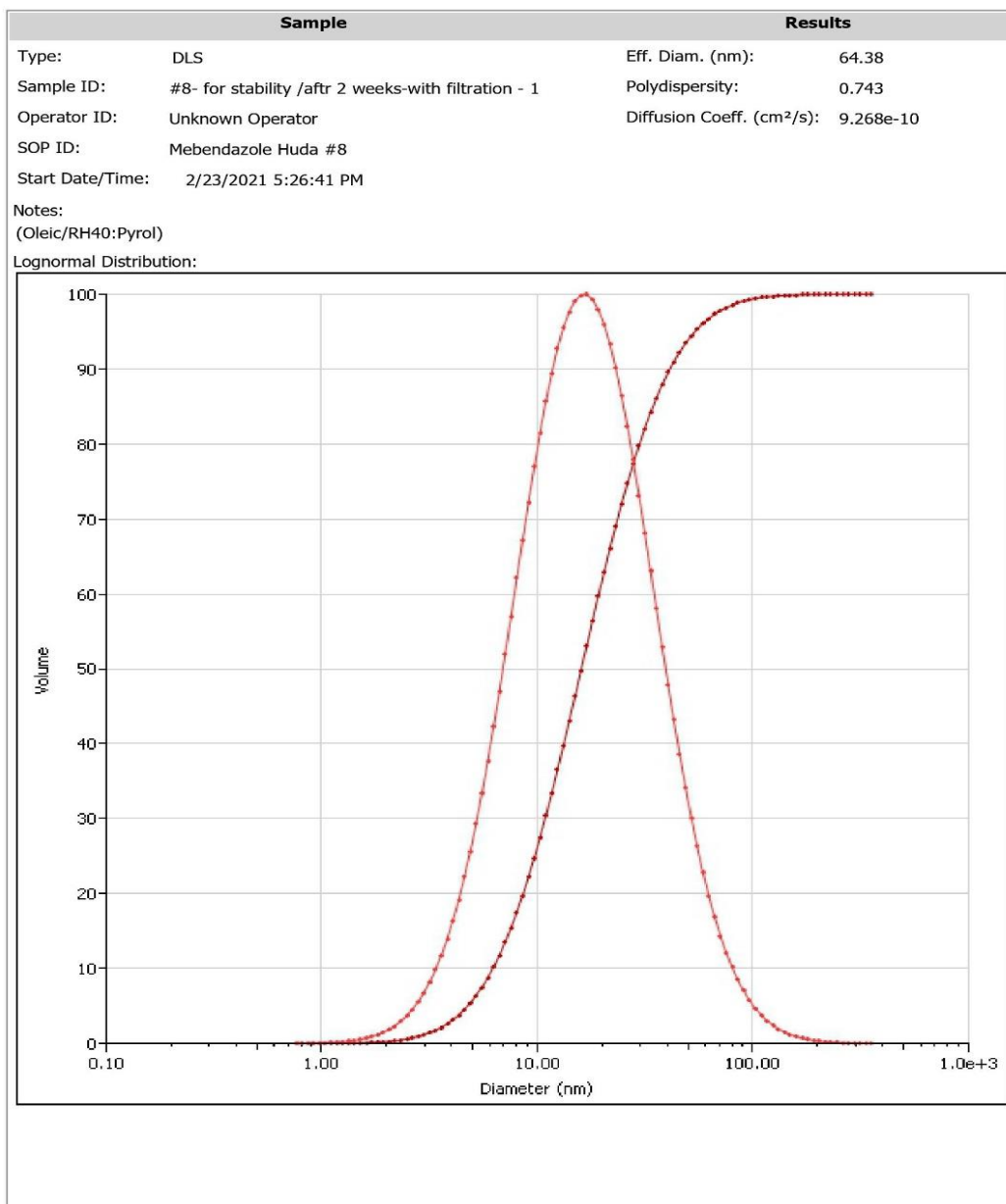
Signal: VWD1 A, Wavelength=300 nm
  
```

RetTime [min]	API Name	Area [mAU*s]	Halfh. Width [min]	USP Symm. Tail.	Plates	Resolution
2.111	Mebendazole	5516.8	0.06	0.94	1.08	6250

### Appendix 3: DLS report for ME#8 using DLS Brookhaven Instruments.



#### Basic DLS Report





#### Appendix 4: Photos from the work



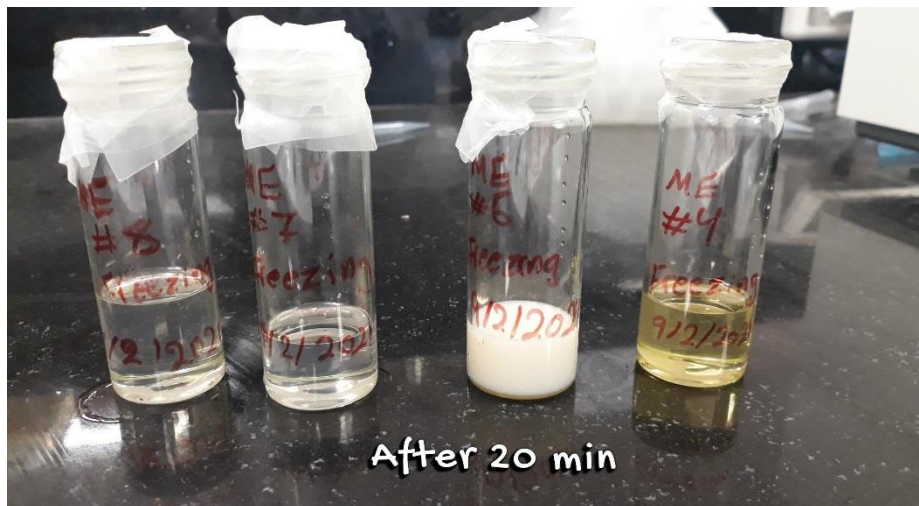
Permeation study using Franz diffusion cells



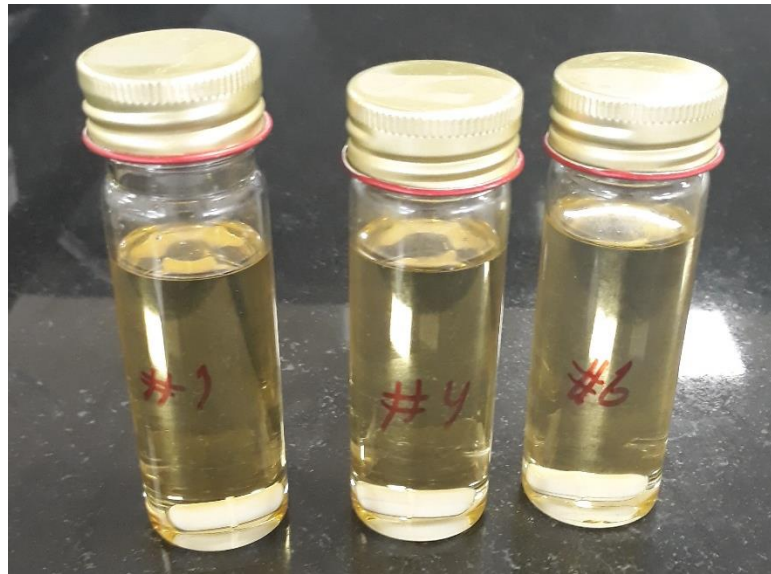
Some microemulsion formulations during preparation



ME#4, ME#6, ME#7, and ME#8 After freezing



ME#4, ME#6, ME#7, and ME#8 at room temperature for 20 minutes after freezing



ME#1, ME#4, and ME#6



Some ailed formulations